University of Strathclyde
Department of Naval Architecture and Marine Engineering

Structural Strength and Reliability Analysis of Composite Structures

by

NANA YANG

A thesis presented in fulfilment of the requirements
for the degree of Doctor of Philosophy

June 2010

- Dedicated to my dearest parents Delin Yang and Wenbo Yu -

For educating me and for their endless love and support

- Dedicated to my darling husband Yanzhuo Xue-

For his endless love, support, patience and encouragement

Acknowledgements

I would like to express my limitless thank to my supervisor, Professor Purnendu K. Das for giving me this opportunity to work under his supervision. If it were not by his trust, support and guidance, I would not have been able to start my doctoral study and have carried it on all the way till this stage. I am indeed very grateful.

I would like to express my deep appreciation to Professor Xiongliang Yao for his support and encouragement throughout the past four years.

I am particularly thankful to Mr. Brian Hayman (Det Norske Veritas) and Dr. James I.R. Blake (University of Southampton) for their valuable suggestions and comments during my research studies.

Special thanks are sent to Prof. Peilin Zhou, Dr. Yunlong Zheng, Dr. Qing Xiao, Dr. Qiuxin Gao and Dr. Li Xu who directly or indirectly inspired me during this research. The administrative staffs of the department are a delight to know and work with, Thelma Will, Fiona Cameron and Nicola Pollock always ready to help, and always with a warm smile.

I warmly thank all my colleagues and friends for their valuable advice and friendship and for making the city of Glasgow pleasant to live and work in. My sincere thanks to my Chinese friends in Glasgow for organizing warm social activities for relaxation.

I would like to express my deep gratitude to my parents and my dearest husband who have given me endless support, encouragement and understanding over the years. I would not be able to succeed without their support.

The research of this thesis has been carried out at Department of Naval Architecture & Marine Engineering, Universities of Glasgow and Strathclyde, during the years 2006 and 2010. During my PhD studies, I have been partially funded by

MASTRUCT (EU), BAE system and Harbin Engineering University. Financial support is gratefully acknowledged.

Nana Yang
June 2010, Glasgow

Abstract

Current design in marine fibre reinforced plastic (FRP) structures has traditionally been driven by rule-based deterministic procedures. However, composite structures possess high inherent variabilities as compared with isotropic materials. In addition, due to their anisotropic properties, they require a larger number of variables to describe them. Conventional deterministic methods are simple but inflexible to adjust the prescribed safety margin and do not give a reliable indicator of satisfactory performance for the design of FRP structures. Structural probabilistic method leads to a better design, where a structure can be designed with adequate and consistent level of safety. The main purpose of this thesis is to develop a stochastic approach to the design of composite structures that is able to account for variations in material properties, geometric properties, load effects and processing techniques.

Two main aspects need to be properly considered for reliability analysis of composite structures. One important aspect is the mechanical model, which should be suitable for the development of a reliability-based design method for composite structures of ships. The second important aspect is the probabilistic model which has to be chosen with computational efficiency, which may restrict their applicability.

A closed form solution is produced for the strength prediction of the unstiffened panel and the probabilistic design approach is proposed at design stages. For more general structures with arbitrary geometries and boundary conditions, a progressive failure analysis method is developed using commercial software ANSYS. A multi-frame restart analysis is used to consider the nonlinearity of material properties. The benchmark study is performed on a number of fibre reinforced plates with various thicknesses and imperfections.

An analytical procedure is presented for the strength assessments of hat-stiffened panels made of composite material subjected to pure compressive load, pure lateral load and the combination of compressive and lateral loads. Equivalent elastic

properties are used for laminated composite plates. The importance of the random variables in the prediction of reliability is determined through the sensitivity analysis. A parametric study is performed to study the effects of statistical distribution of the important variables.

Finally, a methodology, incorporating nonlinear finite element method and probability algorithms, performs a probabilistic assessment of composite structure. Following this procedure, it is possible to provide means for a decomposition of the reliability index β of a structure into partial safety factors associated with the individual design variables which is easily used in codes of practice.

Contents

List of Tables

List of Figures

Nomenclature

Notation

(u, v, w)	Displacements in (x, y, z)
(u_0, v_0, w_0)	Displacements of the mid-plane
ϕ_x, ϕ_y	Rotations of a transverse normal about the y- and x-axis
$\{\varepsilon^0\}, \{\varepsilon^1\}$	Membrane and the flexural strains
A_{ij}, B_{ij}, D_{ij}	Extensional stiffnesses, bending-extensional coupling stiffnesses and bending stiffnesses
$[\overline{Q}]$	Transformed coefficients
$[Q]$	Reduced stiffnesses
$\{N\}$	In-plane load
$\{M\}$	Moment
K	Shear correction coefficient
$\sigma_1, \sigma_2, \sigma_3$	Normal stress components in the x, y, z directions
$\sigma_4, \sigma_5, \sigma_6$	Shear stress components in the yz, xz, xy planes
X_t, Y_t, Z_t	Material allowable tensile strengths in the x, y, z directions
X_c, Y_c, Z_c	Material allowable compressive strengths in the x, y, z directions
R, S, T	Material allowable shear strengths in the yz, xz and xy planes.
F_i, F_i, F_{ijk},	Tensor strength factors
E_1, E_2, E_3	Yong's Modulus
G_{12}, G_{13}, G_{23}	Shear Modulus
v_{12}, v_{13}, v_{23}	Poisson's ratio

P	Compressive load
P_{cr}	Critical buckling load
P_f	Probability of failure
β	Safety index
b_1,b_2,b_3,b_4, b_5,d	Geometry dimensions of the cross-section
t_1, t_2, t_3	Thickness of element of section
L, B	Length and breadth of the stiffened panel
a, b	Spacing between longitudinal stiffeners and transverse stiffeners
N_g, N_s,	Numbers of longitudinal and transverse stiffeners
D_g, D_s	Flexural rigidity of girder and stiffener
V_g,V_s	Potential energy of girder and stiffener
q	Uniform pressure load
W_q	Work of the external force
f_{mn}	Deflection parameter
σ_E	Critical compression
M_g	Bending moment of girder
Z	Distance from the neutral plane to the point considered
E_x^m , E_y^m	Equivalent Young's modulus in the x- and the y-direction
A	Total cross-sectional area of a stiffener with attached strip of shell
GA_s	Effective shear rigidity
A_s	Effective shear area
δ_0, δ	Maximum initial imperfection and total deflection
Π	Total potential energy
U	Elastic strain energy

Φ	Magnification factor
M_{qmax}	Maximum bending moment due to lateral load
w_{qmax}	Maximum deflection due to lateral load
B_{e}	Effective breadth
E_f	Young's modulus of fibre
E_m	Young's modulus of resin
G_f	Shear modulus of fibre
G_m	Shear modulus of resin
V_f	Fibre volume fraction
ε_f^*	Tensile failure strain
σ_{utl}	Maximum compressive stress
σ	Applied compressive stress.
X_{u}	Model uncertainty
$\alpha, \delta, \gamma, \eta$	Sensitivity factors
$G(X)$	Structural response
$G(\bar{x})$	Fitted response surface
A,B,C	Undetermined coefficients in response surface function
$\Phi()$	Standard normal cumulative distribution function
Y	Vector of the observations
$\boldsymbol{B}$	Vector of the regression
X	Matrix of the variables
ε	Vector of random errors
SS_R	Regression

SS_E	Residual or Error
X^*	Design point
ϕ	Resistance factor
R	Design strength
γ_i	Load factor for the i^{th} load
L_i	Design value for the i^{th} load

Abbreviations

APDL	ANSYS Parametric Design Language
CALREL	CAL-RELiability
CLPT	Classical Laminated Plate Theory
COV	Coefficient of Variation
ESL	Equivalent Single Layer
FDM	Finite Difference Method
FEM	Finite Element Method
FM	Forced Method
FORM	First Order Reliability Method
FOSM	First-Order Second-Moment
FRP	Fibre Reinforced Plastic
FSDT	First-order Shear Deformation Theory
FSM	Finite Strip Method
GRP	Glass Reinforced Plastic
HM	High Modulus
HS	High Strength
HSDTs	Higher-order Shear Deformation Theories
LRFD	Load and Resistance Factor Design
MCMVs	Mine Countermeasure Vessels
MCS	Monte Carlo Simulation
RSM	Response Surface Method
SORM	Second Order Reliability Method

Chapter 1: Introduction

1.1 Background

There is increasing interest in the use of lightweight, polymer composite structures in ships as composite materials have a higher strength-to-weight ratio, which can lead to reduced weight in the vessel's structures without compromising strength. This provides increased payload, greater speed and reduced fuel usage. Composites also have advantages as compared to steel such as improved resistance to corrosion, non-magnetic, reduced retained stresses from construction, higher damping properties, a longer fatigue life and lower maintenance requirements. The applications of composite materials in marine structures are in the form of single skin stiffened structures as well as monocoque single skin and sandwich configurations.

Current design trends in marine Fibre Reinforced Plastic (FRP) structures are still designed deterministically on safety factor, which is quantified by the margin between the predicted load and the structure's calculated capacity. However, composite structures possess high inherent variabilities in design variables as composite structures could be designed with different fibre types, fibre architectures, core materials, orientations of reinforcement in the different lamina and the stacking sequence in the laminates. This larger freedom has the counterpart that the strength of composite materials is more uncertain. Furthermore, due to their anisotropic properties, composite materials require a larger number of variables to describe them. In addition, because composite structures usually operate in hostile and random service environments, it is difficult to predict the structural performance due to inadequate knowledge of physical phenomena associated with loads**.**

To ensure the structures can perform their intended functions with desired confidence,

these uncertainties or variabilities must be considered during structural design. Traditional methods of dealing with these uncertainties are to use conservative, fixed values in equations to guard against the possibility of structural damage. In this deterministic analysis, it is assumed that all factors affecting the load applied to the structure are known, the probability or statistical nature relating the material properties, load, and geometric properties are usually ignored. Thus, the deterministic values are usually used as the representative variables. However, in reality, these relationships are only approximations. Material strength and dimensions exhibit appreciable variability in statistical sense and the loads assumed in design generally contain a high degree of uncertainty. High implied margins of safety as in this case, are introduced by ensuring that the estimates of such parameters are conservative. This method of structural analysis gives lower bound solutions to collapse loads and the applied loads are multiplied by suitably large safety factors. The conventional deterministic methods are simple but inflexible in adjusting the prescribed safety margin and do not give a reliable indicator of satisfactory performance for the design of FRP structures.

With the development of reliability technology, probabilistic method has been used in reliability-based design for the marine and offshore structures. Structural probabilistic method allows designers to limit the probability of undesirable events occurring and leads to a balanced design. Reliability-based design is more flexible and consistent than corresponding deterministic analysis because they provide more rational safety levels over various types of structures and take into account more information that is not considered properly by deterministic analysis.

Moreover, in a deterministic analysis, the sensitivity of design variables can only be computed by quantifying the change in the performance measure due to a change in the variable value. On the other hand, if a design is based on reliability theory, each random variable is defined by the mean value, coefficient of variance and distribution type, and then sensitivity may be obtained directly after reliability analysis is completed. Furthermore, load and resistance factor design formats can be used by designers to account for uncertainties without a direct use of probabilistic

description of the variables while maintaining the simplicity of deterministic design practice.

There are various established techniques to carry out reliability analysis depending on the type of problems and the complexity of the limit state function, such as first order reliability method, second order reliability method and simulation-based method. One of the difficult problems in composites will be to define the failure surface for various limit states and also the uncertainties of different design variables involved in the definition of the limit states. Surmounting these issues will reduce the level of uncertainty in adopting composites as a construction material and widen the engineer's choice of design solutions.

1.2 Objectives and Scope of the Thesis

The application of reliability methods for metal structures has become relatively common in design, but this is not yet the situation of composite structures. The strategic goal of this thesis is to develop a stochastic approach to the design of composite structures that is able to account for variations in material properties, geometric properties, load effects and processing techniques. The main objectives and scope of the thesis are detailed as follows:

- Identifying the merits of reliability based approaches in composites structures.

- Determining major possible sources of variabilities in composite design and production process.

- Performing a critical review of the existing approaches on the strength prediction of laminated plates and stiffened laminated plates.

- Establishing the mechanics of composite structures based on each identified

failure mode and the details of variabilities in composite structures. The methodology should be suitable for the development of a reliability-based design method for composite structures.

- Providing a methodology for sensitivity analysis of reliability to variations in design parameters including the basic strength variables, load variables, model uncertainties in strength predictors etc. On the basis of this sensitivity analysis, a parametric study should be performed on the important variables. Design strategies are recommended as guidelines for the design of composite structures.

1.3 Outline of the Thesis

The thesis is structured in seven chapters. A brief outline of the content of each chapter is given below:

- Chapter 1, *Introduction*, provides the background to the research presented in this thesis, the overall objectives and scopes of the present research, and the outline of the thesis.

- Chapter 2, *Review*, presents an introduction to composite materials and their marine applications, different methods available for the strength prediction of composite structures and their advantages and disadvantage, the sources of variabilities in composite design and production process, followed by the review of the probabilistic approaches which have been used for the reliability assessment of composite structures.

- Chapter 3, *Methodology for Assessing Structural Reliability*, describes the reliability analysis methods, which are commonly used in engineering applications such as first-order second-moment, first order reliability method,

second order reliability method and simulation-based method. The sensitivity analysis is also presented in detail.

- Chapter 4, *Strength and Reliability Analysis of Unstiffened Plates*, deals with the analytical and numerical methods for the strength prediction of the unstiffened plates. Probabilistic design approach to composite laminates to consider the uncertainty of basic variables at the design stages is proposed.

- Chapter 5*, Strength and Reliability Analysis of Stiffened Plates,* deals with a simplified analytical method for the strength assessment of hat-stiffened panels at the constituent level. The reliability analysis and the sensitivity analysis are performed and parametric study is investigated based on the important variables.

- Chapter 6*, Application of Response Surface Method for Reliability Analysis of Composite Structures,* applies a methodology incorporating finite element method and probability algorithms to perform a probabilistic assessment of composite structure. Based on these methods a reliability-based design format has been suggested for partial safety factors.

- Chapter 7, *Discussions and Conclusions,* summarises the present work, the main conclusions and the recommendations for the future research.

Chapter 2:
Review

2.1 Introduction to Composite Materials

A composite material is a combination of two or more materials so that the properties of the composite are usually superior to those of the constituent materials acting independently. The excellent capabilities of composites include its lack of magnetic properties and electrical conductivity, its resistance to corrosion, its relative sonar transparency, relatively large strength to weight ratio and good fatigue properties. There are many composite materials used in engineering fields. Fibre reinforced plastic is the most commonly used for shipbuilding, especially for hull construction. All composite materials can broadly be classified based on the constituents in the following two groups:

- Resins
- Reinforcements

Before considering their applications, it is necessary to describe the composition of composite materials which, unlike metal, can be tailored to meet a wide range of design requirements because the property of the composition significantly affects the finished product.

(a) Resins

The role of the matrix resin is to maintain fibre alignment, protect the fibres from abrasion and the adverse environmental effects, efficiently transfer external loads to the reinforcements or redistribute the load to surrounding fibres when fracture happens. Therefore, in general, any resin system for use in a composite material must

meet good mechanical properties, adhesive properties, toughness properties and resistance to environmental degradation.

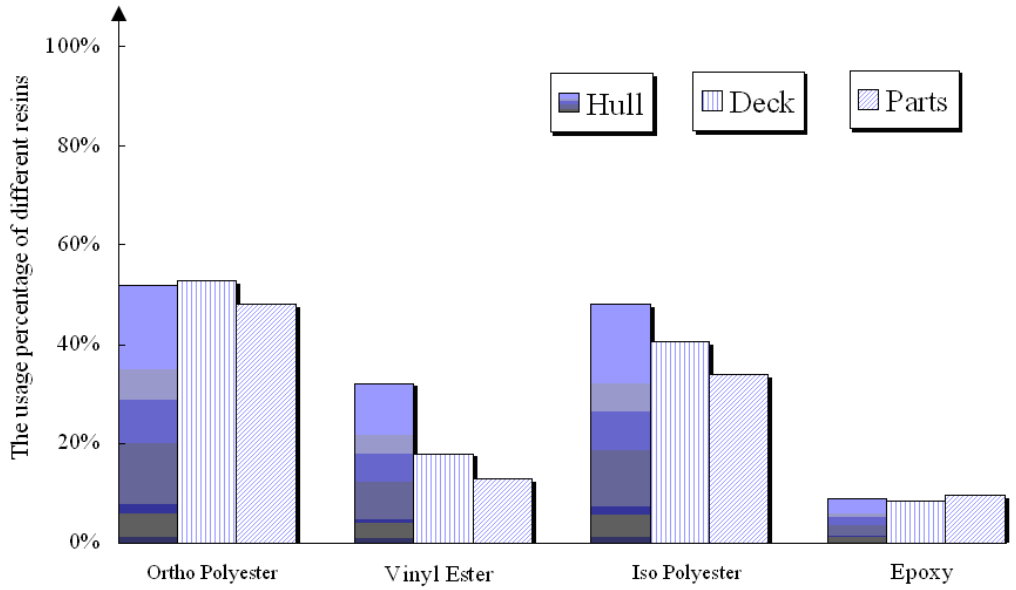

Figure 2.1 Resins used in marine industry (Greene, 1990)

Polyesters, epoxies and vinyl esters are almost always used as the matrix material in reinforced plastics for marine construction. The choice of resin depends to a great extent on mechanical properties and suitability for incorporation into an economical fabrication process. The percent of manufacturers using various resin systems is represented in Figure 2.1. Typical properties of different resins are shown in Table 2.1.

Polyesters are the most commonly used for marine structures since glass fibre-reinforced polyester is a good match in terms of good performance, easy to use and price. The main advantages of polyester resins are low cost, room temperature cure capability and reasonable resistance to water absorption.

Epoxy offers relatively good mechanical properties, superior abrasion resistance, high water resistance, greater bonding strength and much lower shrinkage after curing. However, the disadvantages of epoxies are higher price, toxicity, longer

curing time and complicated processing requirements. Therefore, epoxies are most often used in fields of aerospace and high-performance vehicles and yachts.

Vinyl esters are a compromise between polyesters and epoxies in most respects and more likely to be used in the applications where improved properties are required and polyesters can not quite fulfil the requirement such as racing canoes and speed boats. The disadvantage of vinyl ester is that the cost is about twice that of polyester resins (Smith, 1990).

Table 2. 1 Typical properties of different resins (Smith, 1990)

Material	Polyester (orthophthalic)	Polyester (isophthalic)	Vinyl ester (Derakane 411-45)	Epoxy (DGEBA)	Phenolic
Specific gravity	1.23	1.21	1.12	1.2	1.15
Young's modulus (GPa)	3.2	3.6	3.4	3.0	3.0
Poisson's ratio	0.36	0.36	-	0.37	-
Tensile strength (MPa)	65	60	83	85	50
Tensile failure strain (%)	2	2.5	5	5	2
Compressive strength (MPa)	130	130	120	130	-
Heat distortion temp.(^{0}C)	65	95	110	110	120
Relative cost	0.9	1.0	1.8	2.3	0.8

(b) Reinforcements

The reinforcement is the constituent that primarily provides most of the strength and stiffness to the composites. Mechanical properties of most reinforcing fibres are considerably higher than those of unreinforced resins. Therefore, the mechanical properties of fibre/resin system are dominated by fibre selection.

The most common types of reinforcement used for engineering applications are glass, carbon and Aramid. Glass fibres are the dominant reinforcement in all but high-performance composite applications due to their low cost, relatively good strength and workability characteristics. The usage percentage of different reinforcements in marine industry is given in Figure 2.2. Typical properties of different fibres are shown in Table 2.2. Disadvantages of glass fibres are low stiffness, moisture sensitivity and abrasiveness. E glass (high electrical resistance) and S glass (high strength) are the most used in marine industry. S glass is considerably costlier to produce than E glass and exhibits about one third better tensile strength. The application of glass fibres is often found in leisure boats, mine countermeasure vessels, high-speed passenger ships and some aerospace structures.

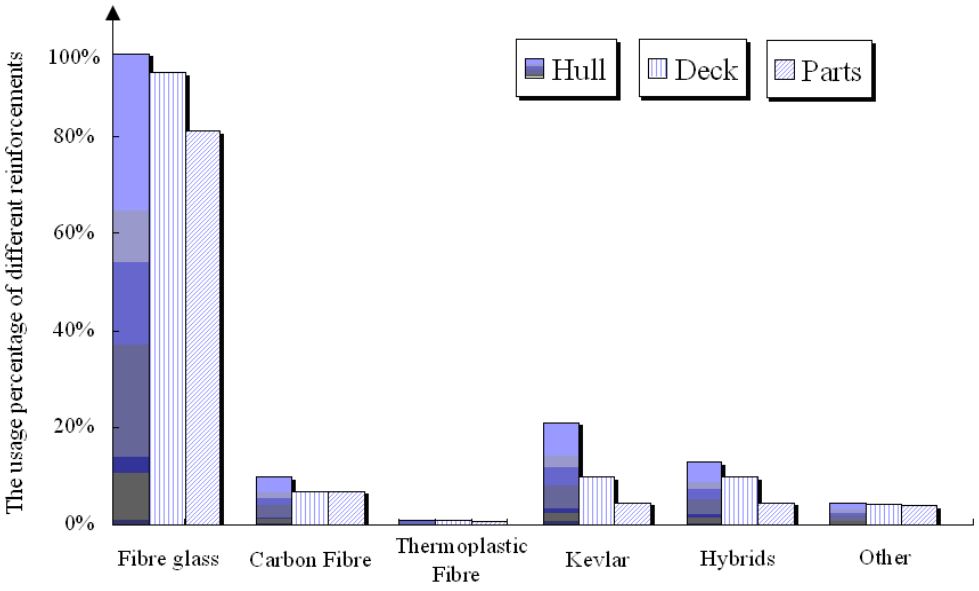

Figure 2.2 Reinforcement materials used in marine industry (Greene, 1990)

Carbon fibres have the highest strength and stiffness characteristics of all the reinforcement fibres, but only High Strength (HS) or High Modulus (HM) can be obtained in the same fibre. The major advantages of carbon fibres are tolerance to high temperatures and corrosive environments as well as lack of moisture sensitivity. The drawbacks are their relative cost, brittleness and conductivity. Due to all carbon fibre types having relatively low density and outstanding mechanical properties, the

applications of carbon fibres are commonly found in the structures where weight saving is the main purpose of design, such as high-performance submersibles, luxury yacht and space craft.

Aramids which have a relatively low density are other important fibres. The advantages of Aramid fibres are their toughness, damage tolerance and fatigue resistance. Compressive performance of Aramids is relatively poor as they show nonlinear ductile behavior at low strain values. Aramid reinforcement is significantly less common in composite applications than glass and carbon and more likely to be used in the applications where energy absorption is required such as aircraft, ballistic armour and safety belts in automobiles. It is also used in the outer skin of some sandwich structures in high performance boats or life boats.

Table 2. 2 Typical properties of different fibres (Smith, 1990)

Material	E-Glass	S2, R-Glass	HS Carbon (Thornel T-40)	HM Carbon (P-12S)	Aramid (Kevlar 49)
Specific gravity	2.55	2.50	1.74	2.18	1.45
Young's modulus (GPa)	72	88	297	826	124
Poisson's ratio	0.2	0.2	-	-	-
Tensile strength (MPa)	2.4	3.4	4.1	2.2	2.8
Failure strain (%)	3.0	3.5	1.4	0.3	2.5
Coeff. of expansion (axial) ($\times 10^{-6}/^{0}C$)	5.0	5.6	-	-	-2.0
Thermal conductivity (axial).($W/m^{0}C$)	1.05	-	-	-	0.04
Relative cost	1.0	8	50	2700	15

(c) Laminate Construction

A fibre-reinforced lamina consisting of many fibres embedded in a matrix material is a typical sheet for structural applications. The type of fibre-reinforced composite lamina can be continuous, e.g. unidirectional or woven, or discontinuous such as chopped strand mat. The unidirectional composite is one in which the majority of reinforcement fibres are oriented in one direction. Thus, unidirectional fibre-reinforced laminae exhibit the higher stiffness and strength in the fibre direction than the transverse direction.

The majority of 0/90° reinforcements are woven fibre materials. A simple woven reinforcement is produced by interlacing of the warp (0°) orientation and the weft (90°) direction. These weave types have good resistance to in-plane shear load and stability. They are generally used in larger vessel construction as they are available in fairly heavy weights, which enable rapid build-up of thickness.

The laminate forms are comprised of more than one unidirectional or woven lamina in different fibre angles. The major advantage of lamination is that it is relatively easy to tailor to efficiently meet design requirements of strength and stiffness of the structural element by varying constituent materials and orientation throughout the plies in a laminate. A potential weak area of laminates is the shear strength between layers of a laminate.

2.2 Marine Applications of Composites Materials

The first attempt to use fibre reinforced plastics to fabricate boat hulls was made by the US Navy between the Second World War and Vietnam War for small personnel boats by the US Navy (Graner, 1982). These earliest applications of composites by the US naval craft were summarized by Mouritz (2001). Other navies began to use

composites on their ships and submarines (Heller, 1967) (Henton, 1967) (Cheetham, 1986) (Lamiere, 1992). Subsequently, a rapid growth of Glass Reinforced Plastic (GRP) boat construction in a very wide range of boat hulls were reported between 1955 and 1980 as the results of their competitive cost, ease in fabricating complex shapes and repair, and low maintenance costs in vessels, such as dinghies, speedboats, sailboards, coastal yachts, lifeboat, pilot and passenger launches, and fishing boats (Cobb, 1968) (Wildman, 1971).

Figure 2.3 HMS Wilton (http://www.tca2000.co.uk)

FRP becomes uncompetitive with steel for construction of ships over about 40m in length because steel has a decisive advantage of the low cost of heavy welded steel construction, except where special requirements exist, such as a nonmagnetic hull is required or weight reduction is necessary for performance reasons (Nishii, 1983). Detailed studies have indicated that GRP cargo ships of up to 140 m might be economically viable (Wimmers, 1966) (Scott and Sommella, 1971).

The most significant naval applications of fibre reinforced plastics among others are in construction of Mine Countermeasure Vessels (MCMVs), which have traditionally been constructed in wood. Different types of MCMVs have been constructed since the UK Royal Navy successfully built a new class of MCMVs named HMS Wilton

using composites shown in Figure 2.3 (Chalmers et al., 1984). In this application, it is the non-magnetic property that is desirable so as not to risk detonating magnetically sensitive mines.

Sharpe (1999) presented survey results of vessel length built entirely of composite materials between 1945 and 2000, in which many of them are up to 50m in length shown in Figure 2.4. Probably the longest naval ship built from sandwich composite panels is the Visby corvette, which is 72m long and 10.4m wide. This ship is the first naval ship to utilize carbon-reinforced construction in sandwich laminates for almost the entire hull. Early design studies showed that thinner laminates would reduce labour costs and the hull weight savings would then allow further weight savings in engines and drivetrain for a given stiffness of carbon reinforced laminates.

Mouritz (2001) predicted that the length of composite ships may be constructed up to 120-160m long around the year of 2020 as fabrication technology develops. The hull structures most commonly are designed as framed single-skin GRP construction (Laros, 1984) (Brown, 1990), monocoque construction (Trimming, 1984) and GRP sandwich hull structures (Sjogron et al., 1984) (Gullberg, 1990).

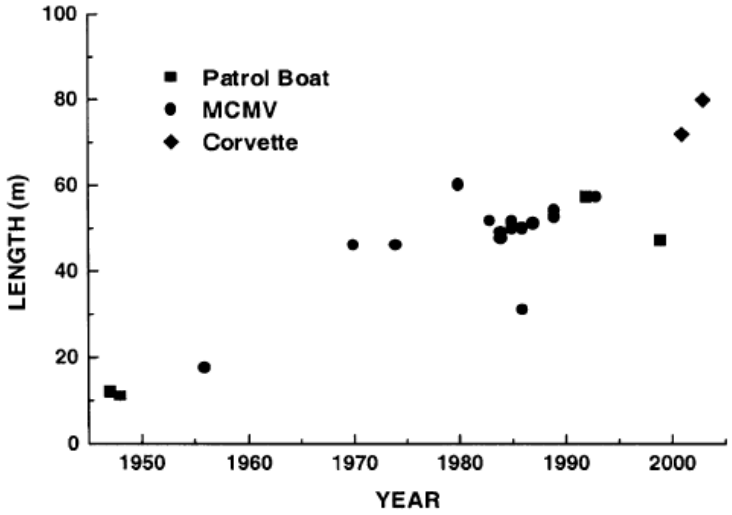

Figure 2.4 Plot of vessel length against year of construction for all-composite patrol boats, MCMV and corvettes (Sharpe, 1999)

Smith (1990) summarized current uses of composite materials in marine structures including small craft, fishing boat, naval vessels, high-performance craft, underwater vessels, submarine casings and appendages, superstructures, masts and funnels in ships and offshore platforms and so on. Mouritz et al. (2001) reviewed in detail other naval application of fibre-reinforced plastics including patrol boats, corvettes, topside structures, masts, propulsion systems, composite secondary structures, machinery, fittings and submarine structures. Marsh (2001) summarized advantage of composite drive shafts and applications for different types of vessels because of reduced weight, resisting to corrosion, absorbing vibration and resonance compared to steel shafts. Morisano (2003) described the techniques in the construction of human-powered submarines to achieve a strong and lightweight structure.

2.3 Available Structural Analysis Methods

2.3.1 Introduction

Three types of behaviour are usually considered in the analysis of a ship structural system: primary (hull girder), secondary (grillage and stiffened panel), and tertiary (unstiffened panel and local details). The primary behaviour is associated with the ship as a whole including the shell, principal decks, main transverse bulkheads and possibly superstructure depending on its effectiveness. The secondary behaviour is associated with grillages and stiffened panels between heavy longitudinal girders or transverse frames. The tertiary behaviour is associated with panels of plate bounded by stiffeners or elements of stiffeners themselves. The different structural types in a structural system have their own particular modes of failure. In this thesis, only secondary and tertiary behaviours will be considered.

2.3.2 Overview of Structural Theories

According to Reddy (2004), the mechanical response of laminated plate could be solved by Equivalent Single Layer theories (ESL), layerwise theories and

three-dimensional elasticity theory. By construction, when composite laminates have their planar dimensions one to two orders of magnitude larger than their thickness, the simplest ESL laminated plate theory can often provide a sufficiently accurate description of global response. ESL plate theories are derived in which the 3-D elasticity theory by making suitable assumptions concerting the kinematics of deformation or the stress state through the thickness of the laminate. These assumptions allow the reduction of a 3-D continuum problem to a 2-D problem. Two commonly used methods of ESL theories are the Classical Laminated Plate Theory (CLPT) and the First-order Shear Deformation Theory (FSDT).

The classical laminated plate theory (Reissner and Stavsky, 1961) is an extension of classical plate theory (Timoshenko and Woinowsky-Krieger, 1959) (Szilard, 1974) to laminated composite plates. It neglects the effects of transverse shear deformation. The displacement field is based on

$$\begin{aligned} u(x,y,z) &= u_0(x,y) - z\frac{\partial w_0}{\partial x} \\ v(x,y,z) &= v_0(x,y) - z\frac{\partial w_0}{\partial y} \\ w(x,y,z) &= w_0(x,y) \end{aligned} \tag{2.1}$$

where (u_0, v_0, w_0) are the displacements of a point on the plane z = 0.

The FSDT was extended to laminated composite plates by Yang et al. (1966) based on the Reissner-Mindlin hypothesis (Reissner, 1945) (Mindlin, 1951), which includes a gross transverse shear deformation in its kinematic assumption. The displacement field is based on

$$\begin{aligned} u(x,y,z) &= u_0(x,y) + z\phi_x(x,y) \\ v(x,y,z) &= v_0(x,y) + z\phi_y(x,y) \\ w(x,y,z) &= w_0(x,y) \end{aligned} \tag{2.2}$$

where $\phi_x = \frac{\partial u}{\partial z}$ and $\phi_y = \frac{\partial v}{\partial z}$ are the rotations of a transverse normal about the y-

and x-axis, respectively.

Second and third-order ESL laminated plate theories are called Higher-order Shear Deformation Theories (HSDTs) (Whitney and Sun, 1973) (Murthy, 1981) (Reddy, 1984, 1990) (Kant and Manjunatha, 1994) (Chen and Wu, 2005). HSDTs involve higher-order terms in the Taylor's expansions of the displacements. The displacement field based on the second-order theory is

$$\begin{aligned} u(x,y,z) &= u_0(x,y) + z\phi_x(x,y) + z^2\varphi_x(x,y) \\ v(x,y,z) &= v_0(x,y) + z\phi_y(x,y) + z^2\varphi_y(x,y) \\ w(x,y,z) &= w_0(x,y) \end{aligned} \tag{2.3}$$

The accuracy of CLPT is restricted to the plates with side-to-thickness ratio of the order of 20 or less. HSDTs can get an accurate prediction of interlaminar shear stresses relative to the CLPT and FSDT solutions but at the expense of increased computational effort. In addition, the higher-order theories introduce additional unknowns that are often difficult to interpret in physical terms. Of the ESL theories, the FSDT with transverse extensibility appears to provide the best compromise for solution accuracy, inherent simplicity and low computational cost (Reddy, 2004). However, the accuracy of the global response predicted by the ESL models decreases as the laminate becomes thicker. Furthermore, when accurate stresses are desired around the regions where the geometric and material discontinuities or intense loading so require, the 3-D theories or Layerwise theories provide the most accurate solutions (Mau, 1973)(Ren, 1986)(Lee et al., 1990)(Xavier et al., 1995).

2.3.3 Analysis of Unstiffened Plates

Analytical solutions of rectangular laminates with various boundary conditions were developed based on the classical laminate plate theory and first order deformation theory, such as the Navier solutions, Levy solutions (Reddy et al, 1987)(Khdeir, 1989)(Khdeir and Reddy, 1991). However, analytical methods to date are limited to specific shapes of plates with a limited set of boundary conditions. For more general

structures with arbitrary geometries and boundary conditions, numerical methods are the most effective means.

Reddy and Pandey (1987) developed a finite element computational procedure for the first-ply failure analysis for laminated composite plates subjected to in plane and/or transverse loads based on first order shear deformation theory. Reddy and Reddy (1992) performed first-ply failure analysis of composite laminated subjected to in-plane and transverse loads using linear and non-linear finite element method. Kam and Sher (1995) presented a finite element method to study the nonlinear behaviour of composite laminates. The accuracy of the finite element results were verified by experimental results. Appropriate failure criteria for composite laminates were suggested.

As can be seen from above literature review, the previous strength assessment of composite structures was mainly concentrated on the first-ply failure of laminated composite plates. However, it is well known that composite plate can sustain considerable loading after the first failure occurrence. Therefore, the ability to predict the ultimate failure is essential for predicting the performance of composite structures and developing reliable, safe designs which exploit the advantages offered by composite materials. Progressive failure analysis of laminated plates has been investigated by many researchers.

The first effort was made by (Petit and Waddoups, 1969), who used gradual unloading model to simulate the property degradation of composite laminates subjected to axial compression. A summary of the past work in progressive failure studies for different type of structures and the loading condition was presented by (Ambur et al., 2001). The summary indicates that the nonlinear geometric effects were not considered initially (Chang and Chang, 1987) (Ochoa and Engbom, 1987).

Englestad et al. (1992) considered both nonlinear geometric effects and postbuckling problem with progressive failure analysis. Subsequently, a number of researches were performed using various different finite element formulations and failure

criteria at different load levels (Shahid and Chang, 1995) (Sleight et al., 1997) (Padhi et al., 1998) (Singh and Kumar, 1998) (Baranski and Biggers, 1999) (Knight et al., 2000).

More recently, Ganesan and Zhang (2004) developed a finite element formulation using the first-order shear deformation theory and the von Karman geometric non-linearity hypothesis to study the progressive failure of laminates under the action of bi-axial compression combined with in-plane negative shear loading. The first-ply failure and the ultimate failure loads and influences of different parameters on the buckling were determined.

Travis et al. (2004) presented a methodology for predicting the response of composite laminates based on the three-dimensional laminated analysis coupled with a progressive failure methodology. The through-the-thickness effects in laminate response were captured as interlaminar load which is particularly important for thick laminated plates.

Chen and Soares (2007) developed a nonlinear finite element analysis with a new explicit through-thickness integration scheme based on a progressive stiffness degradation model.

The progressive failure and ultimate collapse of laminated composite plates subjected to out-of-plane load were also investigated by researchers. Reddy and Reddy (1993) presented a nonlinear finite element progressive failure algorithm. The geometric nonlinearity is taken into account in the von Karman sense, and the stiffness reduction is carried out at the reduced integration Gauss points of the finite element mesh depending on the mode of failure.

2.3.4 Analysis of Stiffened Plates

The solution methods of stiffened composite panels are generally grouped into three categories:

- Engineering methods
- Analytical or semi-analytical methods
- Numerical methods

Different methods for the analysis of stiffened panels based on these three categories are presented as follows

(a) Engineering Methods

Such analysis is carried out by means of simple formulae based on beam and plate theory for initial design purpose such as Euler formula or linear stability analysis for locally buckled panel. This kind method is simple and effective, but needs experience. Up to now much attention has been paid to it but further attempts are needed to improve the procedure.

(b) Analytical or Semi-analytical Methods

- **Folded-plate method**

The folded-plate analysis is represented by an array of parallel beams and interconnected flat rectangular orthotropic plates. The beams of the structure are assumed to behave according to simple beam theory and the plate elements are assumed to be governed by its plane stress equation. Continuity conditions between plates and beams along the interconnecting boundaries can then be defined.

Folded-plate analysis was originally developed for the analysis of isotropic thin-walled prismatic structures (Goldberg and Leve, 1957). This method has also proved useful in the analysis of steel stiffened panels under lateral load and combined lateral and in-plane loads (Smith, 1966, 1968). Extensive work has been carried out in the development of the GRP ship designs by (Smith and Dow, 1985,

1987).

Buckling and vibration problems have been investigated by (Wittrick and Williams, 1968 and 1974) and (Viswanathan et al., 1973). The method has been also applied to cellular structures (Meyer and Scordelis, 1971) (Al-Rifaie and Evans, 1979) (Evans, 1984).

Marsh and Taylor (1990) developed a computer program, incorporating a classical folded plate analysis of an assemblage of orthotropic or isotropic plates to analyse box girders bridges.

Structures which can be treated in this way are normally limited to panels stiffened in a single direction with simply-supported at the extreme ends. Orthogonally stiffened structures may be treated by smearing out the transverse stiffeners as equivalent orthotropic plates together with the plating. The folded plate method can give a complete and accurate solution in less computer time than that needed for the finite element method. However, it is evident that this method is still complicated and time-consuming.

- **Orthotropic Plate Theory Method**

The use of the orthotropic plate theory in solving problems of stiffened plates has been very popular in various applications. The basic idea of this approximation is to convert the stiffened plate into an equivalent plate with constant thickness by smearing out the stiffeners. A cross-stiffened panel may be idealized as an orthotropic plate when stiffeners are relatively numerous and small so as to deflect together with the plating. In addition, it has been said that the application of orthotropic plate theory to cross-stiffened panels should be restricted to stiffened plates with more than three stiffeners in each direction and stiffeners in each direction should be similar (Smith, 1966) (Mansour, 1977).

Cheung et al. (1982) used the orthotropic plate method to calculate the longitudinal moments and transverse shear of multi-spine box-girder bridges. It was concluded that the orthotropic plate method gives accurate results when the number of spines is not less than three. Smith (1990) represented the overall grillage buckling of an orthogonally stiffened panel built of composite material as an equivalent orthotropic plate. The effects of stiffeners were added into flexural rigidities of base plate. Kristek et al. (1990) proposed a method for shear lag analysis of steel and composite box girders of various cross-sectional types using harmonic analysis. The accuracy of the method was illustrated by comparison with results obtained from other sources. Later Evans et al. (1993) extended the harmonic method to consider girders in more general and complex multicellular, composite cross sections. The accuracy of the method was validated by a finite element analysis and a series of experiments. Hosseini et al. (2005) proposed an approximate method to obtain the buckling load for the beaded panels to avoid several time consuming finite element buckling analyses in preliminary design stage of structures.

The validity of representing the stiffened panel by an equivalent orthotropic plate depends to a great extent on the number of stiffeners in each direction, their spacing and how identical they are as far as their stiffness characteristics are concerned. Furthermore, this approach ignores the discrete nature of the structures and does not consider all potential buckling modes.

- **Grillage Analogy Method**

Grillage is the term given to a structure of intersecting beams which is particularly common in ship structures typically in hull constructions. This form of flat grillages is particularly used in the decks, bottoms and bulkhead of ships. Grillage analysis was developed for steel by Vedeler (1945). In a grillage analysis, the structure is idealized as a number of longitudinal and transverse beam elements in a single horizontal plane, rigidly interconnected at nodes. Displacement method, forced method and energy method were used by Clarkson (1965) to find the mechanical response of the grillage.

Cheung et al. (1982) applied grillage analysis based on displacement method in multi-spine box-girder bridges to calculate the longitudinal moments and transverse shear. Finite strip method was used to validate the grillage analogy method. Evans and Shanmugam (1984) used this simplified method to predict the linear and nonlinear behaviour of multi-cellular structures. The effect of shear lag was taken into account by using empirical coefficients. Design curves were presented to account for the reduction in shear and torsional stiffness due to the presence of web openings. Jang et al. (1996) adopted grillage analysis method to consider the interaction effect of longitudinal girders and transverse web frames for optimum design of stiffened plates and complex structures. More recently, a modified grillage method was used by Maneepan et al. (2007) for multi-objective optimization of orthogonally tophat-stiffened composite laminated plates.

The validity of representing the stiffened panel by a grillage becomes particularly critical when the flexural rigidities of the stiffeners are small in comparison with the plate stiffness. The model, however, allows for discontinuities such as hatch openings or different stiffener sizes and spacing within each set of parallel stiffeners.

- **Beam-Column Analysis**

In this method a single beam of the gross panel consisting of a single stiffener and the effective breadth of plating is analyzed. The torsional rigidity of the gross panel, the effect of Poisson's ratio and the intersecting beams are all neglected in this type of analysis. This method is popular among designers because it is relatively simple and less time consuming. The degree of accuracy, however, becomes critical particularly when the plate stiffness is relatively large compared to the stiffener's rigidity.

(c) Numerical Methods

Numerical methods including Finite Difference Method (FDM), Finite Strip Method (FSM) and Finite Element Method (FEM) are the most effective means to get

accurate solutions for stiffened plate problems. In finite difference method, a numerical solution to the differential equation for displacement or stress resultant is obtained for chosen points on the structure. At present, common applications of the finite difference method are in computational science and engineering disciplines, such as thermal engineering and fluid mechanics, etc and less in structural analysis.

A semi-analytic finite difference method developed by Mukhopadhyay (1989a, 1989b) has been extended to the vibration and stability analysis of stiffened plates with different boundary conditions, mass and stiffness properties, and varying number of stiffeners.

A numerical approximation technique FSM is commonly used for the analysis of plate and shell structures. FSM can be considered as a kind of finite element method in which a special element called strip is used. Cheung (1976) may be considered as the pioneer who first presented the concept of finite strip method among others. Subsequent to Cheung, other researchers developed different variations of the method and applied them to different problems over the years. Graves-Smith and Sidharan (1978) proposed the first FSM buckling formulations for isotropic plate structures under edge loading. Yoda and Atluri (1992) investigated the postbuckling of a flat stiffened fibre-reinforced laminated composite plate under compression based on modified higher order shear deformation theory. The finite strip formulation was validated with some typical experimental results. Loughlan et al. (1993, 1996) studied the buckling characteristics of composite stiffened plates under in-plane shear load and some carbon fibre composite stiffened box sections subjected to compressive and bending loading actions. Dawe and Peshkam (1996) re-examined the buckling characteristics of two blade-stiffened panels under combined compressive and shear loads by implementing strips of higher orders so-called superstrips. This is initially analyzed by Stroud et al. (1984) using a finite element method. Ovesy and Assaee (2001, 2003) used the finite strip method to investigate the buckling load capacity of composite stiffened panels subjected to in-plane compression and shear loading. The different lay-up configuration and shapes of stiffeners were studied to consider their effect on the buckling. Yuan and Dawe

(2004) described the development of a B-spline finite strip method for predicting the natural frequencies of vibration and the buckling stresses of rectangular sandwich panels. Razzaq and EI-Zafrany (2005) developed a programming package based on applying a new concept to the finite strip method. Mindlin's plate-bending theory was employed for the derivation of an efficient element for buckling and stress analysis of folded and stiffened plates made of composite layered materials. Zahari and EI-Zafrany (2009) developed a finite strip method for non-linear static analysis based on the tangential stiffness matrix using the new concept of polynomial finite strip elements. A progressive failure algorithm was developed and the accuracy of the method was confirmed through various test cases.

FEM is the most powerful solution tool since computers were used. A significant amount of researches have been devoted to the analysis of buckling and post-buckling strength of stiffened composite panel. Smith and Dow (1985, 1987) investigated the initial compressive buckling and post-buckling behaviour of GRP panels reinforced by longitudinal hat-section stiffeners using non-linear finite analysis together with folded-plate analysis. Compression test on two large-scale longitudinal GRP stiffened panels were carried out.

Fan et al. (1992) studied the buckling, postbuckling failure behaviour of two series of stiffened panels: beam-stiffened panels and blade-stiffened panels under axial compression. The comparison of the computational results with typical tests from CAE, NLR and NASA was presented.

Engelstad et al. (1992) presented the progressive failure analysis to study the postbuckling response and failure modes of various graphite-epoxy panels loaded in axial compression. A progressive damage failure mechanism was applied in the nonlinear analysis. Analytical prediction for the failure mode and location were agreed well with those obtained by Starnes et al. (1981). Subsequently, a number of researchers have extensively investigated and developed the progressive failure analysis with use of various finite element formulations and failure criteria.

Kim et al. (1995) performed an analytical and experimental study of the postbuckling behaviour of stiffened composite cylindrical panels. Progressive failure analysis was implemented for the prediction of failure characteristics and postbuckling ultimate load based on the maximum stress criterion. Kong et al. (1998) investigated the postbuckling behaviour of the laminated stiffened panel by finite element method and experimental study. The maximum stress criterion and the complete unloading failure model were adopted in the progressive failure analysis. Chen et al. (2007) developed a finite element analysis with a new explicit through-thickness integration scheme to predict the postbuckling compressive strength of laminated composite plates and stiffened panels under axial compression. A progressive stiffness degradation model was used and the Tsai-Wu criterion was adopted to predict the failure mechanisms. Orifici et al. (2008) developed a methodology for analyzing collapse in composite structures involving predicting the initiation of interlaminar damage in the skin-stiffener interface.

2.4 The Sources of Variabilities in Composite Material Manufacture

There is a wide range of potential production defects in the manufacture of composite structures. These production defects may arise in the basic lamination processes as well as in the processes involved in assembly and fabrication, and thus introduce uncertainties that are difficult to reduce or eliminate. It is important to know about production defects because these may influence unfavourably the structural performance, particularly important for composite structures since they have so many possible types of defects and failure mechanisms that may be triggered by them. It is also important to better understand the effect of the production defects on strength of composite structures so that reliability can be achieved without having to apply excessively large factors of safety. A brief overview of production defects for single-skin laminates and face laminates of sandwich structures and their causes and effects are given as follows. More detail discussion on manufacturing defects can be found in (Äström, 1997).

(a) Delaminations

Delamination is a common form of damage that may occur during the manufacturing process of laminated composites as well as under load in service. It can cause degradation of the performance of structural components because they allow out of plane displacement of plies to occur more easily. During the manufacturing process, this type of defect is produced mainly by contaminated reinforcing fibres or by shrinkage which occurs during the curing phase of the resin and the resulting exotherm. Because of the presence of the delaminations, once buckling occurs the delamination might extend and the compressive strength of the structures can be further reduced.

The early work was performed by Chai et al.(1981), who characterized the delamination buckling models by the thickness and number of delaminations relative to the total plate thickness. Many researchers have studied the effect of delamination on the load-carrying capacity of the composite structures experimentally, analytically using finite element method over the past two decades. (Klug et al., 1996) (Short et al., 2002) (Tafreshi and Oswald, 2003) (Wang et al., 2005) (Cappello and Tumino, 2006) (Züleyha and Mustafa, 2009).

(b) Fibre reinforcement defects

The laminate defects from the reinforcement materials may be raised in following situations:

- The actual fibre orientation does not correspond to the intended orientation. The structural capability of a composite may significantly decrease since even a small misalignment.
- The reinforcement fibres are damaged, which are generally led by incorrect stacking and storage.
- Fibre waviness.

- Variation in fibre content within a component or between components may also affect the mechanical properties of the laminate.
- Inaccurately cut and tailored.

(c) Poor curing of resin

The defects of resin possibly are caused by insufficient of additives with the resin, unsuitable environmental conditions during the production stage or the presence of incompatible ingredients in the resin.

- **Voids**

All composites contain microscopic voids, which may be due to air entrapped in tightly compressed fibre yarns, volatiles from the resin, air in the resin and incomplete consolidation. The presence of voids may cause stress concentrations which can act as crack initiators. Therefore, they are typically limited in the range 1-5 volume present (Shenoi and Wellicome, 1993).

- **Dry spots**

Dry spots are large sections of the insufficiently impregnated reinforcement. It may result from too high injection rate, merging flow fronts entrapping air, too high resin viscosity, premature resin gelation, etc. The influence of dry zones on compressive strength of sandwich face laminates has been investigated both numerically and experimentally by Johansson (2005). The test results showed that the reduction of the compressive strength is up to 60%. This demonstrates that dry spots should be avoided in production processes.

- **Wrinkles**

Wrinkles are a type of production defect that may arise in single-skin laminates and

in face laminates of sandwich composites. A wrinkle is caused by a slight excess of reinforcement in one or more of the plies in relation to the surface area available.

- **Geometric defects**

Component warpage and angles or deviation in component thicknesses from design all belong to geometric defects. They may arise from the layup accidentally being unbalanced or spatial differences in temporary history during consolidation and crosslinking, which result in residual stresses. These undesirable stresses may reduce the load-carrying capacity of the component or may lead to failure. The imperfection problem can never be totally eliminated. However, it is possible to take them into account in design.

- **Cosmetic defects**

The most common cosmetic defects are poor surface finish and discoloration. These defects affect the appearance of the product but have little or no direct effects on the structural performance. Discoloration generally is a result of incompletely dispersed pigments, contaminants or too high a processing temperature.

The mechanical properties of the laminates are strongly dependent on the manufacturing processes in which material defects may be introduced as summarized above. It is impossible to eliminate manufacturing defects altogether, there is consequently a need for the analysis and design methodologies which must take into account the potential variation.

2.5 Reliability Assessment of Composite Components

Conventional failure analyses of composite structures have been based on deterministic approaches, in which the uncertainties are dealt with through

conservative fixed values in equations to guard against the possibility of structural damage. The assumptions are made that all factors influencing the load, strength and others are known. However, composite materials inherently possess a high variability in material properties, geometric properties as well as the effects of the production processes. Because of the existence of such uncertainties, probabilistic failure analysis approaches should be considered in order to design composite structures more effectively. Various probabilistic models describing the strength of composite materials have been studied by researchers.

Fibre composite materials used to fabricate many components are generally brittle in nature. The failure of brittle materials can be described by theories based on the weakest link theory developed by Weibull (1939). Subsequently, a series of studies have been developed by (Daniels, 1945) (Rosen, 1964) (Zweben and Rosen, 1970) (Harlow and Phoenix, 1981, 1982).

Cassenti (1984) developed a theory to predict the probability of failure for a unidirectional composite including the effects of loading history and the location of the failure. This theory based on the Weibull weakest link hypothesis and a good correlation with the limited experimental data was found. Sutherland and Soares (1997) reviewed the probabilistic models of the strength of composite materials and discussed the way in which these models may be used to analyze experimental results. Soares (1997) presented an overview of the different probabilistic approaches that have been used to assess the strength and reliability of laminated components under plane stress conditions.

A lot of investigations are available in the literatures on the static strength reliability assessment methods for composites using the first-ply failure assumption. That means that an entire laminate is assumed to fail if any of plies in the laminate fails. Cederbaum et al. (1990) used the analytical method to derive the reliability of laminates plates subjected to in-plane random static loads. The Hasofer-Lind method was applied and the reliability indices were obtained by considering the various failure modes. However, the stress analysis was based on a linear elastic approach.

Miki et al. (1990) evaluated the first-ply failure reliability of unidirectional fibrous composites using an advanced second-moment method under plane stress condition. The safety margin was defined based on the Tsai-Wu failure criterion and the effects of various factors on the reliability were investigated. Kam et al. (1993) presented a procedure for the reliability assessment of laminated composite plates subjected to large deflections under random static loads. A nonlinear structural analysis technique based on a corotational total Lagrangian finite element formulation was proposed. Reliability analysis was performed by limit state surfaces, which was obtained by performing a series of first ply failure analyses following different load paths in load space.

Kam and Chang (1997) presented a reliability formulation for laminated composite plates on the basis of first-ply failure. The limit state equation was established using an appropriate phenomenological failure criterion and different numerical techniques were used to evaluate the reliability. The feasibility and accuracy of the proposed methods in reliability assessment was verified by experimental investigations.

Lin et al. (1998) presented a procedure for failure probability evaluation of composite laminates subjected to in-plane loads. The stochastic finite element method was used to determine the failure probability of first-ply failure loads and buckling strengths of the laminates. The feasibility and accuracy of the proposed method were validated by the results obtained using the Monte Carlo method.

Jeong and Shenoi (1998) presented a direct simulation method to perform the reliability analysis of mid-plane symmetric laminated plates using different failure criteria on laminate level. Probability of failure was estimated with respect to each ply in the plates and the effects of mean value and variation on probability failure were also investigated. Jeong and Shenoi (2000) extended the previous work and developed a probabilistic strength analysis procedure of anti-symmetric cross-ply and angle-ply laminated plates by applying the Monte Carlo simulation. Different limit state equations were derived from non-linear analysis with various failure criteria.

Onkar et al. (2007) presented a stochastic finite element approach to study the first-ply failure load statistics of composite laminates under transverse loading. A stochastic finite element formulation was developed using layer-wise plate model and Tsai-Wu and Hoffman criteria were used to predict the first-ply failure load.

It is well known that laminated composite plates can sustain a higher load after the first-ply failure. However, most of these studies mentioned above were based on first-ply failure. Very few research works are available on the reliability assessment of the postbuckling compressive strength of laminated composite plates and stiffened panels.

Chen and Soares (2007) presented reliability assessment of the postbuckling compressive strength of laminated composite plates and stiffened panels under axial compression. A progressive failure analysis was used to predict the postbuckling compressive strength. An improved first-order reliability algorithm coupled with the finite element analysis was proposed for reliability assessment. The capabilities of the developed method were demonstrated by two numerical examples.

Other studies for the reliability of composite laminates have also been proposed by researchers using the different reliability methods and strength theories. Engelstad and Reddy (1993) developed a probabilistic finite element analysis procedure for laminated composite shells using a degenerated three-dimensional laminated composite shell element. Reliability analysis was performed by using the first-order reliability method combined with sensitivity derivatives from the finite element analysis.

Gurvich and Pipes (1995) used a multi-step failure probabilistic model to analyze the random strength response of composites. A numerical algorithm based on Monte Carlo simulation was developed and experimental confirmation was considered through an example of uni-axial bending of laminated composite. Ibnabdeljalil and Curtin (1997) studied the statistical nature of composite failure under local load sharing conditions in which the stress is transferred predominantly from broken

fibres to the nearby unbroken fibres. A 3-D lattice Green's function model was used to calculate the stress field and weakest link statistics were used to investigate reliability and size effects of composite. Lin (2000) performed reliability analysis of laminated composite plates subjected to transverse loads using Monte Carlo simulation, β method and first-order second moment methods. Four different failure criteria were used to construct the limit state equation in the probabilistic failure analyses. The accuracy and feasibility of the different methods in predicting reliability of laminated composite plates were verified using experimental data. Frangopol and Recek (2003) investigated the probability of failure on fibre-reinforced composite material with unidirectional fibres under random loads. The laminate plate was considered as a series system of different layers. The Tsai-Wu failure criterion was used in conjunction with Monte Carlo simulation.

2.6 Failure Criteria

A failure theory is required to assess whether the composite ply has failed or not under an applied stress system. A laminated composite may fail by fibre breakage, matrix cracking, or by delamination of layers depending upon the loading, stacking sequence and specimen geometry. Various failure criteria have been proposed in the literatures. In general, failure criteria for composite materials can be categorized into two groups: independent (non-interactive) failure criteria and interactive failure criteria. The former is simple to apply, but it neglects the effect of stress interactions in the failure mechanism. The latter includes stress interactions, but it does not give the mode of failure.

(a) Non-interactive Failure Criteria

A non-interactive failure criterion is defined by a comparison between the individual stress or strain components and the corresponding material allowable values separately. These criteria ignore the complexities of composite failure mechanisms

and the associated interactive nature of the various components. The maximum stress and maximum strain criteria belong to this group.

- **Maximum Stress Criterion**

Failure is assumed to occur if any stress value in the material axis directions exceeds their respective ultimate strength (Tsai, 1984)

$$\sigma_1 \geq X_t \quad \text{or} \quad |\sigma_1| \geq X_c$$

$$\sigma_2 \geq Y_t \quad \text{or} \quad |\sigma_2| \geq Y_c$$

$$\sigma_3 \geq Z_t \quad \text{or} \quad |\sigma_3| \geq Z_c$$

$$\sigma_4 \geq R \quad \sigma_5 \geq S \quad \sigma_6 \geq T \tag{2.4}$$

where $\sigma_1, \sigma_2, \sigma_3$ are the normal stress components in the *x*, *y*, *z* directions respectively; $\sigma_4, \sigma_5, \sigma_6$ are the shear stress components in the *yz* , *xz* and *xy* planes; X_t, Y_t, Z_t and X_c, Y_c , Z_c are the material allowable tensile and compressive strengths in the *x* , *y* , *z* directions respectively; *R*, *S*, *T* are the material allowable shear strengths in the *yz* , *xz* and *xy* planes, respectively.

- **Maximum Strain Criterion**

This is similar to the maximum stress theory except that strains are considered instead of stresses. Failure is assumed to occur if any of the following conditions are satisfied (Tsai, 1984)

$$\varepsilon_1 \geq \varepsilon_{xt} \quad \text{or} \quad |\varepsilon_1| \geq \varepsilon_{xc}$$

$$\varepsilon_2 \geq \varepsilon_{yt} \quad \text{or} \quad |\varepsilon_2| \geq \varepsilon_{yc}$$

$$\varepsilon_3 \geq \varepsilon_{zt} \quad \text{or} \quad |\varepsilon_3| \geq \varepsilon_{zc}$$

$$\varepsilon_4 \geq R_\varepsilon \quad \varepsilon_5 \geq S_\varepsilon \quad \varepsilon_6 \geq T_\varepsilon \tag{2.5}$$

where $\varepsilon_1, \varepsilon_2, \varepsilon_3$ are the normal tensile strains in the *x*, *y*, *z* directions respectively; ε_4 , ε_5 , ε_6 are the shear strains in the *yz*, *xz*, *xy* planes respectively; $\varepsilon_{xt}, \varepsilon_{xc}, \varepsilon_{yt}, \varepsilon_{yc}, \varepsilon_{zt}, \varepsilon_{zc}$ are the material allowable tensile and compressive strains in the *x* ,*y* , *z* directions respectively; $R_\varepsilon, S_\varepsilon$ T_ε are the material allowable shear strain strengths in the *yz, xz* and *xy* planes, respectively.

(b) Interactive Failure Criteria

Interactive failure criteria predict the failure load by using a single quadratic or higher order polynomial equation involving interactions between stress or strain components. Most of the interactive failure criteria are polynomial based on curve-fitting data from material test. The mode of failure is determined indirectly by comparing the stress or strength ratios. Interactive failure criteria can fall into three categories:

- **Polynomial Theories**

The polynomial theories use a polynomial based upon the material strengths to describe a failure surface. Tsai-Wu criterion (Tsai and Wu, 1971), Tsai-Hill criterion (Tsai, 1968 and Hill, 1950), Azzi and Tsai criterion (Azzi and Tsai, 1965), Hoffman criterion (Hoffman, 1967), Cowin criterion (Rowlands, 1985) and Chamis criterion (Chamis, 1969) are popular failure criteria. These failure criteria can be represented in terms of general polynomial as follows

$$F_i\sigma_i + F_{ij}\sigma_i\sigma_j + F_{ijk}\sigma_i\sigma_j\sigma_k \geq 1 \quad i, j, k = 1,....6 \tag{2.6}$$

where F_i, F_{ij} and F_{ijk}, are components of the lamina strength tensors in the principal material axes and they are different in the different criteria. σ_i is the component of the stress in the principal material axes.

- **Direct-Mode Determining Theories**

The direct-mode determining theories are usually polynomial equations based on the material strengths but a separate equation is used to describe each mode of failure. Hashin (1980) stated a quadratic failure criterion in piecewise form based on material strengths, where each smooth branch represents a failure mode. In unidirectional composites, there are two primary failure modes: in the fibre mode, the lamina fails due to fibre breakage in tension or fibre buckling in compression; in the matrix mode, failure is due to matrix cracking. Lee (1982) proposed a direct-mode determining failure criterion. This criterion was a polynomial equation for each mode of failure based upon the three-dimensional stress calculations. The modes of failure included fibre failures, matrix failures and delaminations. Christensen (1988) introduced a quasi-three-dimensional laminate theory which accounted for out-of-plane stress terms. Then a strain-based failure criterion was developed to distinguish between fibre failure and fibre-matrix interaction failure.

- **Strain Energy Theories**

Abu-Farsakh and Abdel-Jawad (1994) introduced a failure criterion based on an strain energy concept to predict failure of fibrous composite materials subject to uniaxial, biaxial or multiaxial stress. The total strain energy is composed of the elastic strain energy and the plastic strain energy. Wolfe and Butalia (1998) introduced a non-linear strain energy failure criterion based on the concept that the lamina fails when the sum of the ratios of energy levels to the corresponding maximum energies equals unity. This failure model was verified by Tarunjit et al. (2002) through comparing the numerical predictions obtained from that model with published experimental data (Soden et al., 2002).

Chapter 3: Methodology for Assessing Structural Reliability

3.1 Introduction

In structural engineering, nearly all structures and their environments are not deterministic, but rather they have probability distributions that reflect the nature of uncertainty to various degrees. These variables can be treated as deterministic values chiefly due to either the uncertainties of random variables may be negligible in certain circumstances, or lack of knowledge of the estimation of complete probability distributions of uncertainties. Even for uncertainties that can be mathematically modelled, the computational techniques may be difficult to cope with. Early design codes on deterministic analysis deal with the uncertainties by using so-called safety factors. However, with the development of reliability theory, the analysis involving random parameters has made the design codes more rational. The objective of this chapter is to provide an introduction and summary of the state-of-the art in structural reliability theory.

3.2 The Basic Reliability Problem

Structural reliability theory is concerned with the rational statistical treatment of uncertainties involved in structural engineering for assessing the safety and serviceability of structures. The basic structural reliability problem considers expressions linking the load effect on the structure S and the resistance or strength of the structure R. Then the failure event can be defined in the following ways

$$g(R, S) = R-S \tag{3.1}$$

where the limit state equation g(R,S) is defined as the boundary between the safe and unsafe domain with g(R,S) = 0 being the limit state surface, g(R,S) > 0 being in the safe domain and g(R,S) < 0 being in the failure domain.

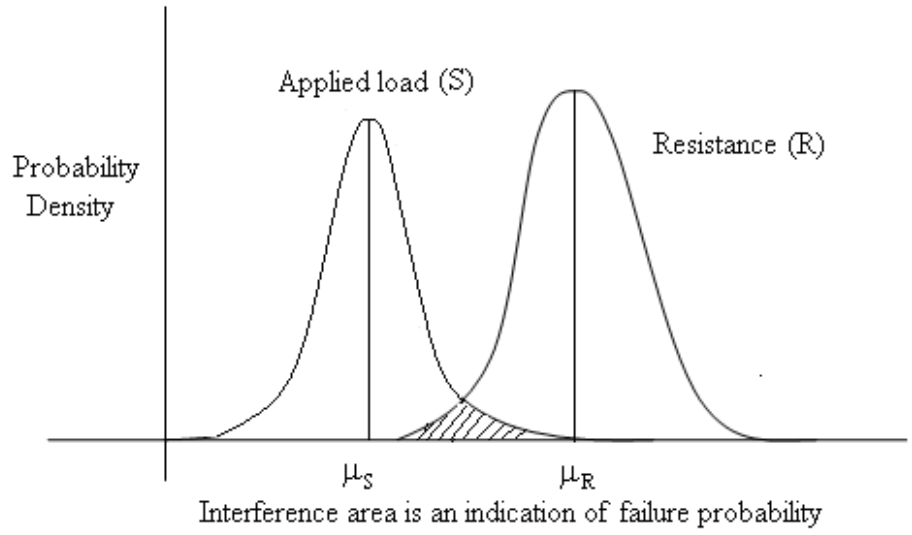

Figure 3.1 Probability density function of the applied load (S) and resistance (R)

Figure 3.1 illustrates the probability of failure defined in the small region of overlap between the two probability distributions of load and resistance. The failure probability is defined as

$$P_f = P[g(R,S) \le 0] = \iint_{g(R,S)\le 0} f_{RS}(r,s)drds \tag{3.2}$$

where $f_{RS}(r,s)$ is the joint density function of R and S

3.3 Levels of Reliability Based Design

The reliability based design code and design practice are currently categorized under

four different levels that depend on the available input information and the application of the probabilistic design approach adapted in design procedure as follows (Madsen et al., 1986).

(1) Level I : Partial Safety Factor Method

Level I procedure is based on the partial safety factor concept. The uncertainties of parameters are modelled by their characteristic values for each design variable. Safety factors traditionally are adopted on the basis of intuition and experience (Pugsley et al.1955). However, the partial factors of the level I may be measured by probability methods, which ensure that the resulting design will have a specified reliability level.

(2) Level II : Semi-Probabilistic Approach

In this level, a semi-probabilistic approach is introduced. Originally, first order second moment analysis was used to assess the safety of the structures. Later a more consistent invariant method such as first order reliability method and second order reliability method were developed. Because of the approximations to the failure surface and the distribution information of random variables, Level II approach is not exact but very efficient.

(3) Level III : Fully Probabilistic Approach

The basic concept of Level III reliability method is that a probability of failure of a structure can be estimated by the integration of the joint probability distributions of the design variables involved in the load and strength of the structure defining the failure domain. The failure probability is estimated as the measure of reliability. However, it is difficult to determine the joint probability density function of the variables in the applications of actual structures.

(4) Level IV : Decision Methods

In this method, probability of failure plus economical optimization, such as minimum cost or maximum benefit are considered. This type of analysis can generally be reserved for the use in those projects whose failure has weighty consequences such as significant economic loss or fatalities.

There are two main reasons for Level III reliability analysis which can be very difficult to apply in practice, e.g. the lack of information to determine the joint probability density function of the design variables and the evaluation of the resulting multiple integrals. Therefore, Level II was developed for the reliability of engineering structures.

3.4 First Order Reliability Methods

The First-Order Second-Moment method (FOSM), which is based on the Taylor expansion of the limit state function, was first developed (Cornell, 1969). In this method, only first two moments of the limit state functions are taken into account i.e. by its mean and covariance. The reliability index is defined as

$$\beta = \frac{\mu_g}{\sigma_g} \tag{3.3}$$

in which μ_g and σ_g represent the mean value and standard deviation of the g-function, respectively.

For the simplest case of two independent normally distributed random variables, the structural reliability can be given by

$$\beta = \frac{\mu_R - \mu_S}{\sqrt{(\sigma_R^2 + \sigma_S^2)}} \tag{3.4}$$

$$P_f = \Phi^{-1}(-\beta) \tag{3.5}$$

where Φ is the standard normal cumulative distribution function; $\Phi^{-1}()$ is the inverse of the standard normal cumulative distribution function.

The first-order second-moment method only deals with the problem of variables being statistically independent normal or lognormal distributions. The performance function is a simple additive or multiplicative function of these variables. In addition, the reliability index defined by Cornell in Eq.(3.4) is not invariant with respect to the choice of failure function (Ditlevsen,1973).

An advanced first-order second-moment method commonly termed as First Order Reliability Method (FORM) was proposed in order to improve the accuracy (Hasofer and Lind, 1974) (Rackwitz and Fiessler, 1978). In this method, Taylor expansion of the limit state function is performed at the so-called design point on the failure surface. The first order reliability method solved the invariance problem and extended the concept of reliability index to arbitrary distribution of random variables. Therefore this method is considered to be the foundation of probabilistic design theory.

In a broad sense, the reliability of an engineering structure may be defined as the probability of performing its intended function or mission in a given period of time. The performance function is generally defined as follows

$$g(x) = g(x_1, x_2, ..., x_n) \tag{3.6}$$

where $x = \{x_1, x_2, ..., x_n\}$ is a vector of the random variables involved in the structural system. Further, the state of the structural system can be defined such that

$$\begin{aligned} g(x) > 0 &\quad \text{represents a safe state} \\ g(x) = 0 &\quad \text{represents the limit state surface} \\ g(x) < 0 &\quad \text{represents a failure state} \end{aligned} \tag{3.7}$$

Let $f_x(x)$ denotes the joint probability density function for the n-dimensional vector X of basic variables. The probability of failure can be expressed as the volume integral of $f_x(x)$ over the failure region as follows

$$P_f = \int_{g(x)\leq 0} f_x(x)dx \tag{3.8}$$

Due to the complexity of the joint probability density function and the failure domain, except for some special cases, the above integral cannot be performed analytically for most of the practical cases. Therefore, approximate methods have been developed to compute this probability integral.

Generally, reliability methods involve a transformation of random variables *x* in physical space into standard normal variables *u* with a zero mean and unit variance as a first step of the reliability analysis due to these methods take advantage of the special properties of the standard normal space. If all the random variables X_i are normally distributed, then the normalised variables *u* can be written as

$$u = \frac{X_i - \mu_i}{\sigma_i} \tag{3.9}$$

If this is not the case, an intermediate step is required to find a random variable set x' which is uncorrelated, and this new set can then be transformed to the standardized form. Various transformations have been proposed. Rosenblatt Transformation (Hohenbichler and Rackwits, 1981) can be used when joint probability distribution function of correlated random variables is known and conditional probability functions are continuous. Nataf Transformation (Ditlevsen and Madsen, 1996) may be used when the joint distribution of random variables is incomplete and the marginal distribution function and correlation is given.

The equation (3.8) can be written after the transformation of the limit state surface from the original space *x* to the standard normal space *u*

$$P_f = \int_{g(x)\le 0} f_x(x)dx = \int_{G(u)\le 0} \varphi_n(u)du \tag{3.10}$$

where $G(u) \equiv g\left(T^{-1}(u)\right)$ is the limit state function in the standard normal space.

In the first order reliability method, the fundamental assumption is that the limit-state functions are continuous and differentiable at least in the neighbourhood of the optimal point. The failure surface is obtained by the linear expansion of G(u) = 0 in the standard normal space at the so-called design point u^*, which is the point on the limit-state surface nearest to the origin in the standard normal space (Ditlevsen and Madsen, 1996). The design point is found by following a minimisation procedure with a constraint that G(u^*) = 0

$$\text{u*} = \min|u| \tag{3.11}$$

where $|u| = \sqrt{u^T u}$

Because the design point is not known in advance, an iteration or optimisation algorithm has to be employed. Different algorithms were developed to obtain the design point (Rackwitz and Fiessler, 1978) (Chen and Lind, 1982) (Liu and Der Kiureghian, 1990) (Zhang and Der Kiureghian, 1994). The difference between these various algorithms is in the section of the search direction and the merit function.

Once the design point *u** is obtained, the reliability index is computed as shown in Figure 3.2 (Hasofer and Lind, 1974)

$$\beta = \alpha u^* \tag{3.12}$$

where β is the shortest distance from the origin to the design point; $\alpha = -\nabla G / \|\nabla G\|$ is the unit vector at the design point; $\nabla G = \left\{\frac{\partial g}{\partial u_1}, \frac{\partial g}{\partial u_2}, \ldots \frac{\partial g}{\partial u_n}\right\}$ is the gradient vector

of g with respect to *u*.

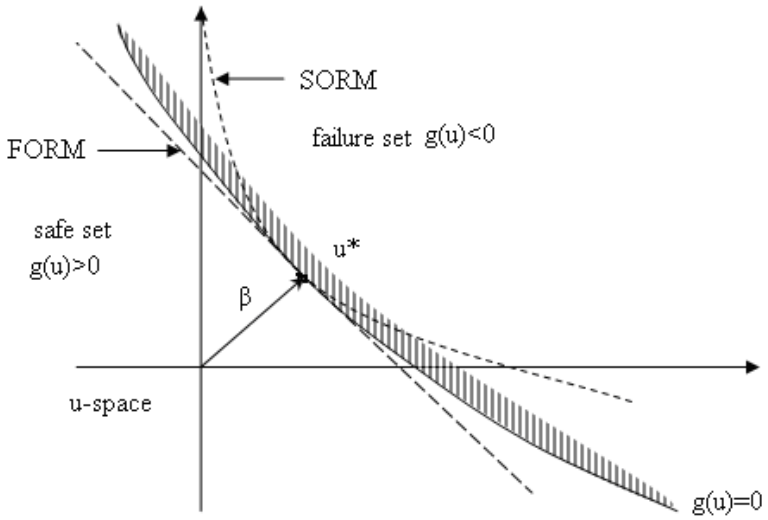

Figure 3.2 FORM/SORM with single-approximation point

This method may work well when the limit state function is a linear function of the uncorrelated normal variables, or when the nonlinear limit state function is represented by the first order (linear) approximation, that is, by a tangent at the design point. The advantage of FORM is that the computing time is small. However, for the limit state surface that is strongly nonlinear, a higher-order approximation, such as second order reliability method, or a simulation-based method is preferable.

3.5 Second Order Reliability Methods

If the limit state surface has significant curvature or even the limit state function is linear in the original space, it may become non-linear when the reliability problem is transformed from the original space to the standard normal space, the approximation from first order reliability method may not be acceptable. In these cases, the limit state function is approximated by parabolic, quadratic or higher order surface around the design point as shown in Figure 3.3 (Fiessler et al., 1979) (Hohenbichler et al.,

1987).

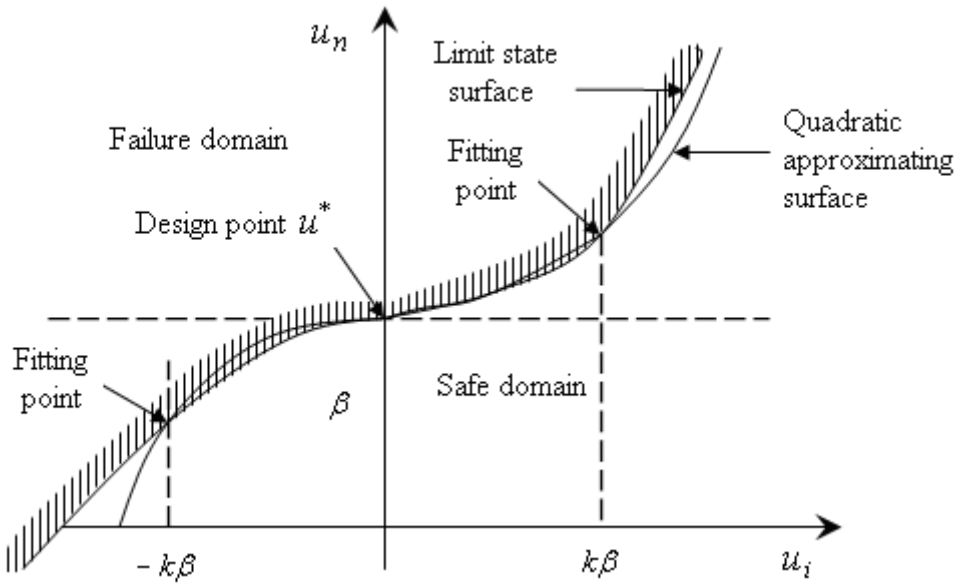

Figure 3.3 Second order approximation to actual limit state surface at design point u^* in u space (Der Kiureghian et al., 1987)

Two distinct methods were developed for second-order reliability analysis. Der Kiureghian et al. (1987) presented a point-fitting SORM method, in which the limit state surface is fitted by a piecewise paraboloid surface at discrete points around the point with minimal distance from the origin. The advantage of this method is that less computation for large number of variables is required and the error is reasonably small.

Another one is the curvature-fitting approximation (Reitung, 1984), in which the paraboloid surface is fitted to the principal curvatures of the limit-state surface at the design point, which is the point on the surface nearest to the origin.

Two algorithms are available for determining the principal curvatures and the corresponding principal directions of the limit state surface. One algorithm is obtained as the eigenvalues of the matrix of second-order derivatives of the surface. Calculation of the second order derivative matrix is time-consuming and 'noise' may

be introduced to the limit state surface. Der Kiureghian (1991) developed an another efficient algorithm, in which curvatures are computed in an iterative manner using the gradient of the limit state function without computing the second order derivative matrix or solving the eigenvalue problem. Generally, second order reliability method yields better estimates of the failure probability but it is computationally more intensive than the first order reliability method.

3.6 Simulation-based Method

If the limit state function is not differentiable or the failure domain cannot be represented by linear or quadratic form, FORM, SORM are no more suitable. In these cases, a simulation-based method is an attractive alternative. Monte Carlo Simulation (MCS) is based upon simulating artificially a large number of experiments and observing the distribution or probability of an output without much of the algebraic complexity associated with the approximate methods.

In the case of analysis for structural reliability, each of the input variables x_i is randomly given a sample value $\hat{x}_i$ according to its probability distribution function. The generated sample values are then substituted in the limit state function whose value is computed and the random output is recorded. If the limit state is violated (i.e. $G(\hat{x}_i) \le 0$), the structure or structural element has 'failed'. This process is repeated many times until the number of simulations provides the desired accuracy. If N trials are conducted, the probability of failure is approximated by

$$P_f \approx \frac{n(G(\hat{x}_i) \le 0)}{N} \tag{3.13}$$

where $n(G(\hat{x}_i) \le 0)$ denotes the number of trials n for which $(G(\hat{x}_i) \le 0)$.

When the probability of failure is estimated by an approximate probability

distribution for g(x) using the trial values (Thoft-Christensen and Baker, 1982), the probability of failure is then determined from

$$P_{\mathrm{f}} \approx \int_{-\infty}^{0} f_M(m)dm \tag{3.14}$$

where M = g(x) is a random variable representing the margin and $f_M(m)$ is its probability density function as estimated from the fitting process.

This method is simple and applicable to problems for which the limit state function and the distribution type of random variables may have many forms. After sufficient simulations, the Monte Carlo method will always converge to the same result. For this reason, Monte Carlo method is generally the baseline against which other methods are compared. Moreover, it may be used for calibrating a novel structural design based on new rules or design methods. However, the number of simulations required to build an accurate distribution of the output may be very large, especially for small-probability problems, since very few of the simulations will be failures.

Shinozuka (1983) proposed importance sampling techniques as an extension of Monte Carlo simulation. At present a number of papers have been published (Schueller and Stix, 1987), (Hohenbichler and Rackwits, 1988) (Melchers, 1990) (Ibrahim, 1991) (Wu, 1994) (Torng et al., 1996). These methods have been developed to reduce the simulation cycles by adjusting the sampling domain to the important region near the most probable points of failure instead of spreading them out evenly cross the whole range of possible values. Engelund and Rackwits (1993) suggested that the most robust and efficient approach is importance sampling for single limit state problems by a comparison of the simulation methods for a range of single limit state applications. Generally speaking, the importance sampling technique is of more interest among researchers in structural reliability analysis as MCS is a costly means to examine a problem.

3.7 Sensitivity Analysis and Importance Measures

In a practical structural design, knowing the most important design parameters and their impact on safety index enables the designer to know where to look to improve reliability. In a deterministic analysis, the sensitivities of design variables can only be computed by quantifying the change in the performance measure due to a change in the variable value. On the other hand, if a design is based on reliability theory, then each random variable is defined by the mean value, coefficient of variance and distribution type. Once the probabilistic model is established, probabilistic analysis is run and then the sensitivity factors are obtained in order to determine the importance of a random variable.

Since the complexity of the mathematical reliability program is greatly influenced by the dimensionality of the space of variables in the analysis, therefore it is important to reduce the number of variables and thereby increase the efficiency of the reliability analysis. The variable having a small sensitivity factor might be assumed to be of fixed value rather than being a random variable in subsequent analyses. The discussions of this kind of sensitivity analysis are fully described in (Thoft-Christsen and Baker, 1982) (Hohenbichler and Rackwitz, 1986) (Bjerager and Krenk, 1989). The following four important sensitivity measures for each random variable were considered in CALREL (CAL-RELiability) program (Liu et al., 1989) (Mansour and Wirsching, 1995).

(1) Sensitivity factor α

According to the definition, the reliability index β is the shortest distance from the origin to the design point as shown in Eq.(3.12), in which α is a unit vector normal to the limit state surface at the design point. Sensitivity factor α is generally considered as a measure of the sensitivity of the reliability index β with respect to the standard normal variable u_i^* in the literature. It provides some insight into the relative

weight that each one has in determining the final reliability of the structures. A larger α_i implies more sensitivity of reliability index β to the standard variate u_i^*

$$\alpha_i = \frac{\partial \beta}{\partial \mathrm{u}_\mathrm{i}^*} \tag{3.15}$$

It can be checked that $\sum_{i=1}^{n} \alpha_i^2 = 1$

(2) Sensitivity factor γ

The sensitivity factor γ represents the relative contributions of the original random variables x_i (i=1,,,n) to the total variance of the linearized limit-state function. γ coincides with α when the random variables x are statistically independent.

$$\gamma_i = \frac{\partial \beta}{\partial \mathrm{x}_\mathrm{i}^*} \tag{3.16}$$

These two sensitivity factors usually provide an importance ranking of input variables and always numerically equal, so either one can be used for analysis. However, these two factors are not useful for design purpose as they are dependent on mean value, standard deviation and distribution type of random variables. Another two sensitivity parameters δ and η referred to as sensitivity of β with respect to the mean and the standard deviation of each basic random variable in question are more useful for design.

(3) Sensitivity factor δ

Sensitivity to the mean value is considered as δ in the CALREL program. The positive sensitivity factors δ obtained by Eq.(3.17) are treated as strength parameters. That means the safety index increases with increasing of mean value of the variables. The negative sensitivity factors δ are treated as load parameters and that indicates that safety index decreases with increasing of mean value.

$$\delta_i = \frac{\partial \beta}{\partial \mu_i} \sigma_i \tag{3.17}$$

where μ and σ represent the mean and standard deviation of basic random variables, respectively.

(4) Sensitivity factor η

The sensitivity factor η expresses the level of uncertainty associated with one of the variables to quantify the effect on risk. If a variable has a small value of η, that means this variable has a small impact on the probability of failure estimate. Another function of the important factor η is that the larger sensitivity factor means that it is better to reduce the uncertainty of these variables rather than other in terms of their relative importance with respect to variations in their standard deviations.

$$\eta_i = \frac{\partial \beta}{\partial \sigma_i} \sigma_i \tag{3.18}$$

Chapter 4:
Strength and Reliability Analysis of Unstiffened Plates

4.1 Introduction

After having discussed the applications of composite materials for shipbuilding it is clear that the advantages of FRP over steel and other materials lie in increased strength, stiffness, fatigue life and fracture toughness, environment resistance, reduced weight, reductions in tooling as well as assembly costs and many more when the appropriate constituents are chosen. The failure analysis of laminated composite plates is much more complex than that of isotropic materials. Composite laminates may fail in a variety of ways. It is well known that a composite plate can sustain a much higher load after the first failure occurrence of damage (Petit and Waddoups, 1969). Therefore, knowledge of the failure characteristics related to the first-ply failure and ultimate strength will permit the composite structures to be designed efficiently and economically.

For the ultimate strength of laminated composite structures, a progressive failure methodology embedded within a nonlinear finite element analysis is developed. The Tsai-Wu criterion is adopted to identify the material failure of structures. In order to have confidence in the progressive damage model and the corresponding computer code, a validation study is performed by comparing the results with those obtained from published experiments. A benchmark study is also performed on a number of fibre reinforced plates of various thicknesses with different imperfections in order to investigate the process of progressive failure analysis and the influence of various seizes of geometrical imperfections on the compressive strength. Finally, a probabilistic design approach is proposed to laminate composite plates at design

stages in order to treat the uncertainty of basic variables in a more realistic way.

4.2 Analytical Method

The mechanical response of laminated plate based on the classical laminated plate theory, first-order shear deformation theory and higher-order shear deformation theory have been reviewed in Chapter 2. As described in Section 2.3.3, classical laminated plate theory provides an acceptable result when the slenderness ratio of the plates is larger than 20. As the plate slenderness ratio decreases, the transverse shear effect cannot be ignored. The analytical solution based on first-order shear deformation theory provides the best compromise of a sufficiently accurate description of global response, economy and simplicity for thin to moderately thick laminates. For this reason, first order deformation theory is chosen in the probabilistic design approach for deterministic analyses.

(a) Assumptions

Certain assumptions are made in FSDT

- Straight lines perpendicular to the mid-surface before deformation remain straight after deformation.
- The transverse normals do not experience elongation.
- Transverse shear stresses are considered as a constant state and the transverse normals do not remain perpendicular to the mid-surface after deformation.

(b) Displacement Field

Due to small strain and displacement assumptions, the displacement field (u, v, w) in FSDT is assumed to be such that

$$\begin{aligned} u(x,y,z) &= u_0(x,y) + z\phi_x(x,y) \\ v(x,y,z) &= v_0(x,y) + z\phi_y(x,y) \\ w(x,y,z) &= w_0(x,y) \end{aligned} \tag{4.1}$$

where (u_0, v_0, w_0) are the displacements of a point on the plane $z = 0$; $\phi_x = \dfrac{\partial u}{\partial z}$ and $\phi_y = \dfrac{\partial v}{\partial z}$ are the rotations of a transverse normal about the y- and x-axis, respectively

(c) Strain Field

The strains associated with the displacement field can be computed using the linear strain-displacement relations given by

$$\{\varepsilon\} = \{\varepsilon^0\} + z\{\varepsilon^1\} \tag{4.2}$$

where $\{\varepsilon^0\}$ and $\{\varepsilon^1\}$ are vectors of the membrane and the flexural strains or bending strains.

The membrane and the flexural strains are given by Eq. (4.3)

$$\{\varepsilon^0\} = \begin{bmatrix} \varepsilon^0_{xx} \\ \varepsilon^0_{yy} \\ \gamma^0_{yz} \\ \gamma^0_{xz} \\ \gamma^0_{xy} \end{bmatrix} = \begin{Bmatrix} \dfrac{\partial u_0}{\partial x} \\ \dfrac{\partial v_0}{\partial y} \\ \dfrac{\partial w_0}{\partial y} + \phi_y \\ \dfrac{\partial w_0}{\partial x} + \phi_x \\ \dfrac{\partial u_0}{\partial y} + \dfrac{\partial v_0}{\partial x} + \dfrac{\partial w_0}{\partial x}\dfrac{\partial w_0}{\partial y} \end{Bmatrix} \quad \{\varepsilon^1\} = \begin{bmatrix} \varepsilon^1_{xx} \\ \varepsilon^1_{yy} \\ \gamma^1_{yz} \\ \gamma^1_{xz} \\ \gamma^1_{xy} \end{bmatrix} = \begin{Bmatrix} \dfrac{\partial \phi_x}{\partial x} \\ \dfrac{\partial \phi_y}{\partial y} \\ 0 \\ 0 \\ \dfrac{\partial \phi_x}{\partial y} + \dfrac{\partial \phi_y}{\partial x} \end{Bmatrix} \tag{4.3}$$

Once the displacements (u_0, v_0, w_0) of the mid-plane and ϕ_x, ϕ_y are known, strains at any point in the plate can be computed using Eqs.(4-2) and (4.3).

(d) Constitutive Relations

The constitutive equations of laminated plate for FSDT can be obtained using Eqs.(4.4) and (4.5)

$$\begin{Bmatrix} \{N\} \\ \{M\} \end{Bmatrix} = \begin{bmatrix} [A] & [B] \\ [B] & [D] \end{bmatrix} \begin{Bmatrix} \{\varepsilon^0\} \\ \{\varepsilon^1\} \end{Bmatrix} \tag{4.4}$$

$$\begin{Bmatrix} Q_y \\ Q_x \end{Bmatrix} = K \begin{bmatrix} A_{44} & A_{45} \\ A_{45} & A_{55} \end{bmatrix} \begin{Bmatrix} \gamma_{yz}^0 \\ \gamma_{xz}^0 \end{Bmatrix} \tag{4.5}$$

where A_{ij}, B_{ij}, D_{ij} are extensional stiffnesses, the bending-extensional coupling stiffnesses and the bending stiffnesses, respectively.

$$(A_{ij}, B_{ij}, D_{ij}) = \sum_{k=1}^{N} \int_{z_k}^{z_{k+1}} \overline{Q}_{ij}^{(k)} (1, z, z^2) dz \tag{4.6}$$

where $[\overline{Q}]$ are the transformed coefficients and can be expressed as $[\overline{Q}] = [T]^{-1}[Q][T]^{-T}$.

The superscript -1 and T denote the matrix inverse and transpose, respectively. $[Q]$ is the plane stress-reduced stiffnesses given in terms of the engineering constants of the lamina

$$[T] = \begin{bmatrix} \cos^2\theta & \sin^2\theta & 0 & 0 & 0 & \sin 2\theta \\ \sin^2\theta & \cos^2\theta & 0 & 0 & 0 & -\sin 2\theta \\ 0 & 0 & 1 & 0 & 0 & 0 \\ 0 & 0 & 0 & \cos\theta & -\sin\theta & 0 \\ 0 & 0 & 0 & \sin\theta & \cos\theta & 0 \\ -\sin\theta\cos\theta & \sin\theta\cos\theta & 0 & 0 & 0 & \cos^2\theta - \sin^2\theta \end{bmatrix}$$

As can be seen from Eq. (4.3), the transverse shear strains are constant through the

laminate thickness. Therefore, the transverse shear stresses will also be constant. However, it is well known that the actual stress varies at least quadratically through the thickness of plate. A shear correction coefficient K is often used to correct the transverse shear force.

The stress-strain relations for FSDT are given for the kth lamina in the laminate coordinates

$$\begin{Bmatrix} \sigma_{xx} \\ \sigma_{yy} \\ \sigma_{xy} \end{Bmatrix}^k = \begin{bmatrix} \overline{Q}_{11} & \overline{Q}_{12} & \overline{Q}_{16} \\ & \overline{Q}_{22} & \overline{Q}_{26} \\ sym. & & \overline{Q}_{66} \end{bmatrix}^k \begin{bmatrix} \varepsilon_{xx} \\ \varepsilon_{yy} \\ \gamma_{xy} \end{bmatrix} \tag{4.7}$$

$$\begin{Bmatrix} \sigma_{yz} \\ \sigma_{xz} \end{Bmatrix}^k = \begin{bmatrix} \overline{Q}_{44} & \overline{Q}_{45} \\ \overline{Q}_{45} & \overline{Q}_{55} \end{bmatrix}^k \begin{Bmatrix} \gamma_{yz}^0 \\ \gamma_{xz}^0 \end{Bmatrix} \tag{4.8}$$

The Navier solutions developed by Reddy (2004) for rectangular laminate with simply supported boundary conditions is described comprehensively in Appendix A.

4.3 Numerical Method

4.3.1 Introduction

Analytical methods are limited to specific shapes of plates with a limited set of boundary conditions. For more general structures with arbitrary geometries and boundary conditions, numerical methods are the most effective means. Furthermore, most composite materials exhibit brittle failure with the first-ply failure being only the beginning of damage in plates. The propagation of the failure mechanism in composite structures must be understood in order to develop reliable designs which exploit the advantages offered by composite materials. Hence, a progressive failure analysis method is developed for predicting the ultimate strength of laminated composite plates under compressive load. A nonlinear finite element technique,

including the multi-frame restart analysis, is adopted using commercial software ANSYS.

4.3.2 The Procedure of Progressive Failure Analysis

The detailed flow chart of the solution is shown in Figure 4.1. Generally speaking, in the first step a linear static analysis is performed to find out the bifurcation point. The next step is to perform a linear stability analysis in order to form the initial geometric imperfection which serves as a trigger for the geometric nonlinear analysis. The geometry of the finite element model can be updated directly at the deformed configuration according to the displacement results of the linear stability analysis by scale factor.

The initial small pressure value P_0 (or displacement value) is specified to ensure no element failure. Nonlinear analysis is run to establish the equilibrium equation and a displacement (or force)-controlled convergence criterion is employed to control the analysis. The on-axis stresses of elements are then determined from the nonlinear analysis and used to determine whether any failures have occurred at each load increment according to adopted failure criteria. If the failures are detected, a reduction in the value of the engineering material constants corresponding to that particular mode of failure will take place using a material degradation model, which will be discussed in the following section. The layer number and the element number of the failed element are then recorded.

After the material properties have been degraded, the historical databases are updated for the current load step by modified material properties for the particular layer of failed element. The static equilibrium is re-established by restarting analysis at the current load level. The iterative process of obtaining nonlinear equilibrium solutions is continued until no additional failure is detected. The material properties in the elements are not changed and an incremental pressure of ΔP (or displacement) is added until further failure is achieved. In what follows, the loading procedure is cycled until the solution is completed.

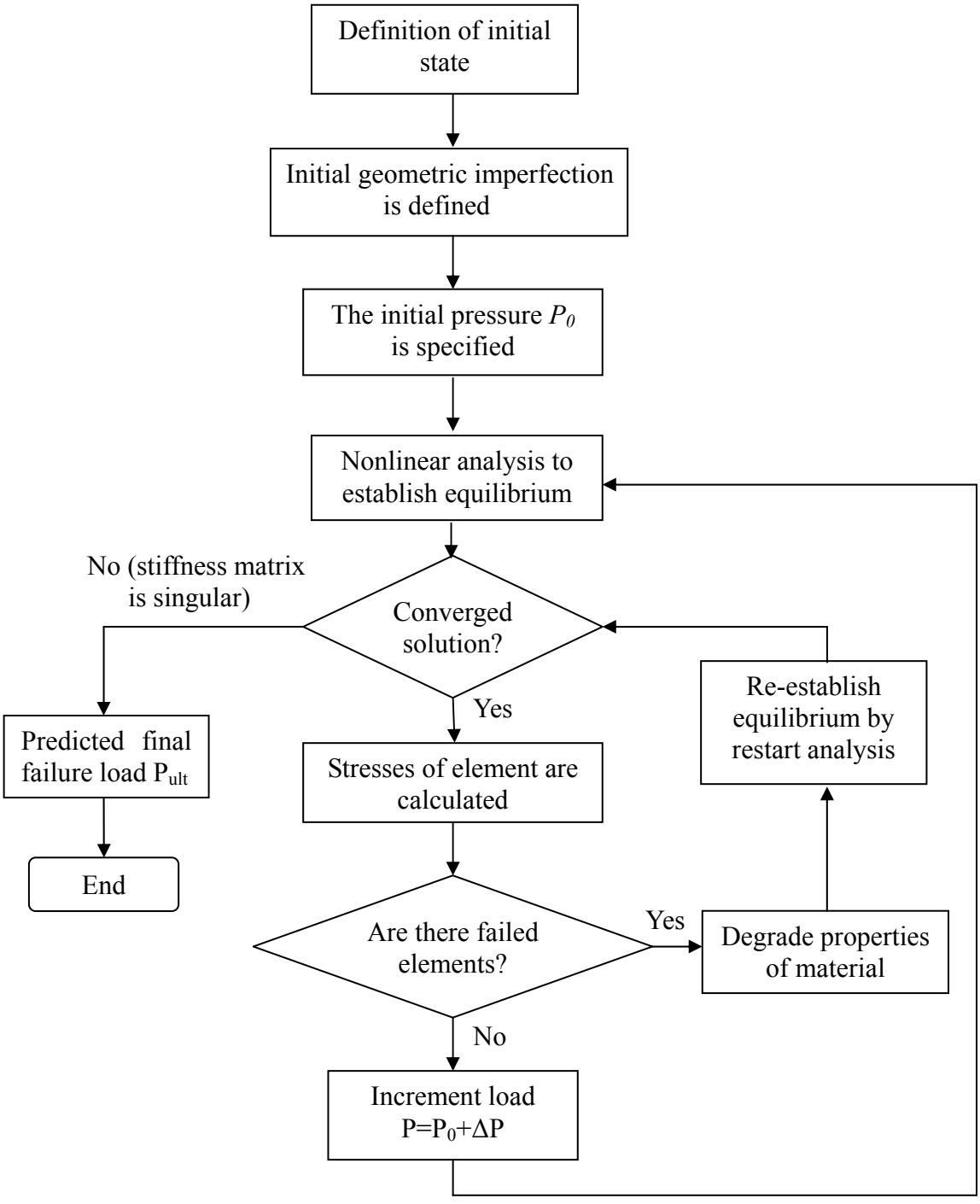

Figure 4.1 Flow chart of progressive analysis methodology

4.3.3 Failure Criteria and Property Degradation Model

A failure criterion is required to assess whether the laminated plate has failed under a load system. Laminate composite may fail by fibre breakage, matrix cracking, shear failure or delamination. The modes of failure depend upon the loading, stacking sequence, specimen geometry and so on. Various failure criteria have been discussed in Section 2.6. The Tsai-Wu criteria is the most commonly used one among existing failure criteria and is adopted in this analysis (Hinton et al., 2002). As indicated previously, the principal stresses associated with particular elements are computed and the failure criterion is used on these principle stresses. According to the Tsai-Wu criterion, the failure is said to have occurred when the following criterion is satisfied at any element of the lamina:

$$F = \sum_{i=1}^{6} F_i \sigma_i + \sum_{i=1}^{6}\sum_{j=1}^{6} F_{ij}\sigma_i\sigma_j \geq 1 \tag{4.9}$$

In the above expression σ_i are stresses in material directions and F_{ij} and F_i are the tensor strength factors, which are expressed as

$$F_1 = \frac{1}{X_t} - \frac{1}{X_c}, \quad F_2 = \frac{1}{Y_t} - \frac{1}{Y_c}, \quad F_{11} = \frac{1}{X_t X_c},$$

$$F_{22} = \frac{1}{Y_t Y_c}, \quad F_{44} = \frac{1}{R^2}, F_{55} = \frac{1}{S^2}$$

$$F_{66} = \frac{1}{T^2} \qquad F_{12} = F_{12}^{*} / \sqrt{X_t X_c Y_t Y_c} \tag{4.10}$$

where X_t, Y_t and X_c, Y_c are the tensile and compressive strengths of a lamina in the fibre direction and in direction transverse to fibre, respectively. R, S and T are shear strengths of a lamina in the principal material planes yz, xz and xy, respectively.

In a progressive failure analysis, a reduction in the corresponding lamina modulus must be introduced. The degrees of property loss are strongly dependent upon the

failure mechanisms resulting from damage. The effect of damage such as fibre breakage or matrix cracking can be taken into account in an average sense. In that way the damaged material could be replaced with an equivalent material of degraded properties. A number of material property degradation models have been proposed for progressive failure analysis since the first effort was made by Petit and Waddoups (1969). Most of them can be grouped into the following three categories (Sandhu, 1974) (Nahas, 1986) (Chang and Chang, 1987) (Murray and Schwer, 1990) (Reddy and Reddy, 1993) (Padhi et al., 1998) (Liu and Zheng, 2008)

- Total discount method: material properties of a failed ply are degraded instantly to zero. This approach may lead to a conservative estimate of the laminate strength as it ignores that the failure is localized.

- Limited discount method: this is the most common method used for material properties degradation. In this method, one or more of the elastic material properties associated with that mode of failure are set to zero or a small fraction of the original properties of the undamaged material once failure is detected somewhere.

- Residual property method: the material properties are gradually reduced depending upon the extent of damage accumulation within a lamina until the lamina has completely failed.

The Tsai-Wu failure criterion identifies the failure of composite material, but it does not distinguish between the different modes of failure. The following terms were used to determine that the failure is caused by resin fracture, fibre breakage or shearing failure (Engelstad et al., 1992):

$$H_1 = F_1\sigma_1 + F_{11}\sigma_1^2 \quad H_2 = F_2\sigma_2 + F_{22}\sigma_2^2$$
$$H_4 = F_{44}\sigma_4^2 \quad H_5 = F_{55}\sigma_5^2 \text{ and } H_6 = F_{66}\sigma_6^2 \tag{4.11}$$

The largest H_i term is selected to be the dominant failure mode and the

corresponding material properties are reduced to a negligible quantity. In the present study, a simple and effective limited stiffness reduction model is summarized in Table 4.1. For example, when H_1 is the maximum value, the failure is assumed to be caused by the fibre breakage. In this case, the values of the material properties and E_1, ν_{12}, ν_{13} are set to an extremely small value such as 1×10^{-10} instead of zero as setting the material properties to zero may cause the lack of ability to invert the structural stiffness matrix.

Table 4.1 Material property degradation model

Primary failure mode	Fibre failure H_1	Matrix failure H_2	Shear failure		
			H_4	H_5	H_6
Degraded properties	E_1, ν_{12}, ν_{13}	E_2, ν_{12}, ν_{23}	G_{23}	G_{13}	G_{12}

4.3.4 FE Analysis

(a) Choice of Element

Modelling the behaviour of composite materials is more complex than isotropic materials such as steel. Thus, the type of elements should be carefully selected to obtain high accuracy. Shell elements based on the first order shear deformation theory are designed to efficiently model thin to moderately-thick laminated composite shells or sandwich construction. Shell 91, Shell 99 and Shell 181 are commonly used when modelling the laminated composite plates in the ANSYS program.

Shell 91 may be used for modeling thick sandwich structures. For laminated composite plate with more than three layers, Shell 99 is usually more efficient than Shell 91 because it uses less time for elements with more layers. However, Shell 99 does not have some of the nonlinear capabilities of Shell 91. Both of two elements

are defined by eight nodes with six degrees of freedom. Shell 281 is another element which has been used in ANSYS 12.0 version instead of Shell 91 and Shell 99.

Shell 181 is a 4-node element with six degrees of freedom at each node. It is suitable for analyzing thin to moderately-thick shell structures and especially suited for linear large rotation or large strain nonlinear structures. The accuracy in modeling composite shells is governed by the first order shear deformation theory. Out of the several elements available in the ANSYS library for modeling laminates, the Shell 181 element is selected for this purpose.

(b) Nonlinear Analysis

In linear finite element analysis it is assumed that the stiffness of the structure remains constant during the analysis.

$$F = K \cdot U \tag{4.12}$$

where K is the stiffness matrix; U is the displacement vectors; F is the applied force vector

This assumption is valid in some cases of engineering applications with reasonable results. However, when the structures undergo large deflections, nonlinear stress-strain relationships or creep response, then nonlinear finite element analysis is required. The nonlinear behaviour can be grouped into geometric, material and boundary nonlinearities.

The geometrically nonlinear behavior due to the large deflection experienced by the structures during loading and the material nonlinearity due to the damage mentioned earlier are considered in this analysis. To implement and perform the progressive failure methodology within a nonlinear finite element analysis, the ANSYS-APDL (ANSYS Parametric Design Language) is used as a subroutine, in which the multi-frame restart analysis is repeatedly used to account for the effect of degradation of material properties

Restart analysis is used where more load steps are added after the initial run has been completed, continuing calculations after some aspects of the model have been changed, or recovering an analysis from a convergence failure in a nonlinear analysis. The single-frame restart and the multi-frame restart can be supported for static structural analysis in ANSYS. The single-frame restart analysis allows resuming the analysis at the point at which it was stopped during the analysis. The multi-frame restart analysis can resume a job at any point for which information is saved.

It is well known that a nonlinear analysis usually requires a more refined mesh to get accurate results compared to a linear analysis. In addition, nonlinear analysis is also sensitive to load increment size as it is essentially a piece-wise approximation technique. The size of load increment and the finite element mesh should be determined based on the requirement of accuracy, efficiency and time constraints.

(c) Solution Procedures

The basic problem is to find solutions that satisfy the nonlinear equilibrium equation. In nonlinear analysis, the load is divided into a series of load increments with the stiffness matrix needing to be updated at each load step. An iterative procedure is required to establish equilibrium. Convergence criteria are defined to check the problem convergences. If convergence cannot be satisfied, the out-of-balance load vector is reestimated and the tangent stiffness matrix is updated to obtain a new solution. This procedure is iterative until convergence is reached.

The most widely used iterative scheme for the solution of nonlinear finite element equations is the Newton-Raphson procedure because it generally converges quite rapidly. However, large computational effort is needed to evaluate the tangent stiffness matrix at each iteration. To improve the computational efficiency, a modified Newton-Raphson method is commonly used. The tangent stiffness matrix in this case is not updated at every equilibrium iteration but at each substep. This means that the matrix is not changed during equilibrium iterations at a substep. However, this algorithm may cause severe convergence difficulties in some nonlinear

analyses when tangent stiffness matrix may become singular (or non-unique).

The arc-length method is an effective alternative iteration scheme to search for the equilibrium path along an arc, even when the slope of load-deflection curve becomes zero or negative. The iteration method of Newton-Raphson Approach and Arc-Length Approach are illustrated in Figures 4.2 and 4.3.

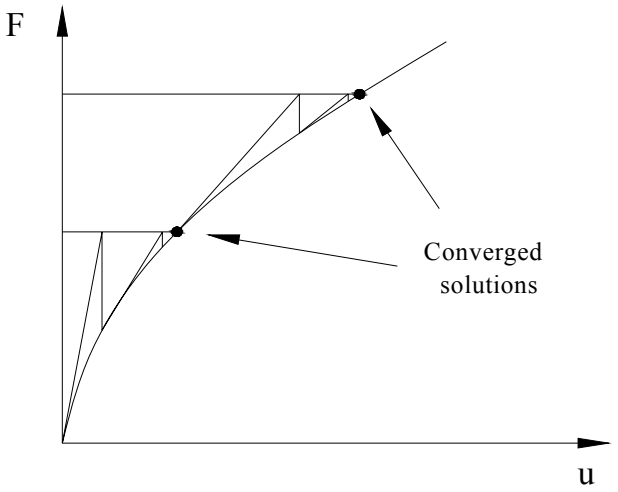

Figure 4.2 Newton-Raphson approach

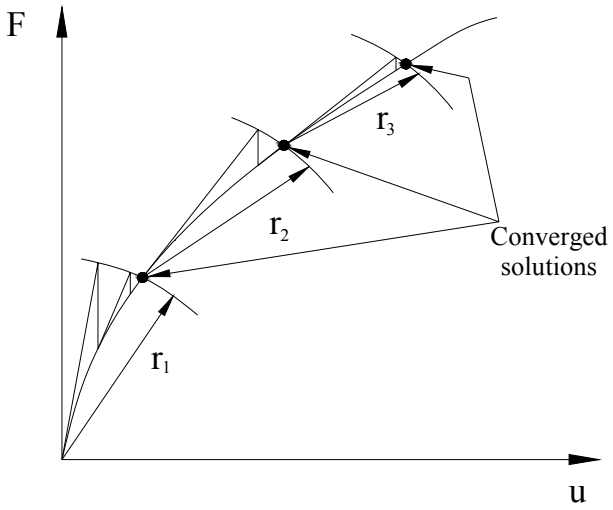

Figure 4.3 Arc-Length approach

4.4 Validation Study

In order to verify the corresponding computer code and the progressive damage model presented in the previous section, a published experimental data by Starnes and Rouse (1981) is used to validate the analysis procedure. A 24-ply unstiffened flat rectangular graphite-epoxy plate loaded in axial compression is adopted in this validation study. The panel is 508mm long by 178mm wide with a stacking sequence $[45/-45/0_2/45/-45/0_2/45/-45/0/90]_s$. The thickness of each ply is 0.14mm. The boundaries are clamped for loaded edges (along width) and simple supported along the unloaded sides (along length) as shown in Figure 4.4. The mechanical parameters of materials are listed in Table 4.2. The mesh 60×21 is modelled and approximately 0.01mm displacement increment size is chosen.

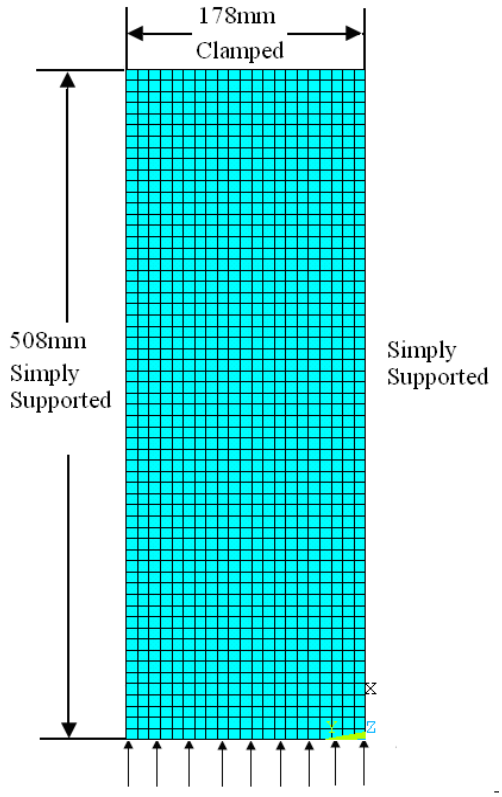

Figure 4.4 Geometry, loading and boundary conditions of panel

Table 4.2 Material properties and strength properties of graphite-epoxy composite material (Starnes et al., 1981)

Mechanical properties	Values	Strength properties	Values
E_1	131.0 GPa	X_t	1400 MPa
E_2	13.0 GPa	X_c	1138 MPa
G_{12}	6.4 GPa	$Y_t = Z_t$	80.9 MPa
G_{13}	6.4 GPa	$Y_c = Z_c$	189 MPa
G_{23}	1.7 GPa	R	62.0 MPa
v_{12}	0.38	$S = T$	69.0 MPa

The first buckling mode from the linear stability analysis has two longitudinal half-waves with a buckling mode line at the mid-length of the panel and one transverse half-wave along the panel width as shown in Figure 4.5. An initial geometric imperfection is formed by using the first buckling mode shape with amplitude 5% of the panel thickness in order to pass the critical buckling point.

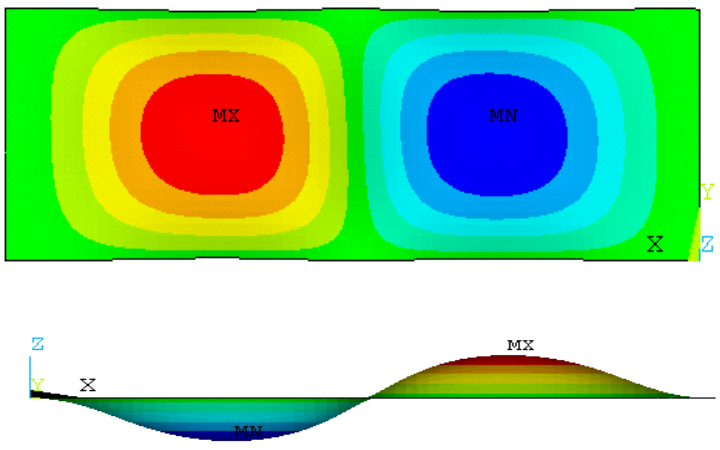

Figure 4.5 First buckling mode of panel

Similar progressive failure analyses have also been performed by (Engelstad et al., 1992) (Sleight, 1999) and (Chen and Soares, 2007). Table 4.3 summarizes the first-ply failure and final failure loads of this study, test results and other analytical results. End-shortening as a function of the applied load from the numerical solution of the panel are presented against experimental results in Figure 4.6. Figure 4.7 shows the out-of-plane deflection response as a function of the applied load at a point of maximum deflection in the plate.

Table 4.3 The experimental results and the corresponding estimated results reported in the literatures

	First-ply failure load (KN)	Final failure load (KN)	End shortening at failure load (mm)	Failure criteria	Dominant failure mode
Present analysis	88.77	101.26	2.31	Tsai-Wu	-
Chen and Soares (2007)	--	101.3	2.4	Tsai-Wu	-
Sleight (1999)	82.83	99.8	-	Christensen	Fibre/Matrix Interaction
	96.91	104.6	-	Hashin	Matrix Tension
Engelstad et al. (1992)	-	111.4	-	Maximum Stress	-
	-	104.3	-	Tsai-Wu	-
Test results Starnes and Rouse (1981)	-	98.0	2.1	-	Transverse Shear

The numerical results obtained from progressive failure analysis as described earlier correlate well with the experimental results up to failure. The load at which the first ply failure occurs predicted by Tsai-Wu failure criterion is 7.17% higher than by Christensen's criterion and 8.4% lower than by Hashin's criterion. The final failure load predicted by Tsai-Wu failure criterion is slightly higher than the experimental results. The fibre failure mode was identified first when the load reached 88.77KN;

failure location is at mid-length of the panel near the boundary, namely, around the nodal line of the buckling mode shape. Soon after fibre compressive failure was detected, the matrix failure and in-plane shear failure at mid-length of panel near the boundaries occurred at 90.56KN and 91.17KN, respectively. In Sleight's study (1999), the dominant failure mode for Christensen's criterion and Hashin's criterion is fibre/matrix interaction and matrix tension, respectively. Starnes and Rouse (1981) reported that the specimen failed along a nodal line of the buckling mode in a shear failure mode in the experiments.

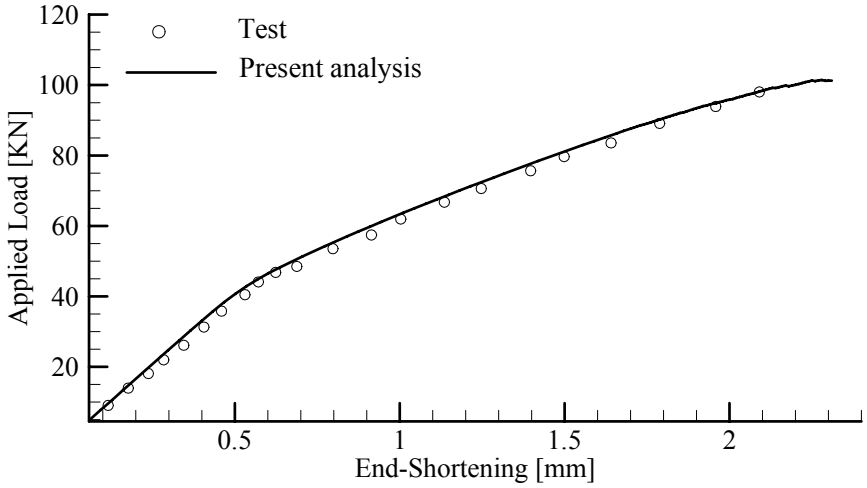

Figure 4.6 End-shortening versus applied load

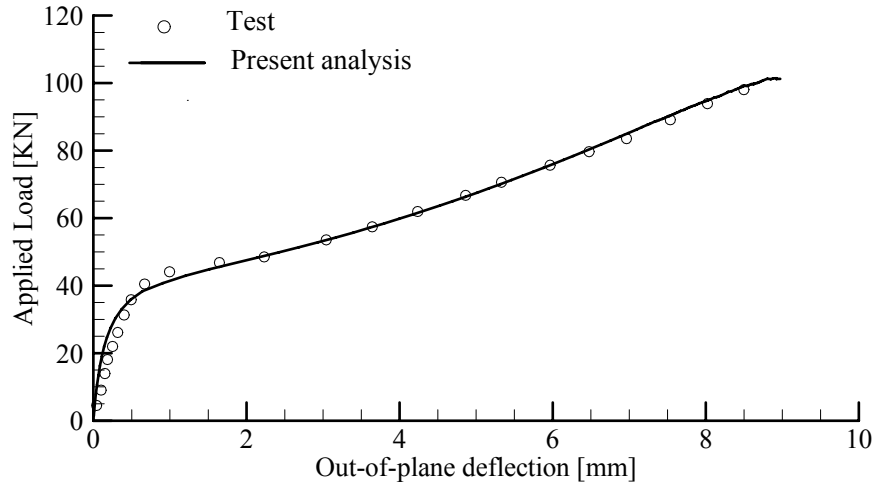

Figure 4.7 Out-of-plane deflection versus applied load

4.5 Benchmark Study

4.5.1 Description of Experimental Studies

In order to investigate the process of progressive failure analysis and the influence of various sizes of geometrical imperfections on the compressive strength of composite plates, the benchmark study is performed on three series of laminated composite panels with various thicknesses and sizes of initial imperfection. Experimental work has been done by Technical University of Denmark (DTU) and National Technical University of Athens (NTUA) from April 2007 to October 2007. The thin and mid-thick plates were fabricated using the vacuum bag moulding method by NTUA. The thick plates were produced by hand-layup and vacuum bagged at DTU (Berggreen, et al. 2009).

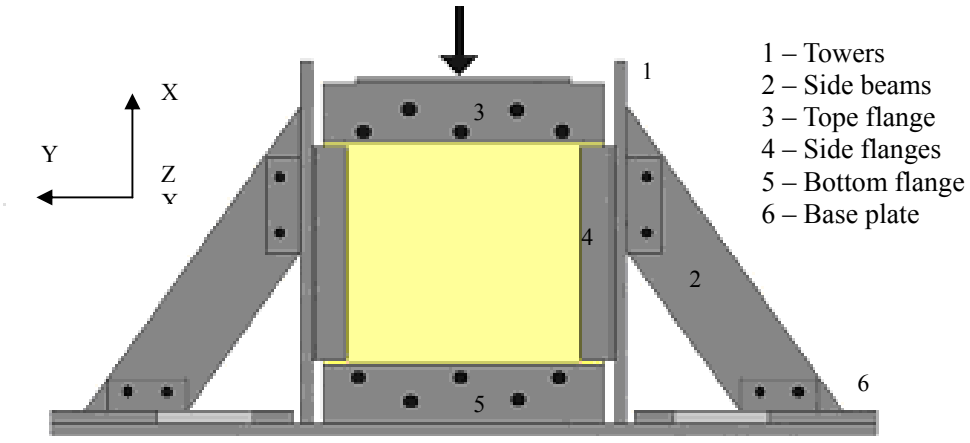

Figure 4.8 Schematic 2-D view of the test-rig (Berggreen et al. 2009)

The dimensions of all the plates are L = 400mm along length direction, e.g. the compressive load direction and B = 380mm along the wide direction. Around 40mm and 30mm plate edges were inserted in the grips along the loaded edges and side edges, respectively. The tests were carried out in the test rig shown in Figure 4.8. The compressive load was applied to the panel by a suitable steel bar, which was placed

between the upper edge of the panel and the testing machine. A similar steel bar was placed between the lower edge of the panel and the base plate of the test rig as well. In all cases, the compressive loading was applied in the form of linearly increasing compressive displacement rate of 1mm/min. The detailed dimensions as measured from the test rig are presented in Figure 4.9.

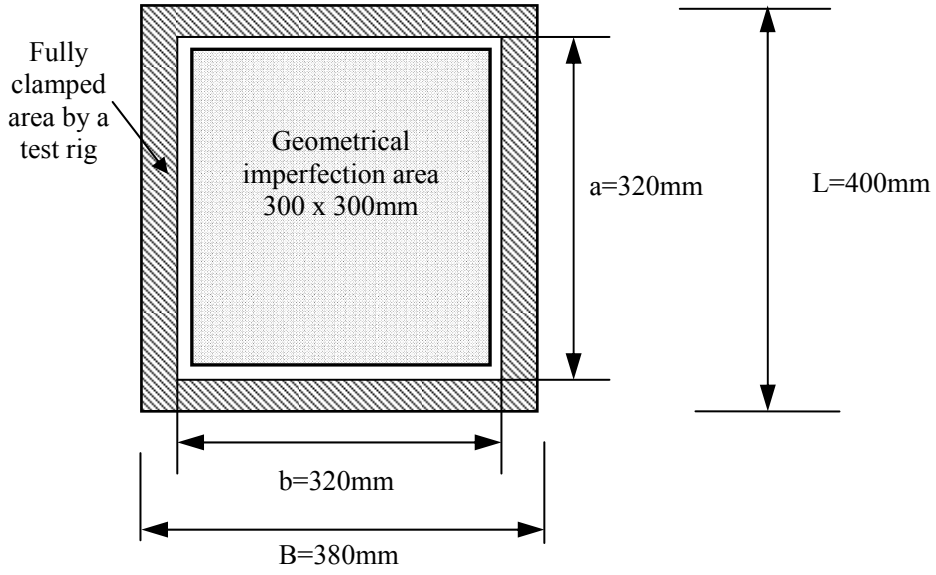

Figure 4.9 Geometry dimensions of the test plates (Berggreen et al. 2009)

Table 4.4 Material properties used in linear eigenvalue analysis

Mechanical properties	Values	Mechanical properties	Values
E_1	46000 MPa	ν_{13}	0.30
E_2	13000 MPa	G_{12}	5000 MPa
E_3	13000 MPa	G_{23}	4600 MPa
ν_{12}	0.30	G_{13}	5000 MPa
ν_{23}	0.42		

As can be seen in Figure 4.9, the unsupported length and width of the plate is 320mm × 320mm after it is fixed by a test rig. The initial imperfection shape of the panels is defined by the first buckling mode shape of a corresponding fully clamped active plate with dimensions 300mm × 300mm. The first buckling mode is calculated by linear eigenvalue analysis with material properties listed in Table 4.4.

These three series of laminated composite plates, termed as S_1 for the thin panel series, S_2 for the mid-thick panel series and S_3 for the thick panel series, are comprised of nine plates: three of these plates are perfect, three have a small imperfection and the rest three plates have a large imperfection. The values of maximum imperfection of each panel are assumed to be a function of the unsupported width 320mm with 1% and 3%, namely 3.2mm for small imperfection and 9.6mm for large imperfection. The thickness of each layer, total thickness and stacking sequence of all these specimens are given in Table 4.5. The material properties and strength characteristics, which were provided by NTUA for the Series 1 and 2 and DTU for the Series 3 are summarized in Table 4.6.

Table 4.5 The dimension properties of the test plates

	The thickness of UD (mm)	The thickness of BIAX (mm)	Total thickness (mm)	Stacking sequence
Thin plates (S_1 series)	0.59	0.36	9.7	$[BIAX/4\times UD(0^o)/ BIAX /3\times UD(0^o)]_s$
Mid-thick plates (S_2 series)	0.59	0.36	15.14	$[BIAX/4\times UD(0^o)/ BIAX/ 4\times UD(0^o)/ BIAX/ 3\times UD(0^o)]_s$
Thick plates (S_3 series)	0.93	0.48	19.62	$[BIAX/4\times UD(0^o)/BIAX/ 3\times UD(90^o)/BIAX/ 2\times UD(0^o)]_S$

Note: UD = unidirectional layer (0^o or 90^o); BIAX = biaxial layers (45/-45)

Table 4.6 Material and strength properties of the test plates

	Thin and mid-thick plates (S_1 and S_2 series)	Thick plates (S_3 series)
E_1	35204 MPa	56210 MPa
E_2	9437 MPa	18075 MPa
ν_{12}	0.268	0.284
G_{12}	2169 MPa	4264 MPa
X_t	698 MPa	1141 MPa
X_c	191 MPa	952 MPa
$Y_t = Z_t$	43 MPa	22 MPa
$Y_c = Z_c$	69 MPa	127 MPa
S	30 MPa	64 MPa

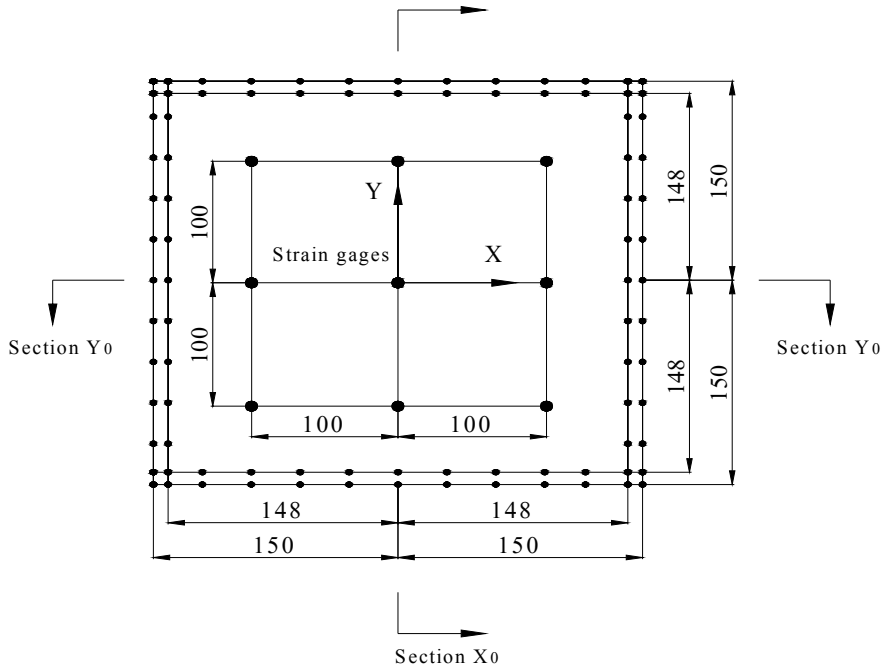

Figure 4.10 The measurement points

During the tests, each edge for the $X = \pm 150$, $Y = \pm 150$, $X = \pm 148$, $Y = \pm 148$ was divided into 11 points, in which displacements in the X, Y and Z directions were extracted. All the specimens were also equipped with nine strain gages to monitor strains of the panels during loading at the selected positions shown in Figure 4.10. The responses of the gages and the end-shortening of the panels were monitored and recorded up to comprehensive failure of the panel

4.5.2 FE Modelling and Boundary Conditions

In the finite element analysis, the boundary condition should be treated with care because minor changes in support can substantially affect results. In these test models, the heavy steel plates were used to fix the edges in order to prevent out-of-plane movements in the experiments. The boundary conditions at the edges of the plate lie somewhere between simple supports and fully clamped. Therefore in order to reproduce the experimental conditions of the test as precisely as possible, the model of active area 300mm × 300mm is modelled by 30 × 30 finite element mesh. The boundary condition of the specimens is considered as nonlinear, and set using the displacement values extracted from experimental data from the NTUA and DTU tests. The displacement values of nodes between these measurement points are linearly interpolated directly and set as table parameters on a function of time and input into ANSYS from external files. The displacement boundary condition is then applied progressively according to the time-load history. The ANSYS solver is set to interpolate linearly between these values through the time-load steps. The following two types of boundary conditions are considered.

(a) Boundary Condition 1

Boundary Conditions1 (BC1) refers to the panels with non-linear boundary condition without rotations. X-direction displacement (along the compressive load direction) and z-direction displacement (out-of-plane direction) are applied in the edges AB and CD of the models. Edges AD and BC of the panel are only constrained by displacement values in z-direction and the remaining degrees of freedom at the nodes

are kept free. In order to constrain the rigid displacement, Y-direction displacement at the centre point of the panel is set to zero. The finite element model with nonlinear boundary condition 1 is illustrated in Figure 4.11.

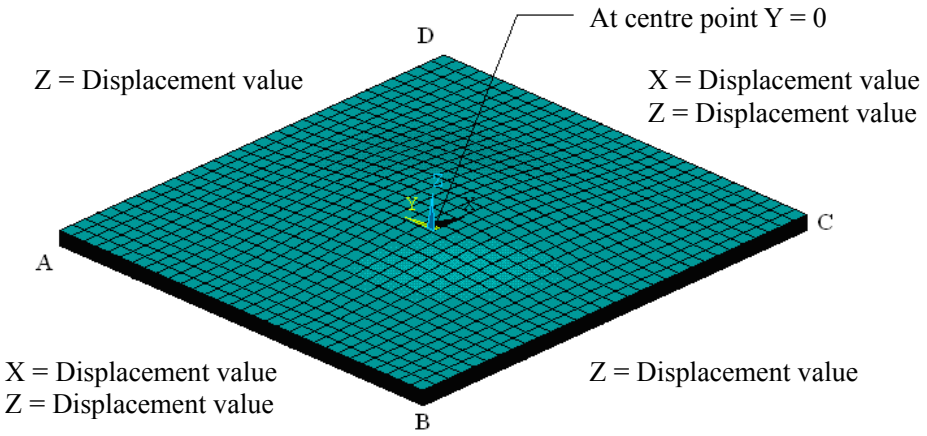

Figure 4.11 Finite element model with nonlinear boundary condition 1

(b) Boundary Condition 2

Boundary Conditions 2 (BC2) refers to a plate with non-linear boundary condition with rotations. Except for boundary conditions given in BC1, the rotations of the AB and CD edges around the Y-axis and the BC and AD edges around the X-axis are applied. These rotation values are obtained by comparing the Z displacement values at positions which have been measured during loading between two closed edges. The finite element model with nonlinear boundary condition 2 is illustrated in Figure 4.12.

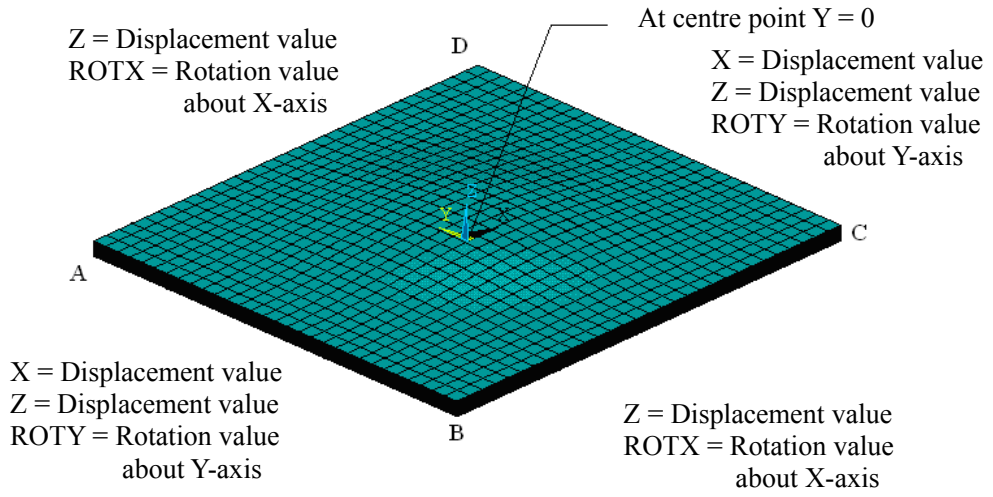

Figure 4.12 Finite element model with nonlinear boundary condition 2

Table 4.7 The maximum values of stress for all plates

	Maximum imperfection (mm)	Test results (MPa)	FEM with BC1 (MPa)	Deviation (%)	FEM with BC2 (MPa)	Deviation (%)
Thin plates (S_1 series)	0	112.6	80.0	-29.0	123.6	9.8
	3.2	93.3	69.8	-25.2	98.01	5.1
	9.6	80.7	64.8	-19.7	80.96	0.3
Mid-thick plates (S_2 series)	0	184.1	-	-	-	-
	3.2	144.6	110.7	-23.4	131.9	8.8
	9.6	137.1	96.4	-29.7	116.5	15.0
Thick plates (S_3 series)	0	***277.7***	***464.0***	***67.1***	***612.5***	***120.6***
	9.6	210.9	156.7	-25.7	150.5	-28.6

Note: FEM = finite element model, BC1 = boundary conditions 1 and BC2 = boundary condition 2

4.5.3 Results and Discussion

The maximum values of stress of all these plates are summarized in Table 4.7. The comparison between the numerical results and corresponding results from the experiments are shown in Figures 4.13 - 4.33. The compressive stresses from the experiments are taken as the total force on the cross-section area of the specimen's full width. For the finite element analysis, the stresses are taken on the active area's width of plates. The out-of-plane displacement variations along the length and width of the panel at the ultimate stress levels are plotted as well (Section X_0 and Section Y_0 shown in Figure 4.10). The out-of-plane displacement distributions at the ultimate load from ANSYS are also shown in Figures.

For the series of thin plates, all plates can get to the final load. The predicted loads are in good correlation with the test results. For the models with boundary condition 1, as expected, progressive failure analysis underestimated the final failure loads compared to test one since the rotations along the edges were not considered. For the models with boundary condition 2, the in-plane stiffnesses and ultimate stresses are larger than experimental results, especially in the case of the plate with imperfection 3.2mm. The maximum difference between the finite element analysis and test is observed up to 29%. The different failure modes can be found for these plates with various imperfections. For the models with boundary condition 1, the initial failures occur around the edges of panel and the failure mode is the fibre breakage. For the models with boundary condition 2, the failures occur around the unloaded edges at early stage of loading.

For the series of mid-thick plates, only plates with imperfection 3.2mm and 9.6mm can get to the final load because of the convergence problem. The overall behaviour of the finite element simulation is similar to the experimental observations for the models with boundary condition 2. As expected, the compressive load versus deflection curves for the models with boundary condition 1 have reduced stiffness of the finite element models and the predicted ultimate stresses are significantly lower

than the experimental one. The maximum deviation is found to be 29.7% between the test results and finite element predictions in the case of the plate with imperfection 9.6mm. The initial failure mode for the models with boundary condition 1 is fibre breakage and for the models with boundary condition 2 is matrix failure mode around the edges of the plates.

For the series of thick plates, experimental results are available only for the perfect model and the model with imperfection 9.6mm. The overall panel responses show significant nonlinear behaviour during loading. The compressive load versus deflection curves from the tests and numerical analysis exhibit a trend similar to that for the thick plate without imperfection although the difference is considerable. The progressive failure analysis over-predicted the final failure loads up to 67.1% for the model with boundary condition 1 and 120.6% for the model with boundary condition 2, respectively. A possible reason for this is that initial geometric imperfections exist and these could be the cause for the considerable influence on the collapse load of the panels. The plate's thickness and geometric imperfection were not measured for the thick plate series because of the unavailability of precisely measured equipment at the Technical University of Denmark. Another possible reason is the delamination of the internal plies of this thick plate which may lead to a lower collapse load. For the thick plate with imperfection 9.6mm, good agreement exists for both models between the test results and the numerical results until the analyses are completed.

The possible reasons for the most significant difference between the experimental measurements and the numerical predictions may be due to the use of nonlinear boundary conditions and conservative damage modelling. For the nonlinear boundary condition, the linearly interpolated displacements between the measurement points may cause discontinuities on the edge surfaces which result in occurrence of high localised stresses, hence, premature failure of their neighbouring elements. In the damage modelling of finite element analysis, the assumption based on that the material property associated with that mode of failure is degraded instantly to zero is conservative, which may cause the lower stresses.

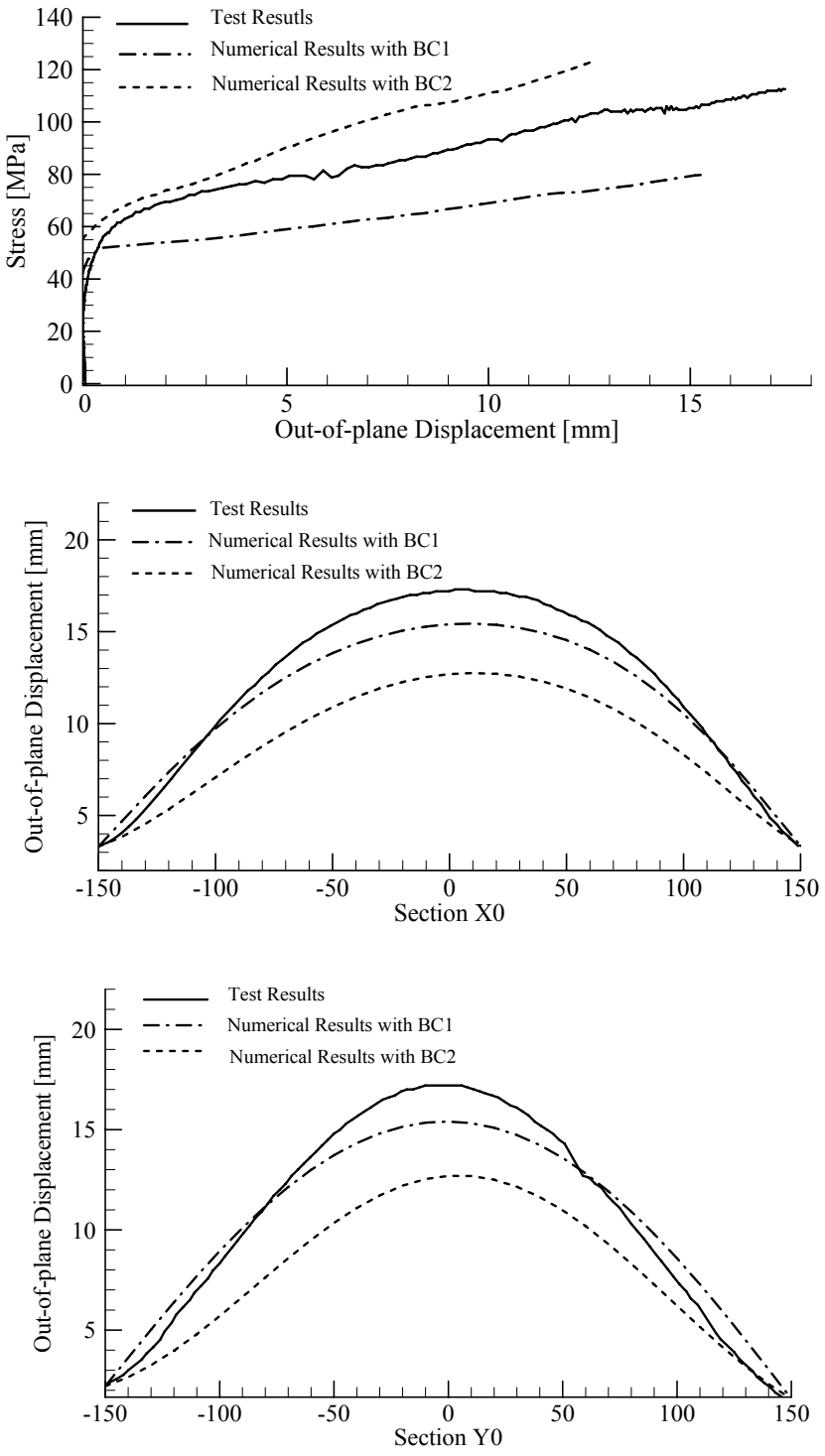

Figure 4.13 Numerical and experimental results for thin plates S_1 without imperfection

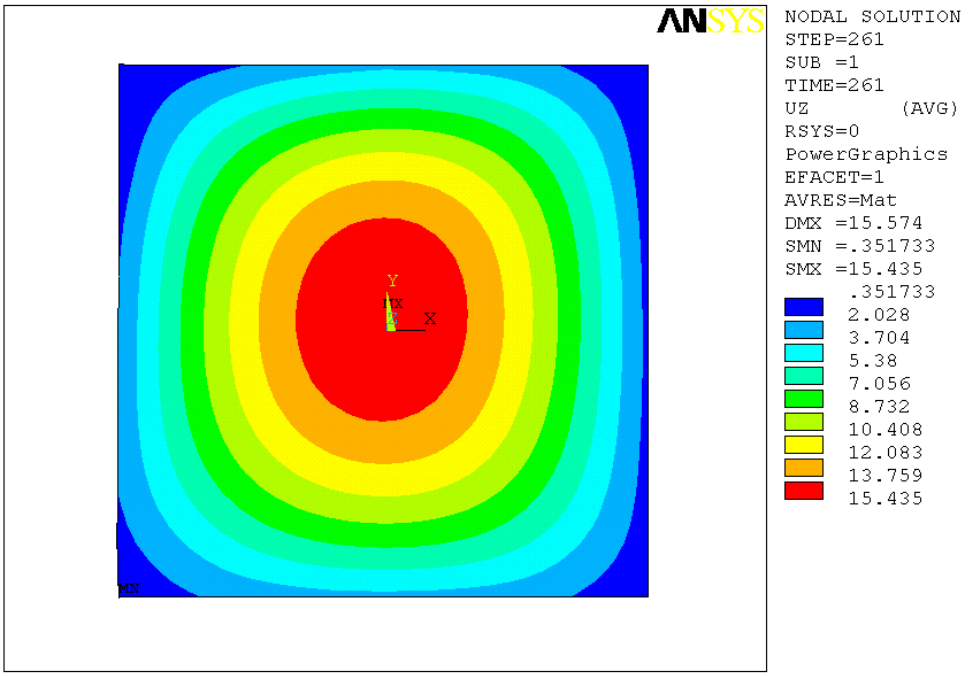

Figure 4.14 The out-of-plane displacement distribution at the ultimate load for thin plates S_1 without imperfection (BC1)

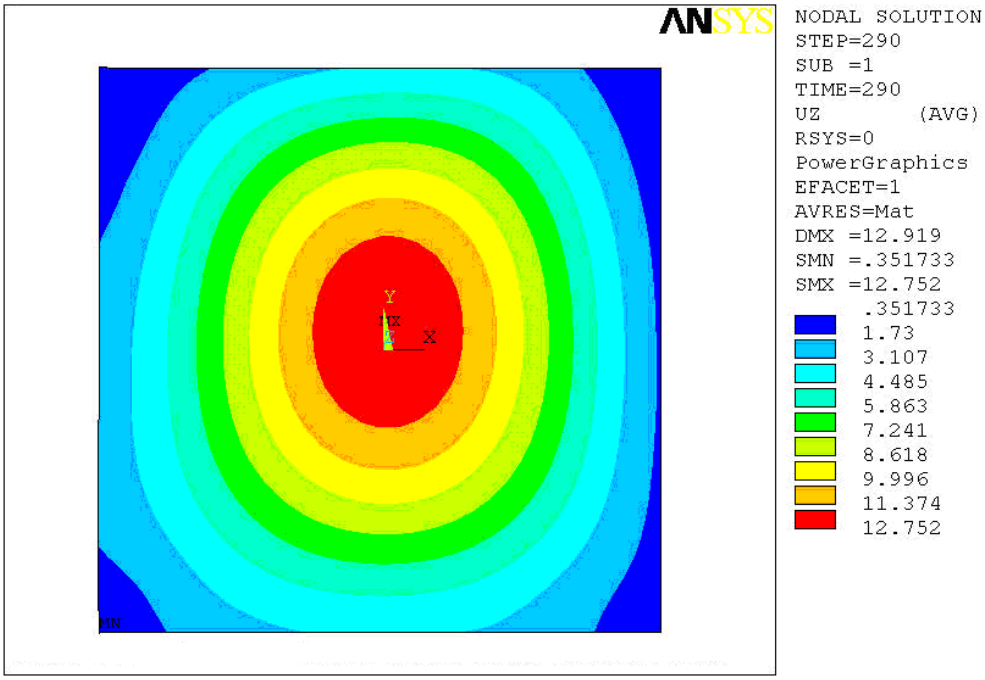

Figure 4.15 The out-of-plane displacement distribution at the ultimate load for thin plates S_1 without imperfection (BC2)

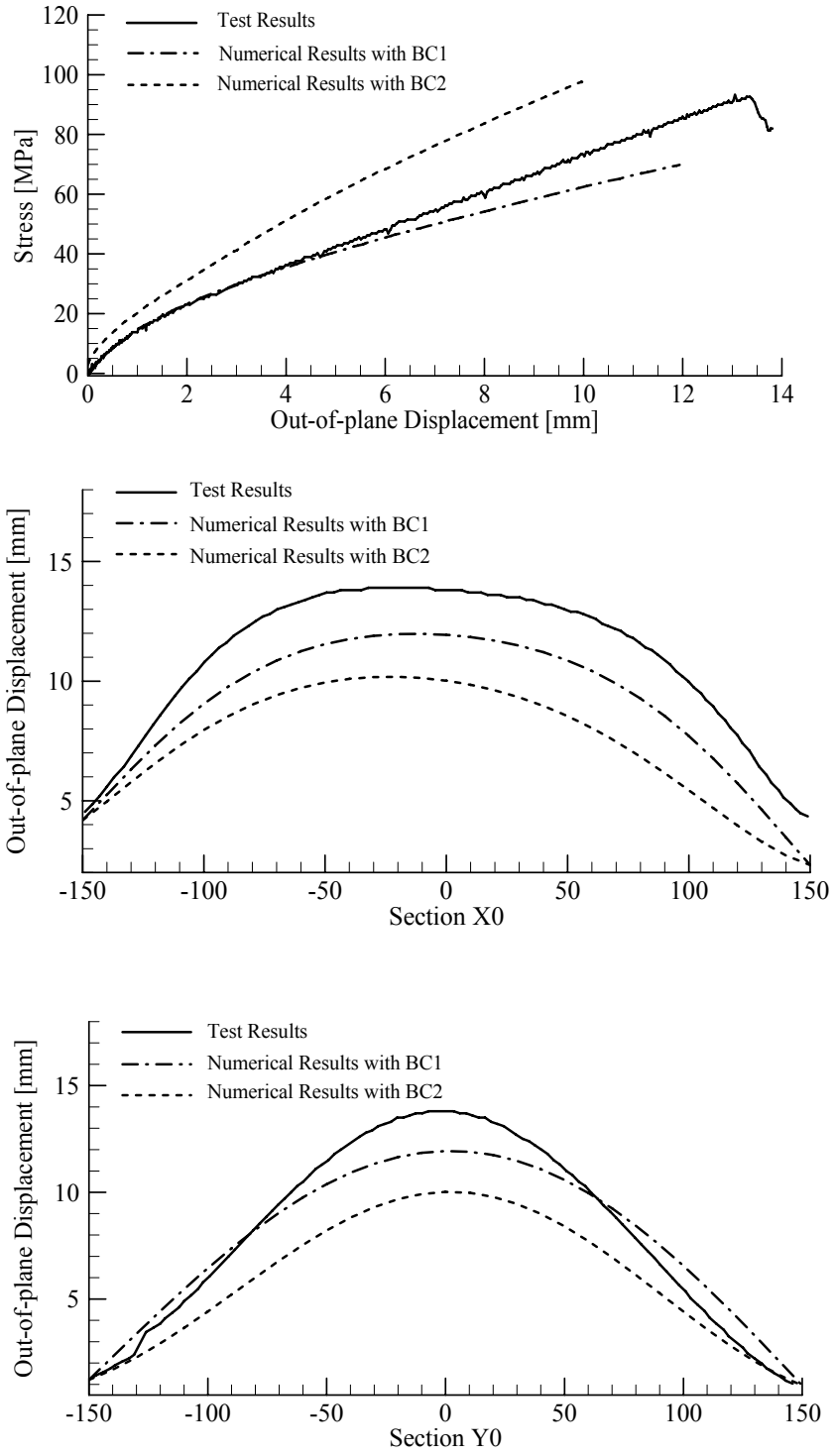

Figure 4.16 Numerical and experimental results for thin plates S_1 with imperfection 3.2mm

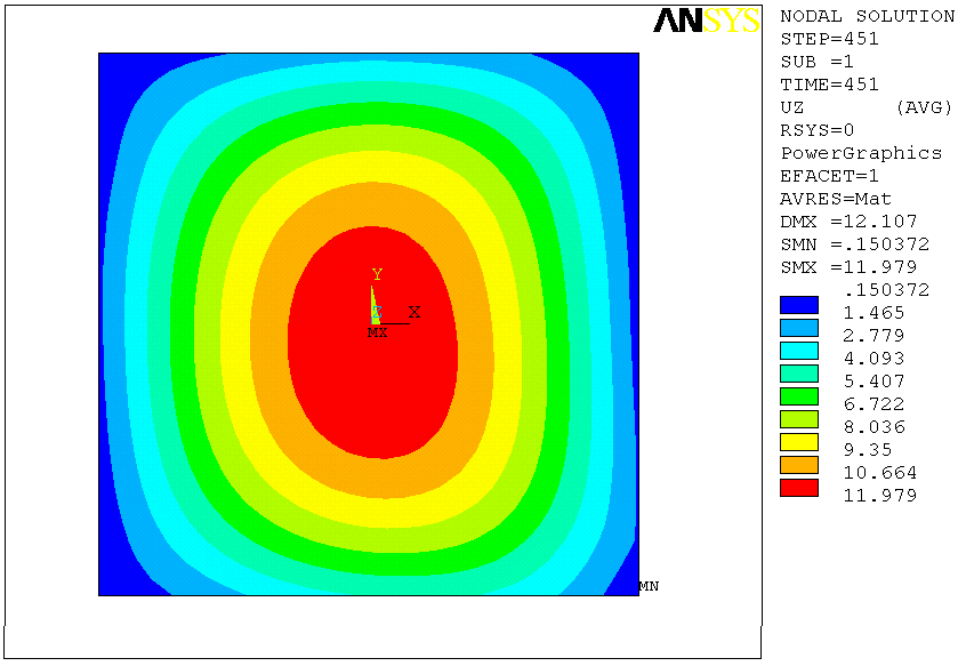

Figure 4.17 The out-of-plane displacement distribution at the ultimate load for thin plates S_1 with imperfection 3.2mm (BC1)

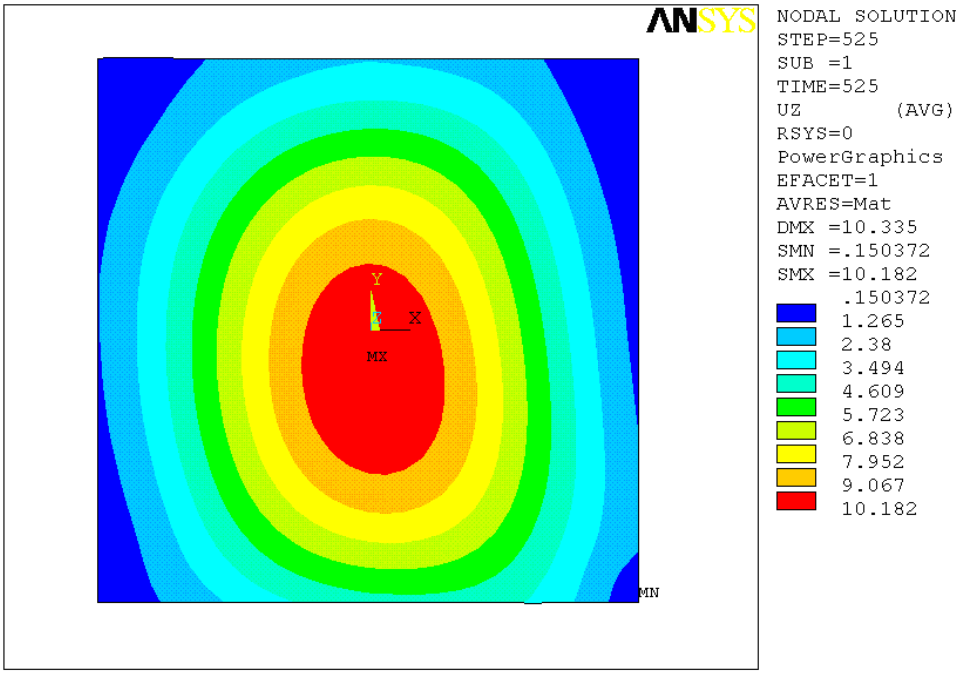

Figure 4.18 The out-of-plane displacement distribution at the ultimate load for thin plates S_1 with imperfection 3.2mm (BC2)

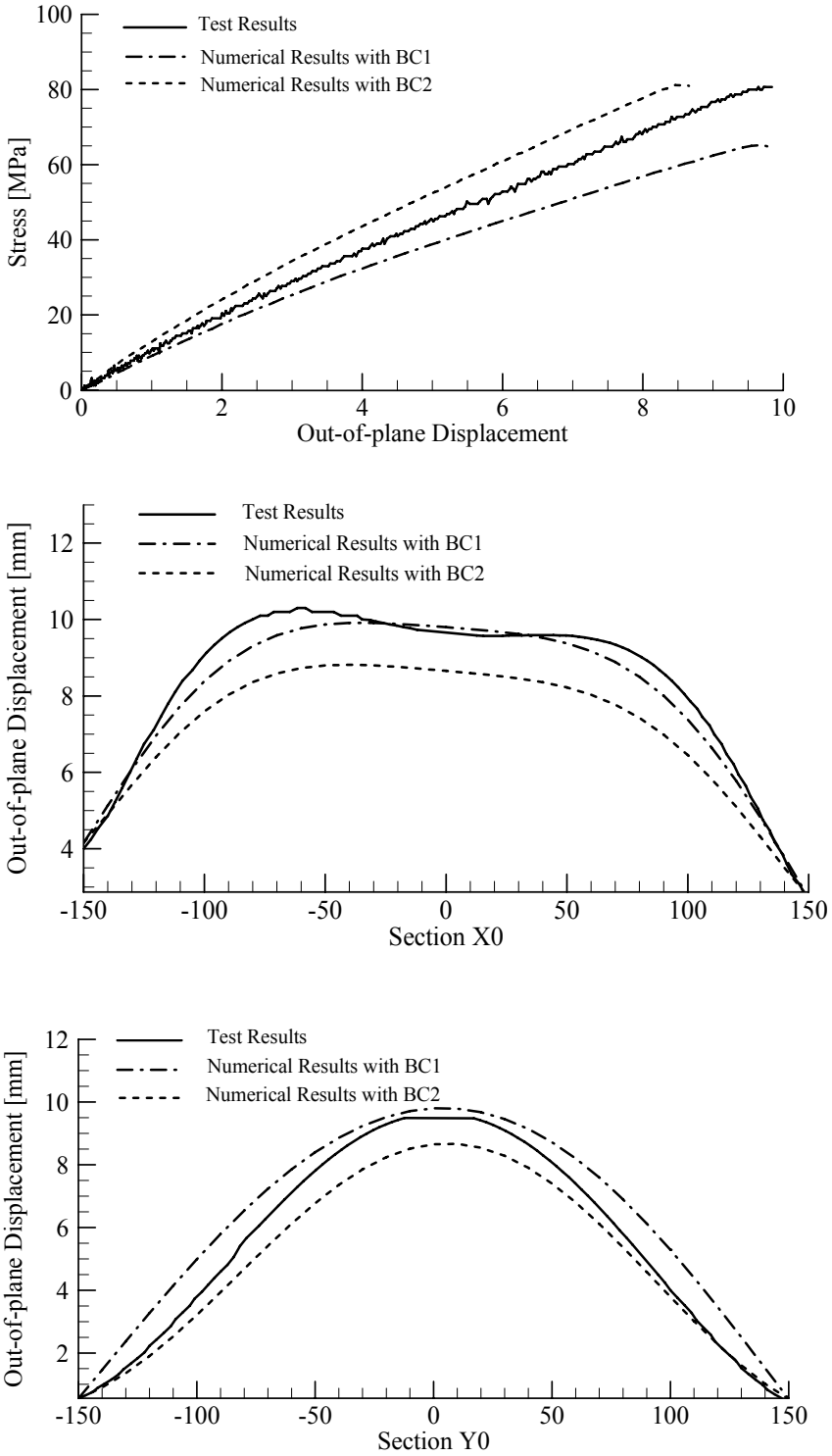

Figure 4.19 Numerical and experimental results for thin plates S_1 with imperfection 9.6mm

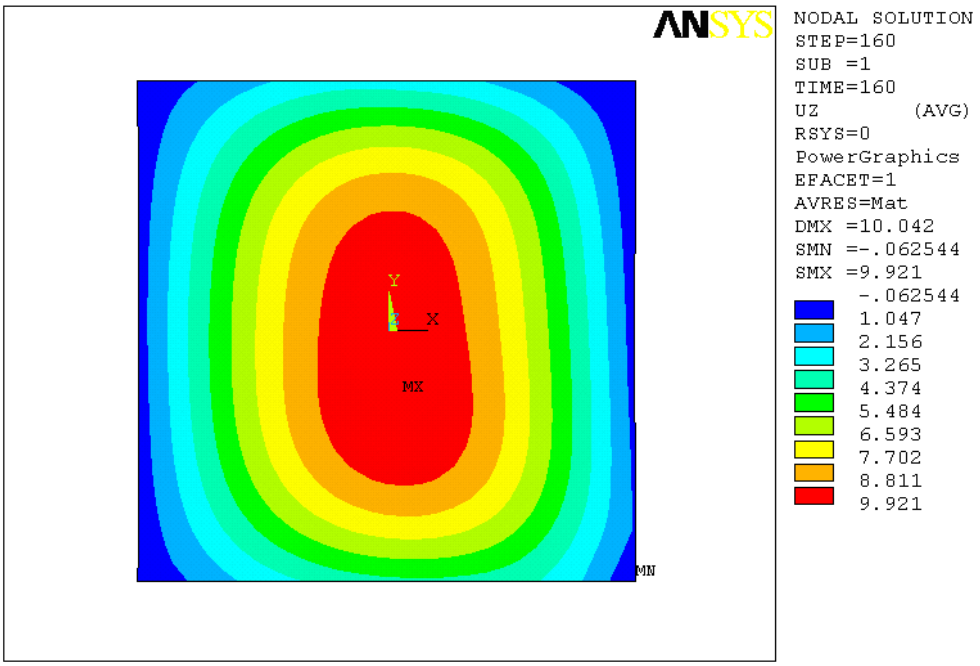

Figure 4.20 The out-of-plane displacement distribution at the ultimate load for thin plates S_1 with imperfection 9.6mm (BC1)

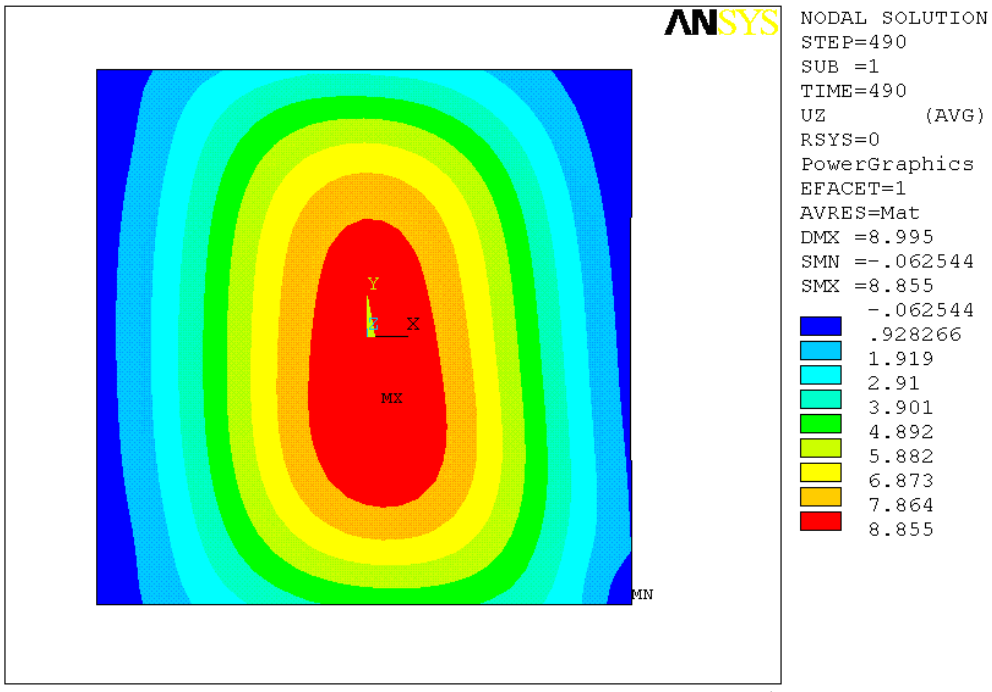

Figure 4.21 The out-of-plane displacement distribution at the ultimate load for thin plates S_1 with imperfection 9.6mm (BC2)

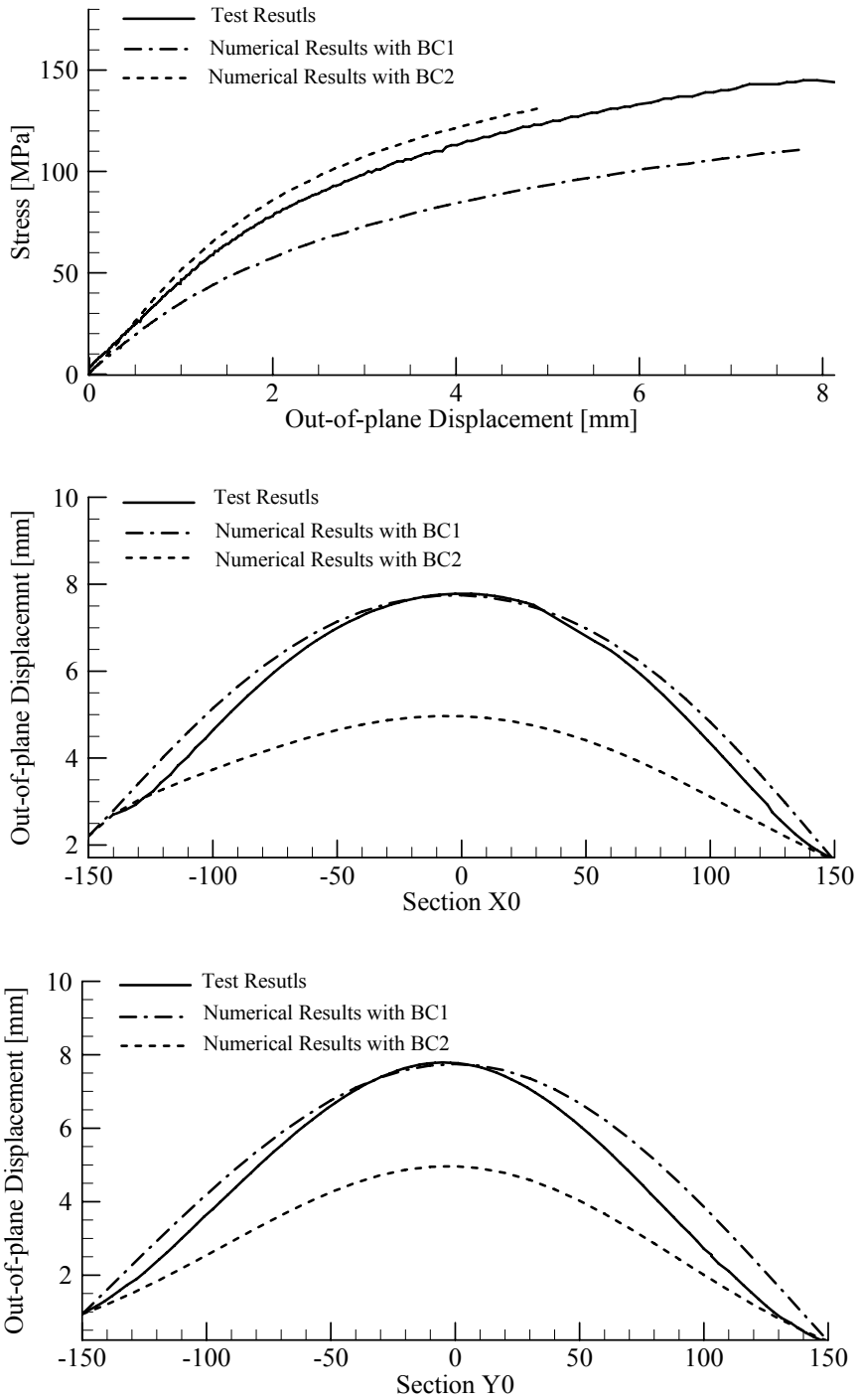

Figure 4.22 Numerical and experimental results for mid-thick plates S_2 with imperfection 3.2mm

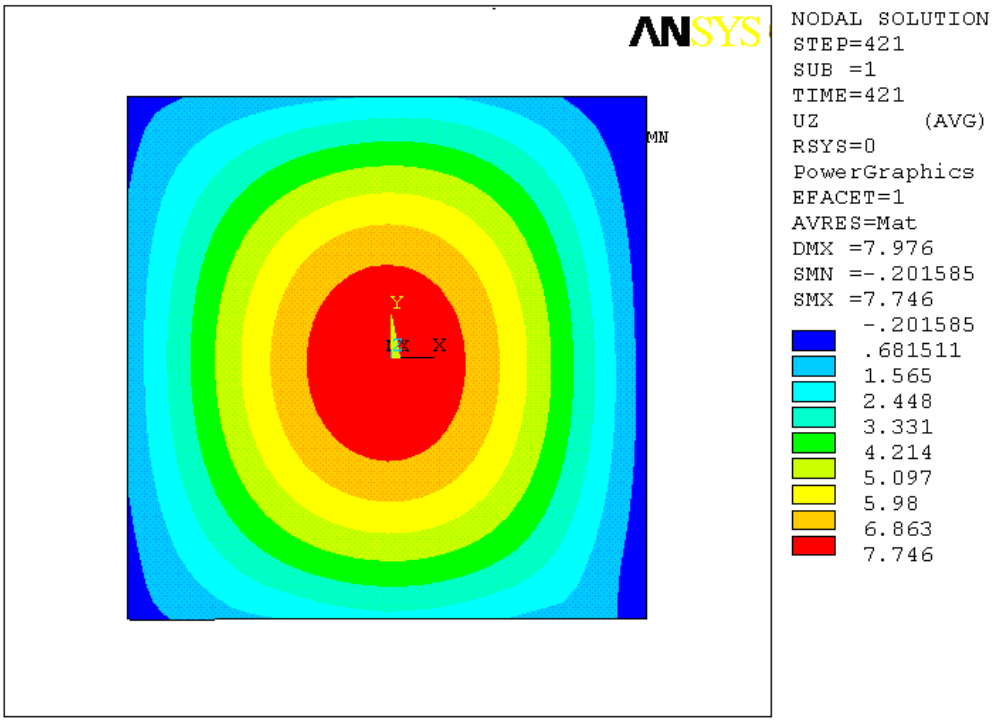

Figure 4.23 The out-of-plane displacement distribution at the ultimate load for mid-thick plates S_2 with imperfection 3.2mm (BC1)

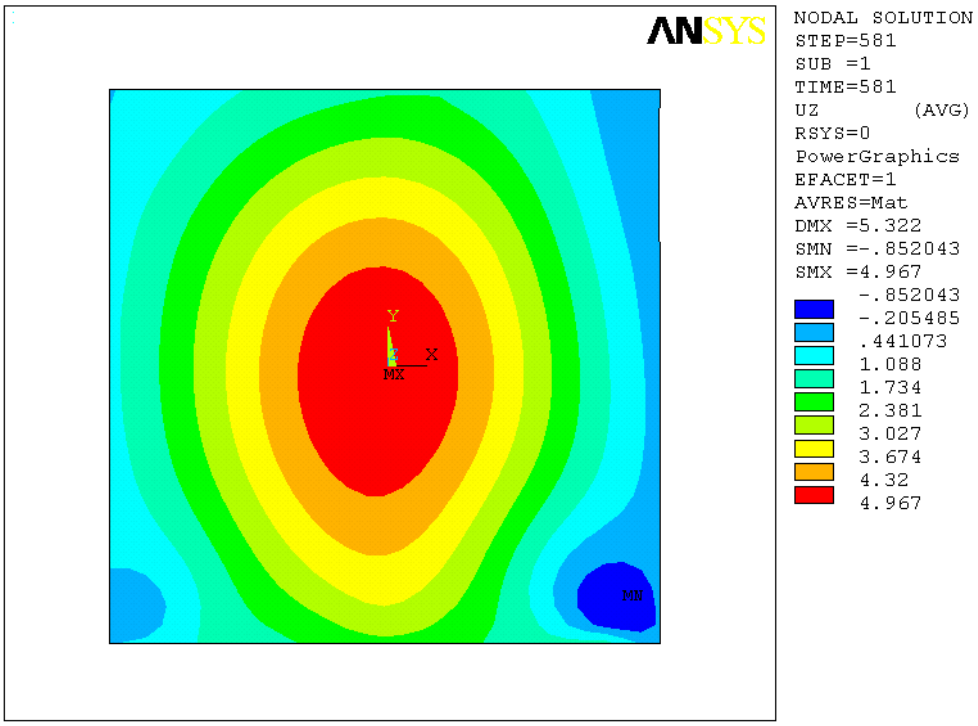

Figure 4.24 The out-of-plane displacement distribution at the ultimate load for mid-thick plates S_2 with imperfection 3.2mm (BC2)

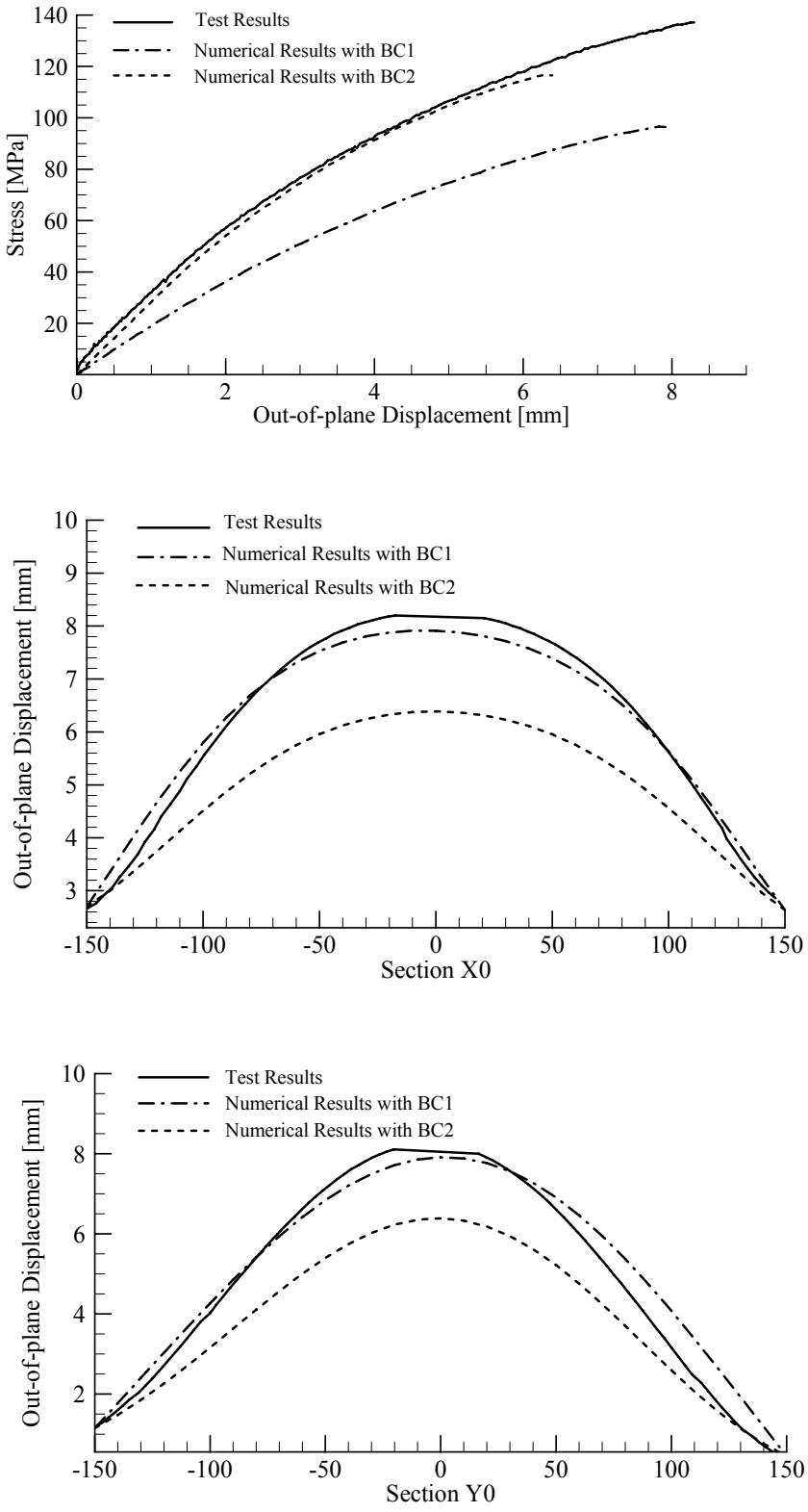

Figure 4.25 Numerical and experimental results for mid-thick plates S_2 with imperfection 9.6mm

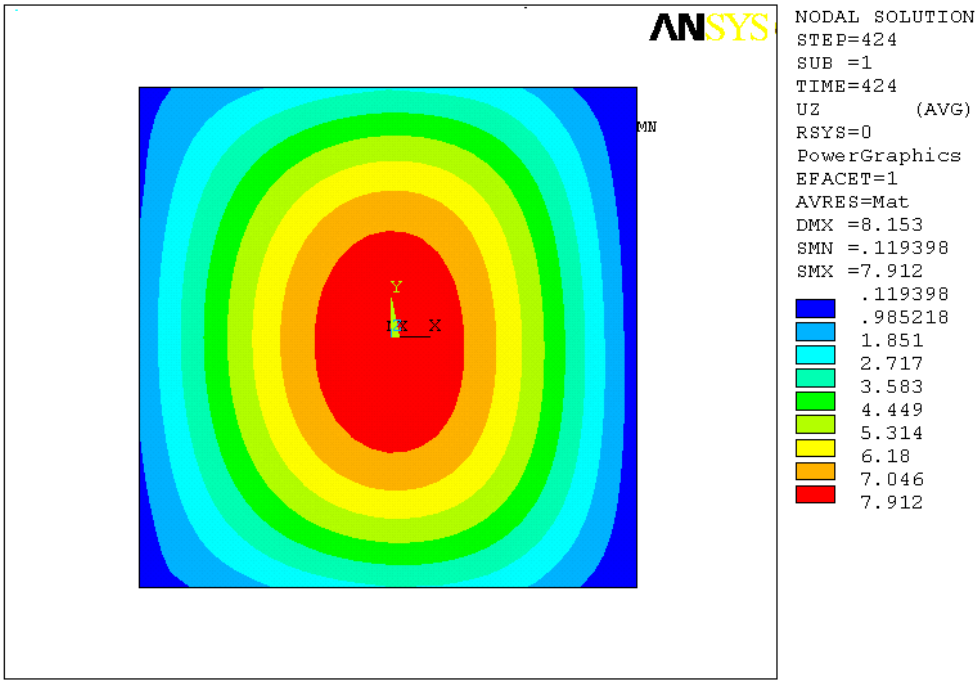

Figure 4.26 The out-of-plane displacement distribution at the ultimate load for mid-thick plates S_2 with imperfection 9.6mm (BC1)

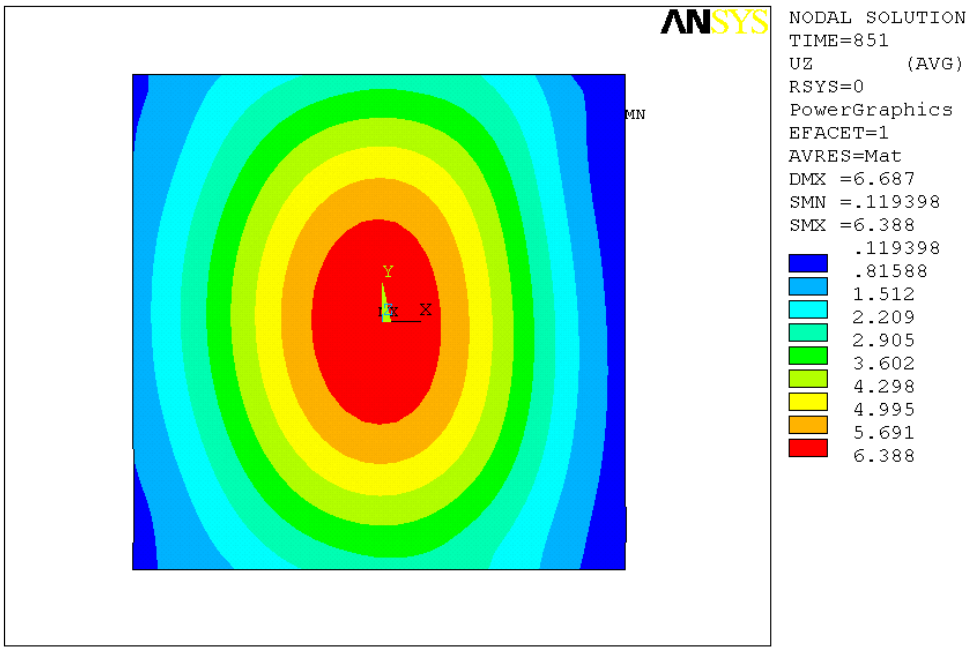

Figure 4.27 The out-of-plane displacement distribution at the ultimate load for mid-thick plates S_2 with imperfection 9.6mm (BC2)

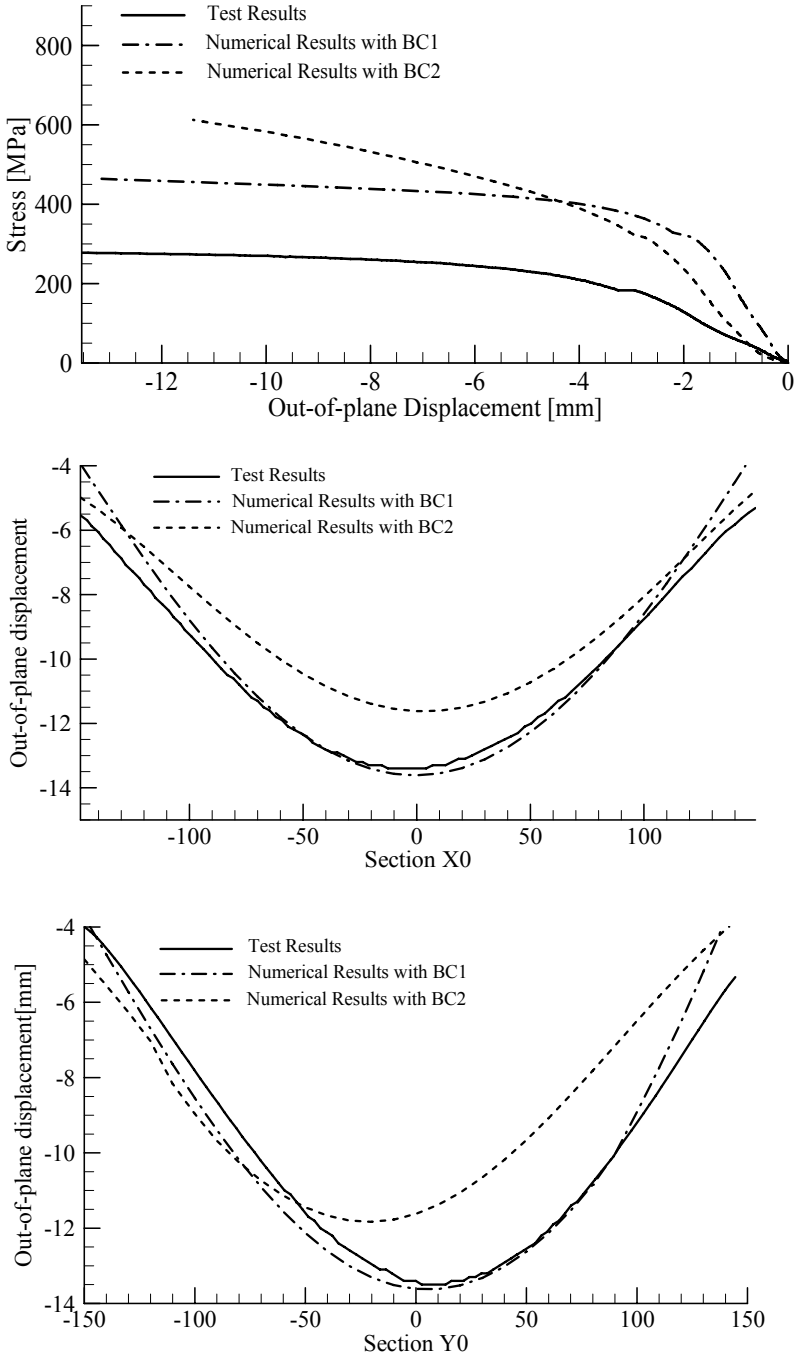

Figure 4.28 Numerical and experimental results for thick plates S_3 without imperfection

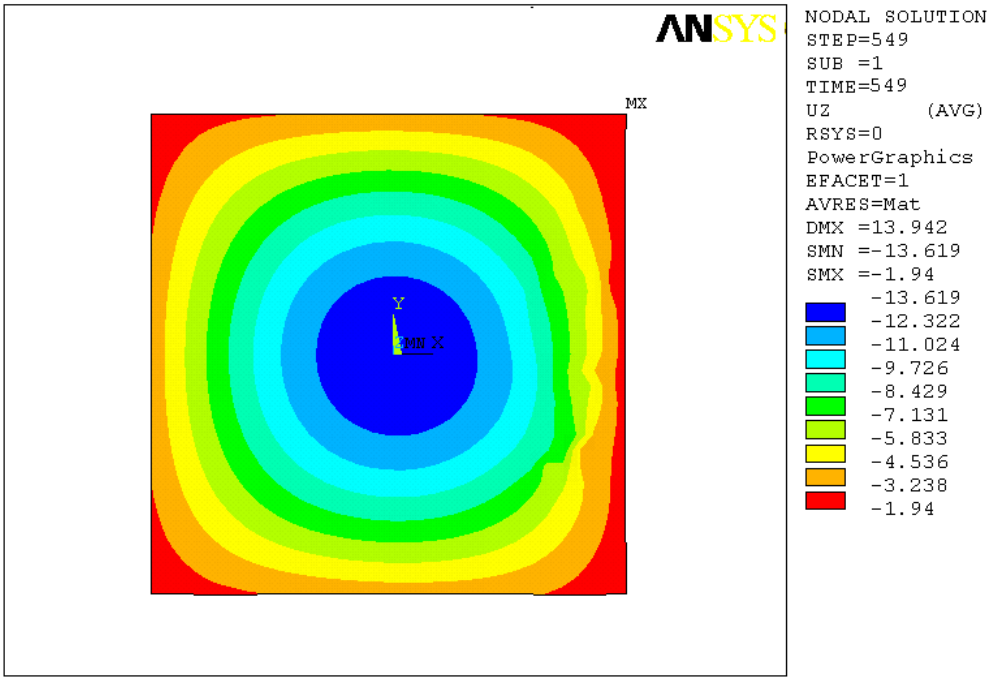

Figure 4.29 The out-of-plane displacement distribution at the ultimate load for thick plates S_3 without imperfection (BC1)

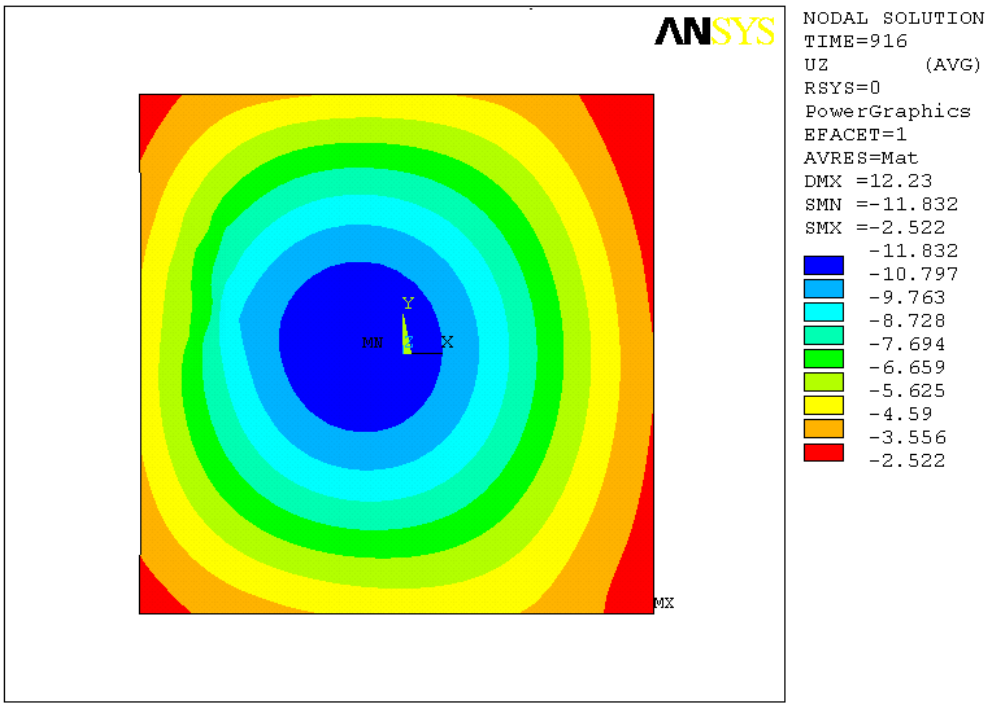

Figure 4.30 The out-of-plane displacement distribution at the ultimate load for thick plates S_3 without imperfection (BC2)

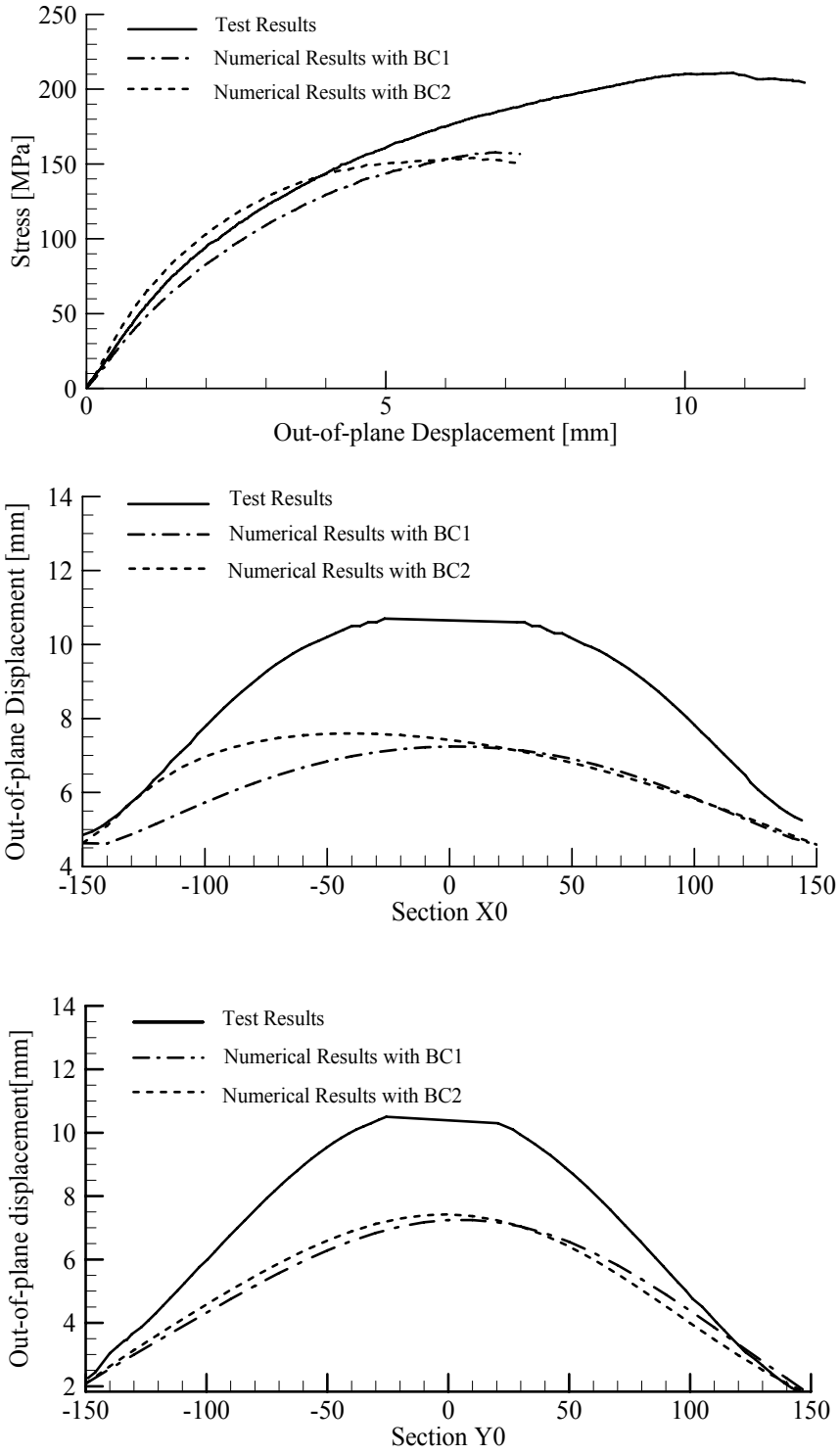

Figure 4.31 Numerical and experimental results for thick plates S_3 with imperfection 9.6mm

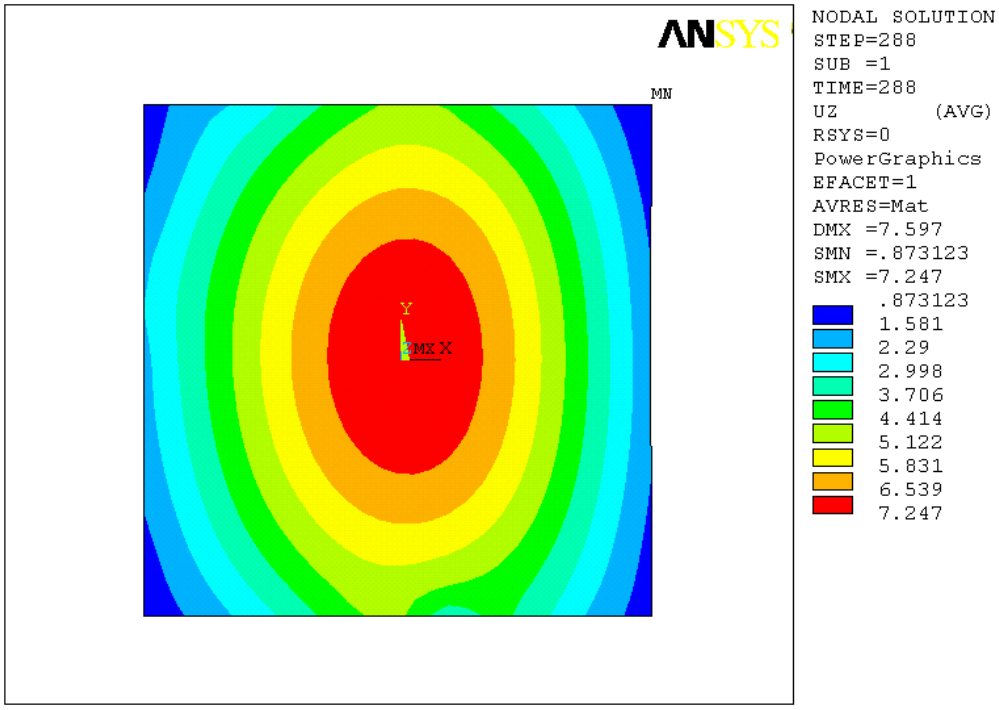

Figure 4.32 The out-of-plane displacement distribution at the ultimate load for thick plates S_3 without imperfection (BC1)

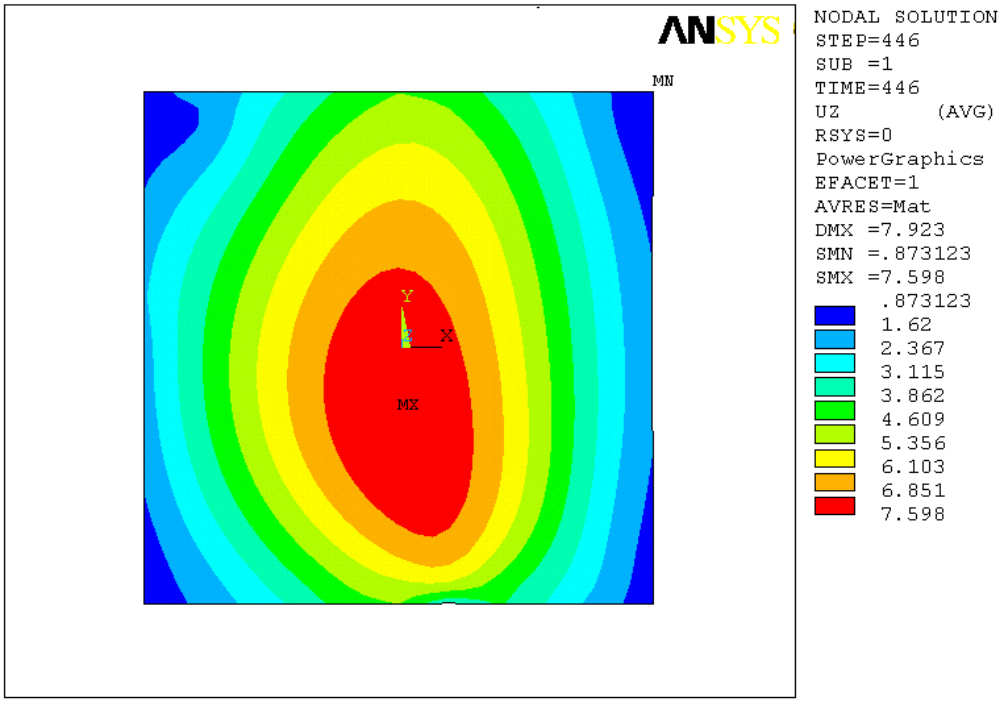

Figure 4.33 The out-of-plane displacement distribution at the ultimate load for thick plates S_3 without imperfection (BC2)

4.6 Probabilistic Approach to Composite Laminate Design

4.6.1 Introduction

One practical example is selected to apply deterministic and probabilistic approaches to design laminate composite plate. The length and breadth of panel are taken as 500mm. The thickness is same for all plies t = 0.98mm. The panel is assumed to have 10 ply woven roving lamina with the material properties provided in Table 4.8. The edges of the plate are assumed to be simply supported and exposed to slam impacts and wave slap 75KPa

Table 4.8 Material and strength properties

Mechanical properties	Values	Strength properties	Values
E_1	17180 MPa	X_t	238.6 MPa
E_2	17180 MPa	X_c	324.5 MPa
G_{12}	3520 MPa	Y_t	238.6 MPa
G_{13}	5150 MPa	Y_c	324.5 MPa
G_{23}	5150 MPa	T	80.9 MPa
v_{12}	0.17	$R = S$	60.7 MPa

The general purpose structural reliability analysis program CALREL (Liu et al, 1989) developed by the University of California is used to perform these analyses. CALREL is a FORTRAN-based program and designed to be used in a wide variety of component and system structural reliability analyses. Once the probabilistic model is established, a variety of useful information such as reliability index, probability of failure and a variety of sensitivity measures are obtained.

4.6.2 Probabilistic Analysis Based on Strength Limit

The FSDT analysis gives a maximum stress level of 65.51MPa at the outer fibre of the laminate. If this stress is considered, then the safety factor is 238.6/65.51 = 3.64, which has a greater safety margin than required by the Lloyds Register classification rules (2004), which require a safety factor of 3. In the reliability analysis, material and strength properties, thickness of plate and distributed transverse load are treated as independent random variables given in Table 4.9. The above model with the following safety margin equation is run for reliability analysis based on strength limit

$$G = X_t - \sigma \tag{4.13}$$

where X_t is the ultimate tensile stress and σ is the maximum stress in the plate calculated by FSDT programme.

Table 4.9 Statistical properties of basic design variables

Property	Mean value	COV	Distribution
$E_1 = E_2$	17180 MPa	0.05	Lognormal
G_{12}	3520 MPa	0.1	Lognormal
t	0.98mm	0.05	Normal
P	75KPa	0.2	Weibull
X_t	238.6 MPa	0.1	Lognormal

Reliability index $\beta = 6.497$ and probability of failure $P_f = 4.09\times10^{-11}$ are obtained by FORM. Loading intensities are rarely known with any uncertainty. Thus the Coefficient of Variation (COV) of load is then changed and these results are shown in Figure 4.34. It is seen that the safety index β becomes 7.03, 5.94, 5.37, 4.83, 4.33 and the probability of failures P_f becomes 1.01×10^{-12}, 1.46×10^{-9}, 3.91×10^{-8}, 6.96×10^{-7}, 7.34×10^{-6} when the COV of load is changed to 15%, 25%, 30%, 35% and

40% respectively. It is thus very sensitive to the statistics of load and the reliability results become more reliable as the statistics are known with more precisely.

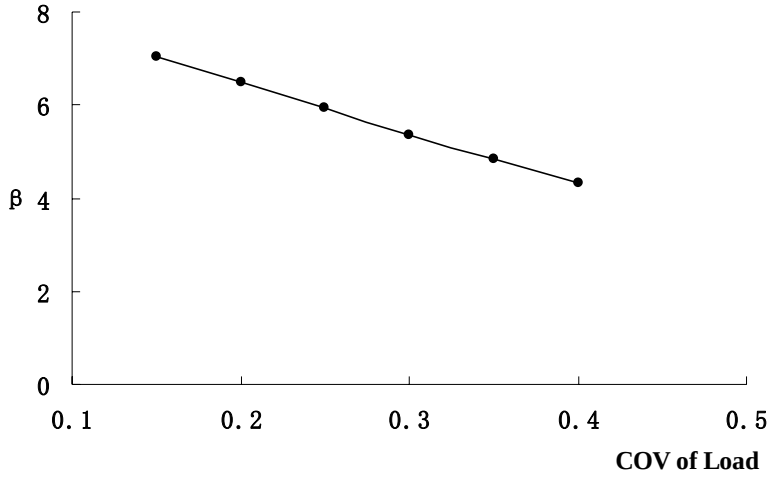

Figure 4.34 Variation of β with change of COV of load

4.6.3 Probabilistic Analysis Based on Stability Limit

The above model is run for reliability analysis based on buckling criteria with the following safety margin equation

$$G = P_{cr} - P \tag{4.14}$$

where P_{cr} is the critical buckling load and P is the applied load, The different ratios of P_{cr}/P are assumed and the results are shown in Figure 4.35

From the Figure 4.35, it is evident that the safety index decreases i.e. probability of failure increases as the design load approaches the critical buckling load for any deterministic safety factor against buckling.

Figure 4.35 can be used to calculate the safety index β and the probability of failure P_f. For the design against buckling, the code recommends safety factor to be used for design. For example, for a safety factor of 3.0, the design load for the example will

be 171480/3 = 57160 N/m, and for this load, the calculated safety index β is 7.1017 or can also be interpolated from Figure 4.35, hence the probability of failure P_f is 6.163×10^{-13}. This means one in 1.62×10^{12} structures will fail if we use the assumed statistics of the design parameter which have been used in deriving Figure 4.35.

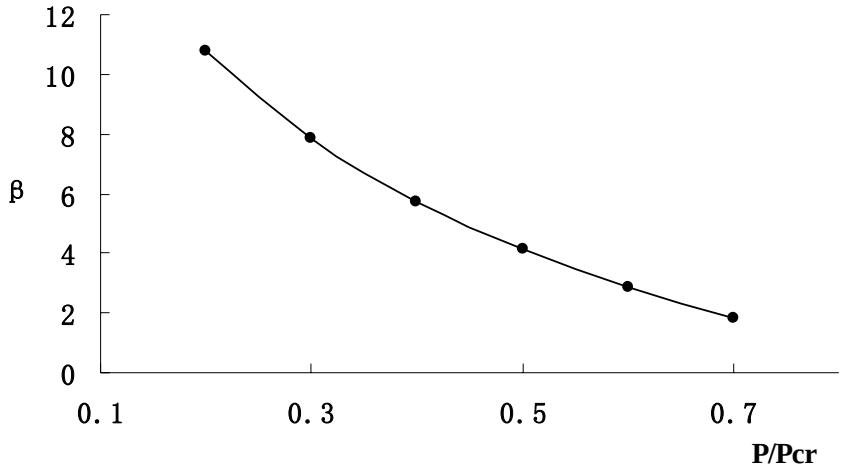

Figure 4.35 Variation of β with change of P/P_{cr}

4.7 Summary

In this chapter, a nonlinear finite analysis technology including the multi-frame restart analysis was developed to predict the first failure and final collapse loads. Both geometric and material nonlinearities were considered. Tsai-Wu failure criterion was used to predict the failure mechanism and a constant degradation method was adopted to degrade the material properties after failure was detected. The numerical accuracy was evaluated with the results published in the literatures and good correlation between the experimental and numerical predictions were obtained. The benchmark study was then performed on a number of fibre reinforced plates with various thicknesses and imperfections.

Finally, the probabilistic approach was considered to laminate composite plates in

order to tackle the design in a more realistic way based on one practical example. The effects of material properties, geometric properties and load on strength limit and stability limit was considered for the application of the probabilistic design approach.

Chapter 5:
Strength and Reliability Analysis of Stiffened Plates

5.1 Introduction

Grillage or stiffened panels comprising a plate, longitudinal stiffeners and transverse frames are important components in ship and offshore structures. Most of these structures can be found in decks, bottoms, bulkheads, side shell and superstructures. The primary purpose of these structures is to absorb lateral loads and contribute to sharing those loads with the ship's primary structure. The panel members can also carry part of the longitudinal bending stress depending on the location of the panels. Top-hat stiffened single skin structure is an excellent structural style because it is intensively used in ship construction as a result of reduced costs with increasing number of hulls, easy to fit equipment and easy for quality control.

This chapter explores the use of a stochastic approach to the design of stiffened composite panels for which typical application can be found in composite ship structures. Uncertainties associated with basic strength variables (e.g.dimension, material properties, etc), load variables and model uncertainties in strength predictors (e.g. ultimate strength) are considered. Limit state equations have been formulated for use in the reliability and sensitivity analyses. Sensitivity of basic variables is calculated using the CALREL code and the variables that have large impact on structural safety have been identified. Based on the important variables, a parametric study is conducted to investigate any detectable trend in the safety index with various design parameters.

5.2 Analytical Methods Adopted

The definition of a stiffened panel is a panel of plating bounded by other structure, the latter having significantly greater stiffness when compared to the panel and its stiffeners. Examples of the other structures include transverse bulkheads, longitudinal bulkheads, side shell or large longitudinal girders. A typical stiffened panel configuration with the hat-section stiffeners is shown in Figure 5.1. The stiffened panel is referred to x- and y- axis coinciding with its longitudinal and transverse edges, respectively and a z-axis normal to its surface. The cross-section geometry is defined in terms of the six dimensions b_1, b_2, b_3, b_4, b_5 and d. The length and breadth of the stiffened panel are denoted by L and B, respectively. The spacing of the stiffeners is denoted by a between longitudinal stiffeners and b between transverse stiffeners. The numbers of longitudinal and transverse stiffeners are N_g and N_s, respectively. The structures forming a hat-stiffener are made of FRP laminates and they are assumed to be orthotropic plates.

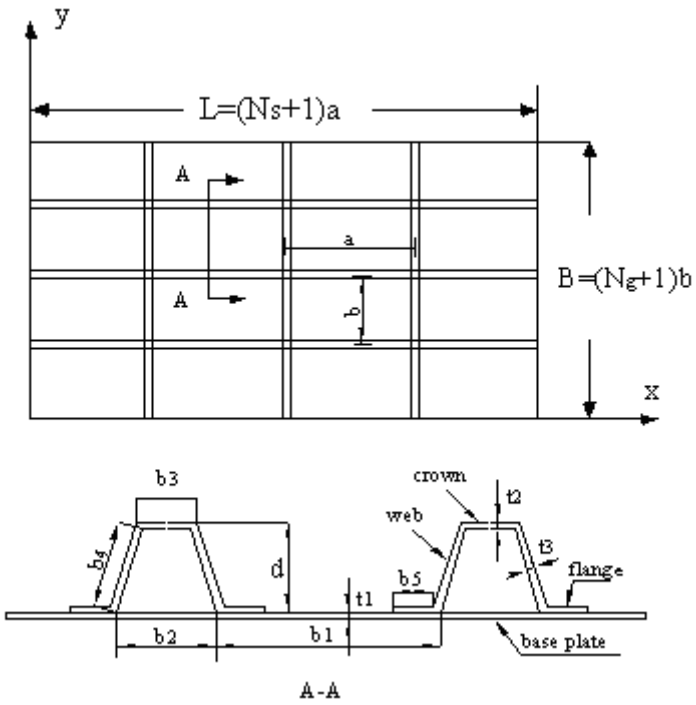

Figure 5.1 Orthogonally stiffened panel configuration with the hat-section stiffeners

According to Section 2.3.4 on the review of available structural analysis methods of stiffened composite plates, although folded plate method and numerical method are capable of giving comprehensive and adequate results, they are not computationally efficient from a design point of view for the considerable preparation and computational time. Particularly if the repeated analyses are required at the preliminary design stage due to the involvement of large number of variables. Simplified analytical methods provide a more time-effective means of calculating the strength of stiffened panels. For engineering practice, most of the necessary evaluation of stresses and deformations can be carried out by means of simple formulae based on beam and plate theory on idealized geometries and boundary conditions.

5.2.1 Grillage Model

Modified grillage analysis method based on energy method is adopted because the advantages of grillage analysis method compared to orthotropic plate method are that the different stiffener size and spacing of parallel stiffeners are allowed and the number of stiffeners in each direction is not restricted. Furthermore, the model allows for discontinuities such as hatch openings.

In the grillage model, the stiffened panel is idealized as a number of longitudinal and transverse beams. Each beam is assumed to consist of the stiffener plus a portion of the plate over which the stress can be assumed uniform with a value equal to the maximum value, i.e. effective flange breadth. In this grillage analysis, the torsional rigidity of the plate and Poisson's ratio effects on the overall behaviour of the stiffened panel are ignored. It is also assumed that those plates are simply supported and the bending deformation of the hat-stiffened panel is analyzed within linear elasticity assumption.

In the general method of grillage analysis, the double series expression for the deflection w of the stiffened panel can be assumed to be

$$w = \sum_{m=1}^{\infty}\sum_{n=1}^{\infty} f_{mn} \sin\frac{m\pi x}{L}\sin\frac{n\pi y}{B} \tag{5.1}$$

which fulfil the end conditions when the plate is simply supported along all edges. The coefficient f_{mn} may be determined by the condition that the change in potential energy due to the assumed deflection is minimum.

The total potential energy of the longitudinal girders and transverse stiffeners are given by

$$V_g = \frac{1}{2}\sum_{i=1}^{Ng} D_{gi}\int_0^L \left(\frac{\partial^2 w}{\partial x^2}\right)^2_{y=y_i} dx \tag{5.2}$$

$$V_s = \frac{1}{2}\sum_{j=1}^{Ns} D_{sj}\int_0^B \left(\frac{\partial^2 w}{\partial y^2}\right)^2_{x=x_j} dy \tag{5.3}$$

where $y_i = \frac{iB}{N_g+1}$, $x_j = \frac{jL}{N_s+1}$ when all girders and stiffeners are arranged at equal distance; $D_{gi} = \sum_{i=1}^{N_g}(EI)_{gi}$ and $D_{sj} = \sum_{i=1}^{N_S}(EI)_{sj}$ are the flexural rigidity of the i^{th} girder and the j^{th} stiffener, respectively.

The total potential energy are given by

$$\mathrm{V} = \mathrm{V_g} + \mathrm{V_s} \tag{5.4}$$

When the stiffened panel is subjected to a uniform pressure load q alone, the work of the external force are given by

$$W_q = \int_0^L\int_0^B q\sum_{m=1}^{\infty}\sum_{n=1}^{\infty} f_{mn}\sin\frac{m\pi x}{L}\sin\frac{n\pi y}{B}dxdy \tag{5.5}$$

When the stiffened panel is subjected to a uniform longitudinal compressive load p in the x-direction, the work of the external force are given by

$$W_{gi} = -\frac{1}{2} p \int_0^l \left(\frac{\partial w}{\partial x} \right)^2_{y_i} dx \tag{5.6}$$

$$W_g = \sum_{i=1}^{Ng} W_{gi} \tag{5.7}$$

The coefficients f_{mn} may be determined using the minimum potential energy theorem

$$\frac{\partial (V - W)}{\partial f_{mn}} = 0 \tag{5.8}$$

The coefficient f_{mn} can be expressed when the stiffened panel subjected to a uniform pressure load alone as

$$f_{mn} = \frac{16qLB}{\pi^6 mn \left[m^4 (N_g + 1) \frac{D_g}{L^3} + n^4 (N_s + 1) \frac{D_s}{B^3} \right]} \tag{5.9}$$

If the stiffened panel is subjected to a lateral load q as well as to axial compression p, the deflection parameter f_{mn} are multiplied by the magnification factor

$$\phi = \frac{1}{1 - \sigma / \sigma_E} . \tag{5.10}$$

where σ_E is the critical compression for the same m and n as the index of the parameter.

The bending moment of i^{th} girder can be found using standard beam formulae

$$M_{gi} = -D_{gi} \left(\frac{\partial^2 w}{\partial x^2} \right)_{y_j} \tag{5.11}$$

The corresponding stress value at any point of the section is obtained by

$$\sigma = \frac{E_{gi} M_g Z}{D_{gi}} \tag{5.12}$$

where D_g is the flexural rigidity of the section of girder; Z is the distance from the neutral plane of the section to the point of the considered element in question.

5.2.2 Beam-Column Model

Because of the high-strength, low-stiffness characteristic of GRP laminates, instability must be carefully considered for the design of FRP hulls as the ultimate tensile and compressive strength of GRP laminates are approximately equal to the yield strength of mild steel. However, the elastic modulus of such laminates is much lower. Thus, the design consideration of composite laminated panels against buckling characteristics is a key point of composite structures made, particularly in bottom shells or deck units subjected to compressive loads by longitudinal wave-induced. Smith (1990) suggested that the possible failure modes of a stiffened panel under compressive load can be divided into four classes:

- **Local buckling of plate between stiffeners (Mode I)**

  When the lowest initial buckling stress corresponds to local buckling of the plate between stiffeners, a substantial postbuckling reserve of strength may exist. Generally, local buckling of the shell is associated with loss of effective width, which may cause a reduction in the flexural rigidity of the cross-section.

- **Column-like buckling (Mode II)**

  This buckling mode indicates a failure pattern in which the collapse is reached by column or beam-column type collapse of the combination of stiffener with the effective plate. Collapse is possibly caused by material tensile or compressive failure in the stiffeners. This buckling occurs first in the case of stiffeners with lower rigidity.

- **Tripping of stiffeners (Mode III)**

  Tripping of stiffener can occur when the ultimate strength is reached by lateral–torsional buckling (or tripping) of stiffener. This form of instability is

susceptible to open-section stiffeners. Hat-section stiffeners which are usually used in composite ships have high torsional stiffness. This buckling mode can be prevented by using stiffeners with good proportions, hence, tripping of longitudinal is not generally considered in this analysis.

- **Overall instability of the stiffened panel (Mode IV)**

  This failure mode refers to the buckling of the gross panel involving longitudinal and transverse frames between the major support members. Overall instability failure mode typically represents the collapse pattern when the stiffeners are relatively weak. This failure mode should be proportioned so that this form of failure is preceded by that interframe collapse mode because this failure involves a large portion of structure and is likely to be more catastrophic.

As a result, the collapse mode of the stiffened panel may be considered by the form of column-like instability of longitudinal stiffeners together with the effective plating so that they would behave as a beam-column. In this mode of failure, the ultimate load carrying capacity of the stiffened panel is governed by column-like flexural buckling of the longitudinal stiffeners.

The critical strength for the flexural buckling of a stiffener, without consideration of initial imperfection and lateral load, may be estimated from the Euler formula with shear deformation included (Smith, 1990)

$$\sigma_E = \frac{\pi^2 D}{Aa^2} / (1 + \frac{\pi^2 D}{a^2 GA_s}) \tag{5.13}$$

where D is the flexural rigidity of a stiffener with associated effective breadth; A is the total cross-sectional area of a stiffener with attached strip of shell; a is the length of the longitudinal stiffener between the transverse frame; GA_s is the effective shear rigidity; A_s is the effective shear area.

In real applications, composite structures exhibit some unavoidable initial shape

imperfections due to the manufacturing process or heavy load connected to the hull. These initial imperfections may trigger buckling or premature strength failures at pressure far below those corresponding to elastic buckling. The initial deformation w_0 and total deflection w are assumed to have the similar shape as follows:

$$w_0 = \delta_0 \sin\frac{\pi x}{a} \tag{5.14}$$

$$w = \delta \sin\frac{\pi x}{a} \tag{5.15}$$

where δ_0 is the maximum initial imperfection and δ is amplitude of the total deflection

The bending moment equilibrium is given by

$$D\frac{d^2(w-w_0)}{dx^2} = -Pw \tag{5.16}$$

The strain-energy-based approach is employed to determine the initially deflected column. The total potential energy can be given by

$$\Pi = U + W \tag{5.17}$$

The elastic strain energy U and the external potential energy W are calculated as

$$U = \frac{D}{2}\int_0^a (\frac{\partial^2 w}{\partial x^2} - \frac{\partial^2 w_0}{\partial x^2})^2 dx \tag{5.18}$$

$$W = Pu = -\frac{P}{2}\int_0^a \left[(\frac{\partial w}{\partial x})^2 - (\frac{\partial w_0}{\partial x})^2 \right] dx \tag{5.19}$$

Applying the principle of minimum potential energy, the amplitude of the total deflection can be found as follows

$$\delta = \frac{\delta_0}{1-\sigma/\sigma_E} = \Phi\delta_0 \tag{5.20}$$

where $\Phi = \dfrac{1}{1-\sigma/\sigma_E}$ is known as magnification factor.

The maximum stress σ at the outer fibre of the cross-section can therefore be obtained by the sum of axial stress and bending stress as follows

$$\sigma = \frac{P}{A} + \frac{M_{\max}}{W} \tag{5.21}$$

where $M_{max} = P\delta$; $W = \dfrac{D}{E_i Z}$; E_i is the membrane equivalent Young's modulus of the element; Z is the vertical distance from the neutral axis to the point in question.

For the plate under combined axial compression P and lateral line load q, the internal bending moment along the span can be obtained by the sum of bending moment due to lateral load and geometric eccentricity which may include lateral deflection caused by external load as well as initial deflection

$$M_{max} = M_{q\,max} + P\phi(w_{q\,max} + \delta_0) \tag{5.22}$$

where M_{qmax} and w_{qmax} are maximum bending moment and maximum deflection due to lateral load alone.

For each element of stiffened panel, the direct stress value at any point in the section can be predicted using Eq.(5.21) in place of the $M_{\max}$ using Eq.(5.22). Because many composite materials are brittle and show no yield point, the maximum stress criterion is used in the principal material direction of each layer at the element of the cross-section, in which the individual stress components are compared with the corresponding material allowable strength values. Failure is deemed to have occured when the maximum stress in any layer equals the ultimate strength in that direction. This method requires an iterative procedure but usually few of iterations are sufficient.

5.3 Equivalent Young's Modulus

For stiffened plates the section is made from an assembly of flat layered laminated composite element such as crown, web and flange, which will be referred to as elements of section. The material properties vary from element to element, depending on the laminate configuration in each element.

In order to perform the analysis of structures made from composite laminated plate using the methods mentioned above, the equivalent Young's modulus value is required for each element. Symmetric laminates are considered here only as they are the majority of laminate configurations used in practice. The coupling stiffness terms B_{ij} are zero for symmetric laminates: impling that there are no membrane-bending coupling effects. From Datoo (2003), the membrane equivalent Young's modulus value of the laminate plate in the x-direction and the y-direction are

$$\begin{cases} E_x^m = (A_{11}A_{22} - A_{12}^2)/A_{22}t \\ E_y^m = (A_{11}A_{22} - A_{12}^2)/A_{11}t \end{cases} \tag{5.23}$$

where A_{ij} are called extensional stiffness; t is the total thickness of the laminate element under consideration.

5.4 Effective Flange Breadth

For a stiffened panel, the plate flange of a stiffener is usually not fully effective because plate buckling and shear lag results in a non-uniform stress distribution. Effective breadth is used to describe the effectiveness of plating in acting as a flange to stiffeners and hence in contributing to the overall flexural rigidities of a stiffened panel. In this way, the distribution of stresses along the beam flange is assumed to be

constant. The effect may often be neglected when panels with closely spaced longitudinal stiffeners or stiffened panels subjected to uniform lateral pressure (Smith, 1990).

The effective breadth of steel and aluminium plating has been extensively researched and can be evaluated with reasonable accuracy from data curves accounting. As a matter of GRP reinforced plates has peculiar differences with respect to steel plates, not many formulae are available in literatures but that presented by Classification Societies, in which only simple relationships are provided. Dario Boote (2007) summarised the formulas for effective breadth calculation from different Classifications Societies (Appendix B). The formula from B.V. is chosen for this calculation.

$$B_e = B \text{ or } 0.2L + b_1 \tag{5.24}$$

where B_e is effective width between stiffeners; B is the physical width between longitudinal stiffeners, b_1 is the stiffener base width (no overlap) and L is the distance between the transverse stiffeners. The choice of effective width is dependent on the consideration of either the transverse beam stiffeners or the longitudinal girders.

5.5 Validation Studies

5.5.1 Case 1

A tophat-stiffened panel under lateral pressure is considered to verify the numerical accuracy of developed program on the modified grillage method. The comparisons are made with finite element method using ANSYS package, in which the laminated shell element SHELLl181 is used to model the element of stiffened panel. The plate is assumed to consist of 3 girders in the length of L and 2 stiffeners in the width of B. The geometric properties and mechanical properties of all elements are given in Tables 5.1 and 5.2. The results along with the comparison are presented in Table 5.3

and 5.4. The maximum deflection and stresses at two positions A and B on this stiffened panel are compared as shown in Figure 5.2.

Table 5.1 Geometric properties of stiffened panel for case 1

		Single layer thickness(mm)	Total thickness (mm)	Lamination scheme
Longitudinal girder	Top flange	$(0.9625)_8$	7.7	$[0/90/45/-45]_s$
	Web	$(0.9625)_8$	7.7	$[0/90/45/-45]_s$
Transverse stiffener	Top flange	$(0.9625)_8$	7.7	$[0/90/45/-45]_s$
	Web	$(0.9625)_8$	7.7	$[0/90/45/-45]_s$
Shell		$(0.77)_{12}$	9.24	$[0/90/45/-45/0/90]_s$

Table 5.2 Material properties of stiffened panel for case 1

Particulars	Value
Young's modulus E_1 (GPa)	140
Young's modulus E_2 (GPa)	10
Shear modulus G_{12} (GPa)	5.0
Poisson's ratios v_{12}	0.31

As can be seen from Table 5.3 and 5.4, the maximum deflection from the grillage method is larger 13.54% than the FEM result. The stresses at every layer from the grillage method are generally conservative, with maximum difference of 20.7% in these two positions with respect to FEM results. The time required for FEM analysis is much higher compared to the simplified grillage method. It is concluded that in spite of many simplifying assumptions made in the simplified analysis of grillage model, the results are within acceptable limits for use in the preliminary stages of

design. Therefore, the simplified grillage method can make reliability analysis, involving a large number of iterative analyses, possible within a reasonable time frame.

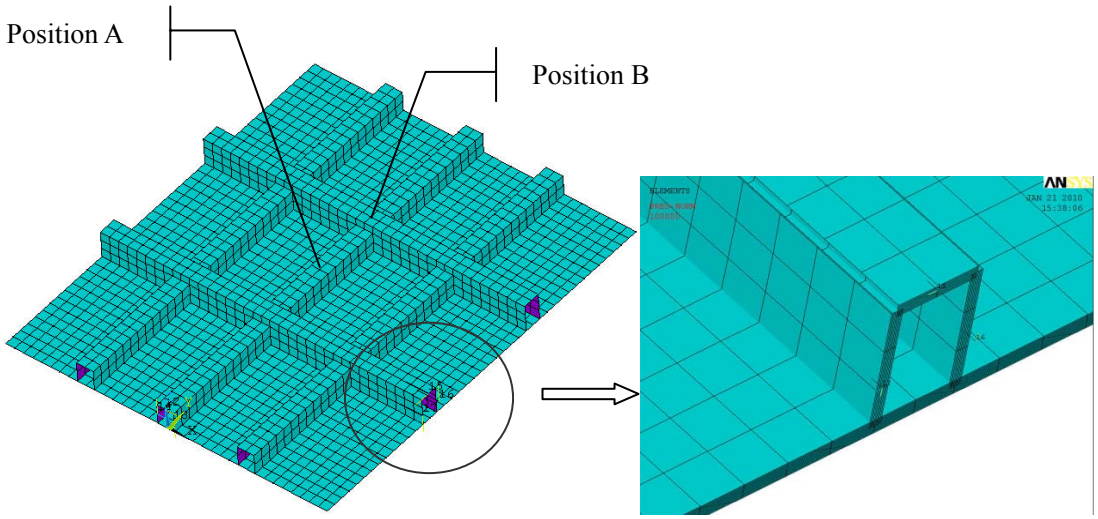

Figure 5.2 Finite element model of stiffened panel

Table 5.3 Comparison between the different methods at location A

Method			FEM	Grillage Method	Difference (%)
Deflection (mm)			4.351	4.94	13.54
Stress (MPa)	Layer1	σ_1	179.2	184.1	2.8
		σ_2	-0.51	-0.08	--
		σ_6	0.037	0.02	--
	Layer3	σ_1	65.02	66.13	1.7
		σ_2	5.97	6.03	1.0
		σ_6	8.89	8.78	-1.2
	Layer5	σ_1	70.04	67.0	-4.3
		σ_2	6.45	6.14	-4.7
		σ_6	8.89	8.90	0.2
	Layer7	σ_1	-54.1	-56.3	4.1
		σ_2	13.43	12.52	-6.7
		σ_6	0.045	0.002	--

Table 5.4 Comparison between the different methods at location B

Method			FEM	Grillage method	Difference (%)
Stress (MPa)	Layer1	σ_1	273.7	321.7	17.5
		σ_2	2.041	-0.12	--
		σ_6	0.026	0.027	--
	Layer3	σ_1	107.2	115.1	7.4
		σ_2	9.86	10.51	6.6
		σ_6	12.66	15.28	20.7
	Layer5	σ_1	103.8	116.3	12.04
		σ_2	9.457	10.66	12.72
		σ_6	13.55	15.44	13.95
	Layer7	σ_1	-99.7	-97.27	-2.43
		σ_2	19.14	21.64	13.1
		σ_6	0.022	0.003	--

5.5.2 Case 2

The accuracy of buckling strength based on the beam-column model is validated with the results of FEM and compression tests on large-scale longitudinally stiffened GRP panels as shown in Figure 5.3 (Smith and Dow, 1985). The overall length and width of the stiffened panels is 6120 mm and 3200 mm, respectively. The geometric properties and material properties of the stiffened panels from tests are given in Tables 5.5 and 5.6. A series of longitudinally stiffened panels having the same cross-sectional geometry and material properties with the experimental panel are also studied to evaluate interactions between local buckling and overall column-like buckling. The span *a* between transverse frames for a range of 1000, 1500, 2000, 2350, 2670 and 3500mm are considered.

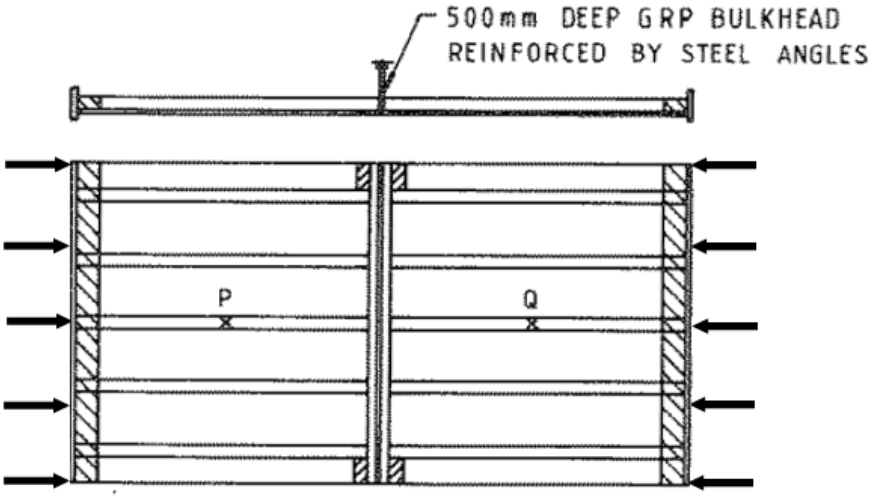

Figure 5.3 Details of test panel (Smith and Dow, 1985)

Table 5.5 Geometric properties of stiffened panels for case 2 (unit: mm)

t_1	b_2	b_3	b_4	b_f	t_2	t_3	d
12.7	108	92	123	54	8.6	4.0	132

Table 5.6 Material properties of stiffened panel for case 2

Particulars	Young's modulus E_1(GPa)	Young's modulus E_2(GPa)	Shear modulus G_{12}(GPa)	Poisson's ratio v_{12}
Plate	15.0	13.5	3.45	0.15
Table	19.5	11.9	3.45	0.18
Web/flange	15.0	13.5	3.45	0.15

To minimize the complexity of the analysis and thereby reduce the time necessary to generate results, the finite element model is idealized by a single longitudinal stiffener with attached shell laminate, extending over two half-frame spaces with

simple support at the position of the transverse bulkhead, a plane of symmetry at the longitudinal and transverse edges shown in Figure 5.4. A more detailed study on the efficiency of finite element model is investigated in Chapter 6. Initial imperfections are assumed to have the form of the interframe column-buckling mode with amplitude W_{os} and local buckling mode with amplitude W_{op}. Uniform compressive displacements are applied at the nodal points along the loaded edge in finite element models. Average compressive stresses against mid-span lateral displacements of stiffeners at positions P and Q are presented in Figure 5.5. The buckling stresses evaluated by simplified method and finite element method are summarized in Table 5.7.

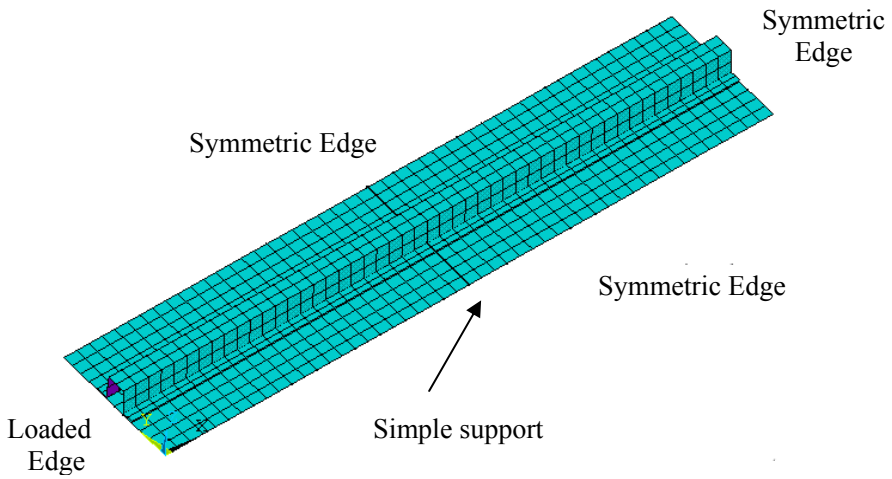

Figure 5.4 Finite element model for case 2

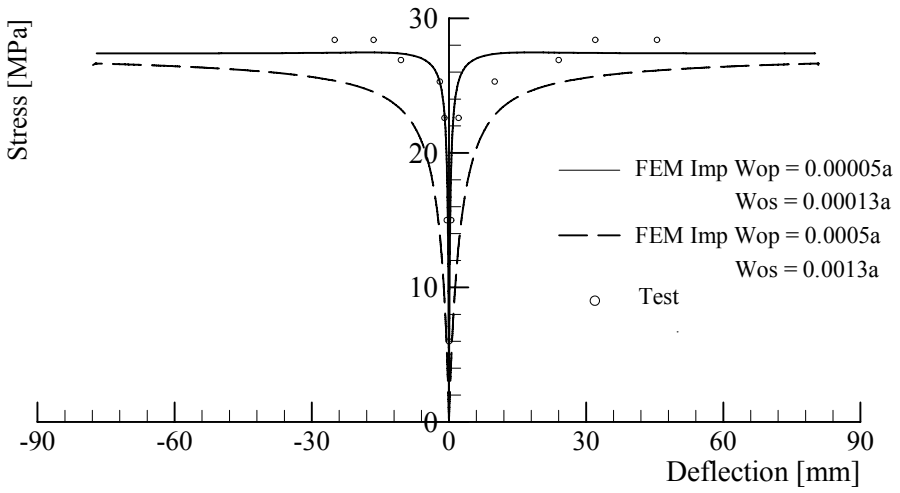

Figure 5.5 Mid-span stiffener displacements at positions P and Q

Table 5.7 The comparison between the analytical method and finite element results

Span *a* (mm)	Simplified method (MPa)	FE result (MPa)	Difference (%)
3500	22.08	21.87	0.96
3060	28.28	27.46	2.99
2670	36.14	34.31	5.33
2350	44.51	41.82	6.43
2000	57.25	53.44	7.13
1500	86.38	78.69	9.77
1000	131.06	89.95	45.7

From Table 5.7, good agreement between the simplified method and finite element simulations was found for the model with span larger than 1500mm. However, the disagreement becomes more remarkable as the span length decreases. The ultimate stress for panel of length 3060mm was found to be 28.28MPa by simplified method and 27.46MPa by finite element method, respectively. These results are in good agreement with the experimental compressive load of 28.4MPa.

It was also noticed that the predicted values by simplified analysis are slightly higher than the values obtained from finite element analysis in all cases. For the case of a panel of length 1000mm, it was found to overestimate the buckling stress by a larger margin 45.7%. That is because the local buckling becomes the dominant mode for the shortest panel and the occurrence of local buckling which results in further reduction of the flexural rigidity of the panel is not considered in this simplified method.

5.6 Reliability Analysis

5.6.1 Example 1: Grillage Model

The grillage model chosen for investigation contains four equal and evenly spaced longitudinal girders and transverse beams. The structure measures 3810mm square and is simply supported at all edges. The longitudinal and transverse beams are 254mm deep × 127mm wide with 18.288mm thick flange and 9.144mm thick web. Unidirectional laminates where all fibres run parallel in one direction throughout the thickness of the laminate are considered in this model. A uniform pressure of 137kPa is applied on the grillage structure. Reliability analyses of a grillage structure made of composite material is performed using the method presented in Section 5.2.1. The material properties of the resin and fibre are listed in Table 5.8.

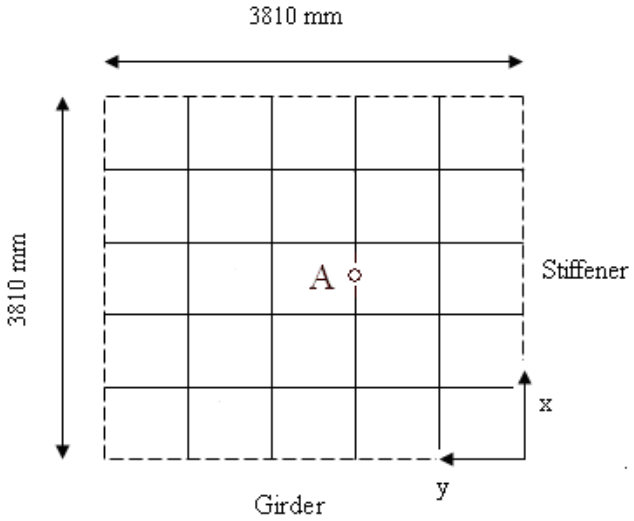

Figure 5.6 Composite beams

Elastic moduli of FRP laminates should be established ideally by tests on specimens, however, a very wide variety of fibre-resin configurations is under consideration such as the variation of fibre content, the moduli of fibre and resin. The representative test data are unlikely to be available. It may be obtained by several simple approximations to the elastic constants with reasonable accuracy.

Semi-empirical equations of moduli derived by Halpin and Tsai (Smith, 1990) are sufficiently accurate for most composites except those with very high fibre content. More details can be found in Appendix C.

Table 5.8 Material properties of resin and fibre (Smith, 1990)

	Young's modulus E (GPa)	Poisson's ratio ν	Shear modulus G (GPa)	Tensile strength (MPa)	Compressive strength (MPa)	Tensile failure strain (%)	Volume fraction
Epoxy	3.0	0.37	1.09	85	130	5.0	0.45
E-Glass	72.0	0.20	30	2400	-	3.0	0.55

- **Deflection Limit State**

Assume the limit state function is

$$g(x) = k \times w_{\max} - w(L, B, P, E_f, E_m, G_f, G_m, V_f) \tag{5.25}$$

where $w_{\max}$ is the maximum displacement using the mean value of design parameters. k is a safety factor and taken as 2 in this problem. The reliability analysis is performed with the assumed statistics of the design variables given in Table 5.9.

The results of the reliability index and probability of failure are presented in Table 5.10. The importance of the dominant variables in the limit state equation on the reliability of the composite stiffened grillage is shown in Figure 5.7. It can be seen that the model dimensions and load for the deflection limit state have quite sizeable contributions to the probability of failure. It is also noticed that Young's modulus of fibre E_f and fibre volume fraction V_f also have important contributions. However, unrepresented in this figure are the sensitivities for the shear modulus of the fibre and the resin G_f and G_m, which play such small roles in contributing to the probability of failure that they can be treated as deterministic constants.

Table 5.9 Statistical properties of random variables for composite grillage structure (Deflection limit state)

Random variable	Distribution	Mean value	COV
L (Length)	Normal	3810mm	0.03
B (Width)	Normal	3810mm	0.03
q (pressure)	Weibul	0.137MPa	0.15
E_f (fibre)	Normal	72.0GPa	0.05
E_m (resin)	Normal	3.0GPa	0.05
G_f (fibre)	Normal	30GPa	0.05
G_m (resin)	Normal	1.09GPa	0.05
V_f (volume of fraction)	Normal	0.55	0.05

Table 5.10 The results of reliability analysis for composite grillage (Deflection limit state)

Method	Reliability index β	Probability of failure P_f
FORM	3.5054	2.280×10^{-4}
SORM	3.5382	2.014×10^{-4}

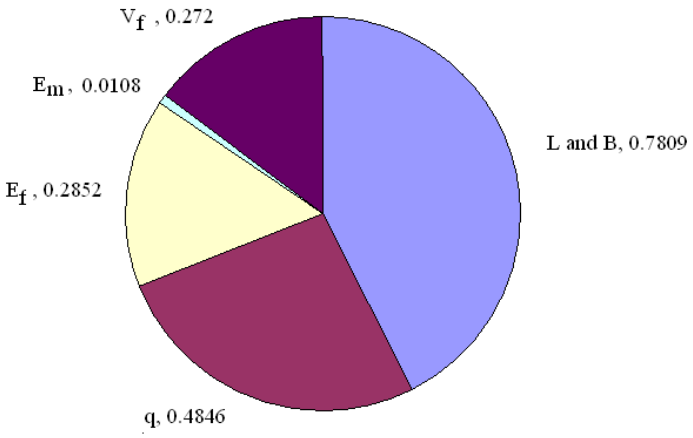

Figure 5.7 Sensitivity factors for a 4×4 box stiffened composite grillage (Deflection limit state)

- **Stress Limit State**

The maximum stress criterion is used here to assess whether the crown of composite stiffener has failed or not. The stress limit state function is considered as the following

$$g(x) = X_t(E_f, E_m, V_f, \varepsilon_f^*) - \sigma_{\max}(L, B, q, E_f, E_m, G_f, G_m, V_f) \qquad (5.26)$$

in which X_t is the ultimate tensile strength determined by the mean values of basic variables and $\sigma_{\max}$ is the maximum stress in the crown of section.

Reliability analysis is performed using the assumed statistics of the design variables given in Table 5.11. The sensitivity of the limit state function on the random variables is also performed and the sensitivity factors of the dominant variables are shown in Figure 5.8.

Table 5.11 Statistical properties of random variables for composite grillage (Stress limit state)

Random variable	Distribution	Mean value	COV
L (Length)	Normal	3810mm	0.03
B (Width)	Normal	3810mm	0.03
q (pressure)	Weibul	0.137MPa	0.15
E_f (fibre)	Normal	72.0GPa	0.05
E_m (resin)	Normal	3.0GPa	0.05
G_f (fibre)	Normal	30GPa	0.05
G_m (resin)	Normal	1.09GPa	0.05
V_f (volume of fraction)	Normal	0.55	0.05
ε_f^* (Tensile failure strain %)	Normal	3.0	0.05

Table 5.12 The results of reliability analysis for composite grillage (Stress limit state)

Method	Reliability index β	Probability of failure P_f
FORM	13.1332	0
SORM	13.1332	0

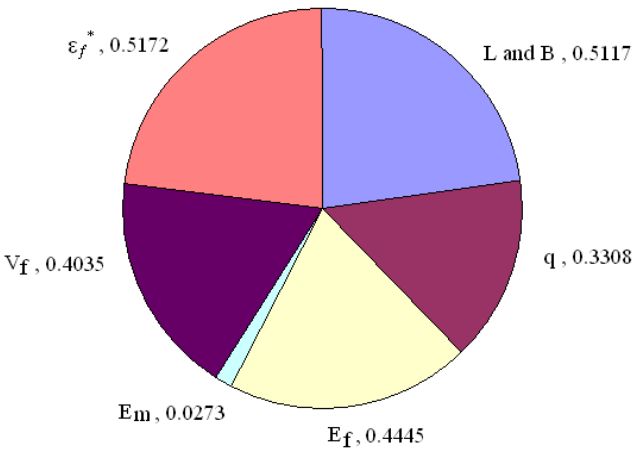

Figure 5.8 Sensitivity factors for a 4×4 box stiffened composite grillage (Stress Limit State)

The results for the reliability index are so large that the "demand" contribution to the stress limit state function is far removed from the grillage "capacity". Not surprisingly any uncertainty in the true value of the tensile failure strain significantly affects the stress limit state equation. The stress is very much dependent on the fibre volume fraction V_f and the Young's modulus E_f for the fibre. The dimension of the panel is also important in this respect. The shear modulus of fibre and resin, G_f and G_m, unrepresented in Figure 5.8, again play a small role in the reliability analysis and as such can be treated as deterministic constants.

5.6.2 Example 2: Beam-Column Model

In this section, a stochastic approach to the design of stiffened composite panel under compressive load and the combination of compressive and lateral loads for ship structures is applied and the importance of different stochastic parameters on the reliability index and failure probability is investigated. The material properties of fibre and resin are the same with example 1 shown in Table 5.8. In this case, the shell and stiffener laminates are assumed to be reinforced by woven rovings laminates, which is balanced laminates of the type and commonly used in ship construction.

Table 5.13 Geometric properties (unit=mm)

	Crown width	Crown height	Web width	Web height	Panel thickness
Longitudinal	50	3.36	3.36	39	15.68
Transverse	100	6.2	6.2	80	
Thickness of single layer = 0.56					

- **Formulation of Limit States**

The failure due to instability or buckling of longitudinal stiffeners (flexural or tripping) or overall buckling is related to the ultimate limit state. The safety margin of structures can be evaluated by a comparison of ultimate strength with the applied loads. The stiffened composite panel is assumed to fail when the applied compressive load reaches or exceeds its ultimate compressive strength as defined in Eq.(5.27).

$$g = X_u \sigma_{ult} - \sigma \tag{5.27}$$

where X_u is the model uncertainty of the strength prediction; σ_{ult} is the maximum compressive load of a stiffened composite panel; σ is the applied compressive load.

- **Random Variable Definition**

A measure of uncertainty should be included to account for the effect of variability in material properties, dimension tolerance and fabrication of the panel as the layup and curing of laminae are complex processes which may involve a lot of uncertainty. In general, the basic variables concerned with external load and geometric values have the largest and smallest coefficients of variation respectively. Therefore, the geometric properties such as dimension of panel a, b_3, b_4 and the thickness of laminae t, which may fluctuate in the vicinity of the given values depending on the manufacturing processes, are considered as random variables. All geometric properties are assumed three percent of COV. Initial imperfection is also taken into account as this problem can never be totally eliminated. The material properties of fibre and matrix, fibre volume fraction, which may affect the mechanical properties of the laminate, are treated as random variables with five percent of COV.

The modelling uncertainty is generally associated with assumptions in the strength prediction model in representing boundary conditions, property degradation model and so on. The modeling uncertainty is usually incorporated into a reliability analysis by the ratio between the actual response and predicted modeling response. Faulkner et al. (1988) suggested that a normal distribution is usually assumed, the mean value and coefficient of variance for strength parameter are assumed to be 1.0 and 10% for simplicity, respectively. All these variables are assumed as independent variables and they are randomly generated according to their assumed probability distribution as shown in Table 5.14.

- **Results and Discussions**

Table 5.15 shows the three sensitivity factors α, δ and η defined in Eqs.(3.15)-(3.18) for the dominant variables. The important factors α for all variables are also shown in Figure 5.9. The safety index 3.67 and failure probability 1.227×10^{-4} are obtained via the proposed method together with the first order reliability method..

Table 5.14 Statistical properties of basic design variables

Symbol	Distribution	Mean value	COV
a	Normal	550mm	0.03
b	Normal	500mm	0.03
t	Normal	0.56mm	0.03
b_3	Normal	50mm	0.03
b_4	Normal	39mm	0.03
δ_0	Normal	0.55mm	0.03
E_f	Normal	72.0GPa	0.05
E_m	Normal	3.0GPa	0.05
G_f	Normal	30.0GPa	0.05
G_m	Normal	1.09Gpa	0.05
V_f	Normal	0.55	0.05
X_u	Normal	1.0	0.10
P	Weibull	0.5 P_{ult}	0.15

From Figure 5.9, the importance of the dominant variables α, by order, is modelling uncertainty of the strength prediction X_u, applied load P, volume of fraction of fibre V_f, the height of section b_4, the thickness of laminae t, the length a, Young's modulus of fibre E_f, and shear modulus of resin G_m. The sensitivity factors of shear modulus of fibre G_f, the Young's modulus of resin E_m, initial imperfection δ_0, the width of crown b_3 and the width b are small compared to the values mentioned above. That means these values can be replaced by deterministic values in the further analysis as they have the least impact on the reliability calculations.

Table 5.15 Sensitivity factors of basic variables

Random variable	α	δ	η	Random variable	α	δ	η
a	0.1786	-0.1786	-0.1167	G_m	-0.0829	0.0829	-0.0250
t	-0.2232	0.2232	-0.1814	V_f	-0.3157	0.3157	-0.3662
b_4	-0.2328	0.2328	-0.1980	X_u	-0.7226	0.7226	-1.9159
E_f	-0.1435	0.1435	-0.0748	P	0.4578	-0.6339	-1.0842

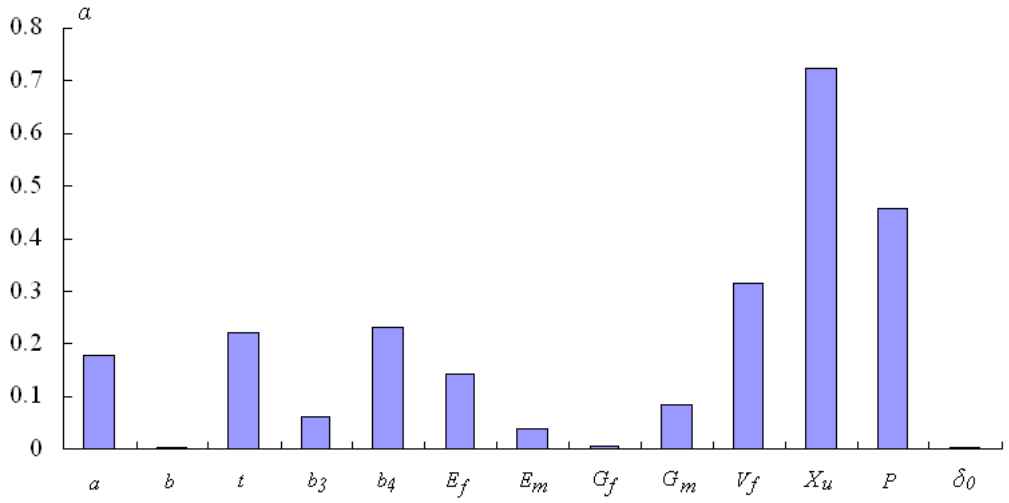

Figure 5.9 Important factors α

The sensitivity factor δ represents the sensitivity of β with respect to the mean values. The positive sensitivity factors δ such as geometric parameters t, b_4 and material properties of fibre and resin E_f, G_m, V_f are obtained and treated as strength parameters. That means the safety index increases with increasing mean value of the variables. The negative sensitivity factors δ are treated as load parameters such as the length of stiffener a and compressive load P. This indicates that the safety index decreases with increasing of mean value.

The combination of in-plane and lateral loading is also considered because lateral loading from sea water pressure or cargo is always present on plates and stiffened plates elements. Pressure load of 131.47kPa with the uncertainty 10% is considered and Weibull distribution is assumed in the reliability analysis. The direction of lateral pressure is assumed to be the same with the initial imperfection towards the stiffeners. The reliability index of the panel decreases from 3.67 to 2.4963 when lateral pressure is considered. The effect of lateral pressure on the stiffened plates is to lower the ultimate collapse load and therefore reduce the reliability index compared with the stiffened plate under in-plane loading alone.

- **Parametric Study**

Although the probabilistic method provides more information than the corresponding deterministic counterparts in the analysis, this method also requires more comprehensive information. Reliability analysis shows that not only the mean value but also COV of random variables play a very significant role in determining the reliability or safety. However, such information is generally indeterminate. Therefore, it is worth studying the effects of the statistical distribution of the various variables, which have the largest sensitivity factors calculated in the previous section on the reliability and probability of failure.

From Table 5.15, the modelling uncertainty $X_{u,}$ the fibre volume V_f, the thickness of laminae t, Young's modulus of fibre E_f and shear modulus of resin G_m are chosen to study the effect of coefficient of variation. The results are computed by varying each of the parameters in turn with other variables held the same as the previous analysis. The results are presented in Figures 5.10 - 5.12. The model has also been analysed for a wider range of load uncertainties by ignoring the actual source of loading. Axial load COVs of 10%, 20% and 30% are considered. The results, in terms of P/P_{ult} versus the safety index β, are presented in Figure 5.13.

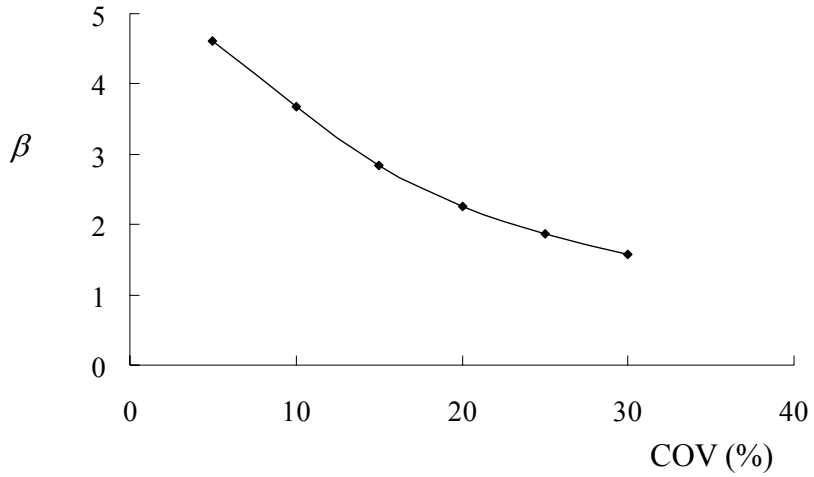

Figure 5.10 Variation of β with change of COV of X_{u}

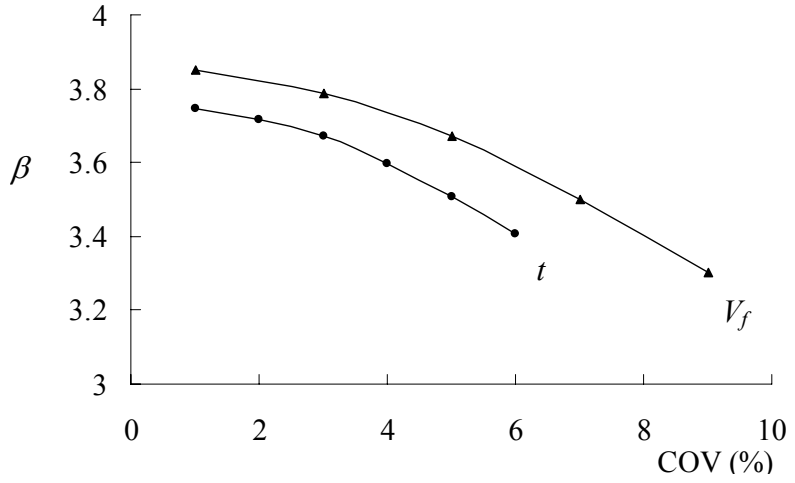

Figure 5.11 Variation of β with change of COV of V_f and t

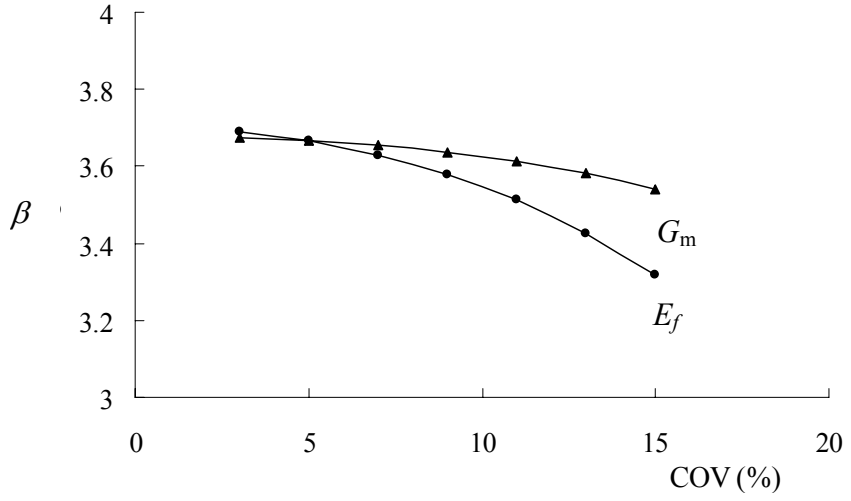

Figure 5.12 Variation of β with change of COV of E_f and G_m

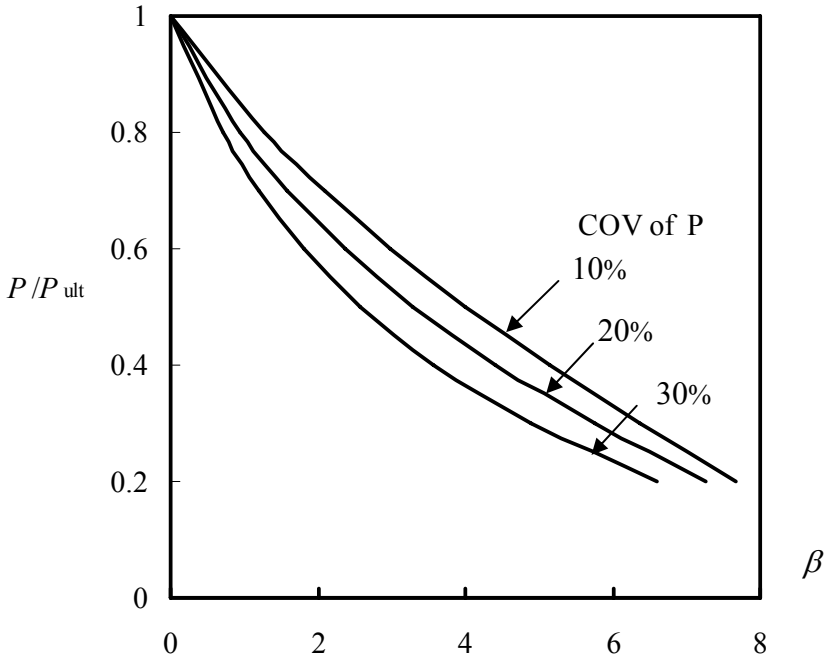

Figure 5.13 Variation of design axial load with safety index

From Figures 5.10 and 5.13, the reliability index of the model uncertainty and applied load reduces rapidly as the uncertainty increases. In other words, these two variables are very sensitive to the statistics of variables. Thus more precisely knowing the statistics of these two design variables will induce more meaningful results in the reliability analysis. For example, increasing the COV from 10% to 15% in the model uncertainty of the strength prediction leads to a reduction in reliability index of 22.8% and around a 20-fold increase in the failure probability. Improving the accuracy of analysis method, such as by applying more advanced analysis method can minimise the modelling error and its variation so as to increase the safety index.

The variations in component thickness and the fibre content within a component from design is caused by production defects, which may arise in the manufacture of composite structures and are difficult to eliminate. The influences of variation in the volume fraction V_f and thickness t on reliability are shown in Figure 5.11. It is evident that the reliability indices are strongly dependent on the variation of these

two quantities. In other words, the minor variation in these two variables has a major effect on the reliability. Therefore, if the uncertainties of such random variables can be reduced through appropriate care or stricter quality control, then reliability can be increased.

Uncertainties in material properties E_f and G_{m} are also investigated as shown in Figure 5.12. It is evident that the influence of the variation in the fibre modulus E_f is stronger than the shear modulus G_{m} on reliability. This enables the designers to know where to look to improve reliability. For example, if the coefficient of variation of the G_m is reduced from 15% to 11%, the failure probability is reduced around 24%. However, the failure probability can then be reduced to almost half if the coefficient of variation of the E_f is reduced by the same percent. This indicates that it is better to reduce the uncertainty of E_f rather than G_{m} in terms of their relative importance with respect to variations in their standard deviations.

5.7 Summary

In the present chapter, an analytical procedure is presented for strength assessment of stiffened laminated panels under pure compressive load, lateral load and the combination of compressive and lateral loads based on grillage model and beam-column model. Equivalent elastic modulus for laminates is used to consider anisotropy. A complete program on the basis of analytical methods has been generated and validated by comparing the results obtained from the finite element calculations and experimental results published in literatures. Reliability estimates have been performed and corresponding probabilities of failure have been determined for different examples. The importance of random variables in the prediction of reliability can be determined through investigation of the sensitivity indices. Finally, a parametric study is performed to study the effects of statistical distributions of the important variables on the reliability estimation.

Chapter 6:
Application of Response Surface Method for Reliability Analysis of Composite Structures

6.1 Introduction

Generally, two main aspects need to be properly considered for reliability assessment of composite structures. One important aspect is the accuracy of the mechanical model. The simplified analysis methods considered in Chapter 5 ignore interactive effects of different buckling modes and consider the buckling modes, separately. The interaction could occur in some cases between local and overall buckling modes, especially for the stiffened panel with a small span length. As can be seen in the Table 5.7, the occurrence of local buckling which results in further reduction of the flexural rigidity of the panel is not considered in this simplified method. Then the simplified analytical method presented in Chapter 5 is not quite accurate for this kind of case. Therefore, stiffened composite panels often require expensive finite element modelling to predict structural efficiencies. Nonlinear models are quite reliable to get accurate results, especially for composite structures characterised by large deflection or material nonlinearity. Progressive failure analysis described in Chapter 4 allows us to accurately model and predict the ultimate capacity of composite structures.

The second important aspect is the probabilistic model which has to be carefully chosen to consider computational efficiency which may restrict their applicability. Structural reliability theory has previously been introduced in Chapter 3. The practicability of structural reliability analysis methods for a specific limit state depends to a great extent on the complexity of the formulation of the limit state. The

solutions of structural reliability based on FORM and SORM procedures are carried out based on the existence of closed-form expressions for the failure functions. It should be clear that in the situation where the limit state function is smooth and not too strongly non-linear, the FORM and SORM are usually sufficient to get a rational estimate of the structural reliability. In other words, when the failure domain cannot be represented by linear or quadratic form and/or the value of limit state function and its gradient can be obtained neither explicitly nor numerically, then FORM or SORM can not be successfully applied. In such an event alternative methods, namely simulation-based methods, are preferable. Structural reliability is calculated by counting the number of failures among the total number of simulations. These methods are attractive for the reliability analysis because they are the only known techniques to accurately estimate the probability of failure regardless of the complexity of the limit state. However, these methods become computationally intensive for reliability analysis when each simulation corresponds to a complete nonlinear mechanical analysis as they lead to very high computational cost, especially for a realistic structure whose reliability is usually high. Furthermore, in many practical problems the performance function may not be a closed form or preferably differentiable form of the random design variables as the performances of the structure can be evaluated numerically by the commercial software such as ANSYS or ABAQUS. This means that the safety domain can be defined only through repeated numerical analyses with different input values. In these situations, the FORM and SORM are not immediately applicable.

To deal with cases where no closed-form functions exist, without incurring excessive computational costs, a Response Surface Method (RSM) has been proposed as a vehicle for incorporating finite element analysis into structural reliability computation. The response surface method was first introduced by Box and Wilson (1951) and has been a topic of extensive research in many different application areas. One of the earliest suggestions to utilize the response surface method for structural reliability assessment was made by Rackwitz (1982).

The goal of the response surface methodology is to construct a predictive equation

relating a response such as stress or deflection to a number of input variables to approximate the true limit state function. Once the Response Surface (RS) has been fitted, the reliability analysis can be carried out by any of the methods previously described using the fitted equation, instead of having to repeatedly run the time-consuming deterministic structural analyses.

6.2 Response Surface Method

6.2.1 Basic Concept of Response Surface Method

Response surface methodology is a collection of statistical tools and techniques used for constructing an approximate functional relationship between input parameters (loading and system conditions) and output parameters (response in terms of displacement, stress etc.). It is assumed that the structural response can be represented by $G(X)$, which depends upon a set of input variables X. However, it is an implicit limit state function of the random variables. The response surface method can be regarded as a system identification procedure to seek a function $\overline{G}(X)$ which best fits the discrete set of values of $G(\bar{x})$. $\bar{x}$ represents a set of points in x space for which $G(X)$ is evaluated. The accuracy of results depends highly on how accurately the characteristics of the original limit state are approximated. There are three key ingredients that need special attention in the RSM technique: the selection of the response surface function, design of the experimental point and solution strategy.

6.2.2 Selection of Response Surface Function

In the response surface method, an approximating function is used to fit the actual performance function. Thus, a key step of the response surface method is to select the response surface form involving the selection of order and the terms of polynomial. The selection of the form of the approximated limit state function $\overline{G}(X)$ should be

based on the shape of the true limit state function $G(X)$. Only the design point region needs to be modelled accurately since the accuracy of the reliability estimate depends on the accuracy of the polynomial approximation in the region where it is evaluated.

Wong (1985) proposed a response surface function $\overline{G}(X)$ including first order terms as well as mixed second order terms and ignoring the square terms, which might lose useful information when square terms are essential. Faravelli (1989) suggested a correction factor term representing the error between the actual function and the estimate of the response function to improve the response surface of the polynomial form.

Bucher and Bourgund (1990) proposed a response surface function containing the constant, linear and square terms but not cross terms in their method. However, Kim and Na (1997) demonstrated that the response surface neglecting mixed terms may not be sufficiently accurate in some cases. Thus, an improved sequential response surface method, in which a linear response surface function in conjunction with a vector projection sampling technique are proposed. On the contrary, Yang et al. (1996) found that the algorithm by Bucher and Bourgund is very efficient and accurate.

Das and Zheng (2000) proposed a modified version, in which the linear, square and cross terms were introduced into response surface function in an iterative fashion so that better accuracy can be obtained while the computational effort is maintained fairly low.

Yu et al. (2002) proposed the response surface function by stepwise regression approach, in which quadratic terms were introduced into or excluded from response surface function according to their contributions.

Generally, a second degree polynomial is enough to approximate the solution around the design points. A higher order polynomial may lead to an ill-conditioned system of

equations and erratic system behaviour (Melchers, 1999). The general form of quadratic polynomial which is most often employed for the response surface is

$$\overline{G}(X) = A + X^T B + X^T CX \tag{6.1}$$

where the undetermined coefficients A,B,C in this polynomial are the constant, linear and quadratic terms respectively.

6.2.3 Design of Experiments

The procedure for choosing a small set of optimal points in the design space to fit the observed responses is termed 'design of experiments'. The convergence of the search algorithm is directly correlated with the quality of the selected experimental design points. Many researchers focused on the experimental design for regression schemes. The 2^n and 3^n fractional factorial and central composite designs are commonly used in RSM.

The two levels 2^n mean that two values or levels are used for each factor denoted by 1 (high level) and 0 (low level). Considering 2^n factorial points for a simple three-variable problem, the full factorial design method generates $2^3 = 8$ possible combinations of the various factors as indicated in Table 6.1. Three of them are associated with the main effect of x_1, x_2 and x_3. Four of them are associated with interactions. The full factorial design method offers the most efficient way to estimate the effects of the individual factors and the interaction between the factors as well. However, for large values of *n*, the number of runs required for a complete factorial design rapidly grows. Therefore frequent subsets are chosen that lead to fractional factorial design, in which certain high-order interactions are negligible and the information on the main effects and low-order interactions are considered. Since the number of experiments can be less than the number of combinations in the full factorial set, fractional factorials are useful when the number of variables is large

The 2^n factorial design is useful in the cases where the response surface function is approximated by the linear equation. Similarly, a 3^n factorial design may be useful

when the response surface function is approximated by a second order model (Myers and Montgomery, 1995). However, the main disadvantage of the fractional schemes, especially the full factorial, is that the number of support points in the design grows exponentially with increasing number of basic variables.

Table 6.1 List of runs for a 2^3 factorial design of full factorial method

Test run No.	1	2	3	4	5	6	7	8
x_1	0	1	0	1	0	1	0	1
x_2	0	0	1	1	0	0	1	1
x_3	0	0	0	0	1	1	1	1

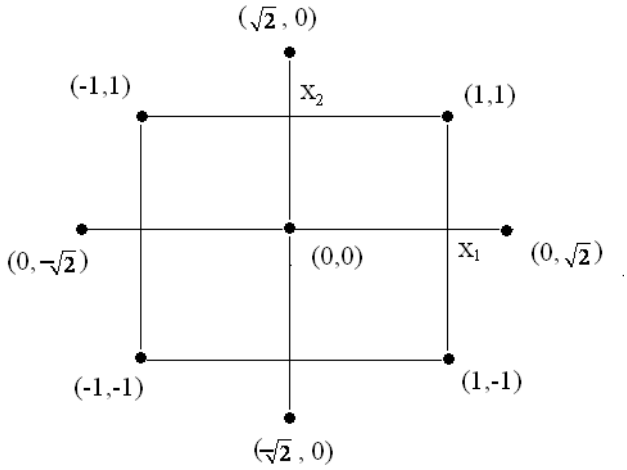

Figure 6.1 Central composite design for two variables with $\alpha = \sqrt{2}$

Central composite design is another efficient class of design for fitting a second-order response surface. It was introduced by Box and Wilson (1951). This design consists of a 2^n factorial design, with each factor at the two-level (1,-1), one central point at the central value of each variable and 2n axial points, which are placed on each axis at a distance α from the centre. Therefore, the design contains 2^n+2n+1 points (Faravelli, 1989). The axial distance α is a very important parameter in the use of the central composite design. The choice of α depends to a great extent

on the region of operability and region of interest. The Figure 6.1 illustrates the central composite design for two variables with the axial distance $\alpha = \sqrt{2}$. The design consists of four runs at the corners of a square, plus four axial runs, plus the centre runs of this square.

Box-Behnken design of experiment is an efficient alternative to the central composite design for fitting a second-order response surface (Box and Behnken, 1960). These designs are formed with incomplete block designs. The example with three design variables is shown in Table 6.2. Every two design variables are paired together as a block while another variable remains fixed at the centre 0. For each block, a 2^2 factorial is scaled by (1,-1). However, this method is not recommended by Jeff Wu and Hamada (2002) when a large number of variables are involved.

Table 6.2 Box-Behnken design of three variables

Test run No.	1	2	3	4	5	6	7	8	9	10	11	12	13
x_1	0	-1	-1	1	1	-1	-1	1	1	0	0	0	0
x_2	0	-1	1	-1	1	0	0	0	0	-1	-1	1	1
x_3	0	0	0	0	0	-1	1	-1	1	-1	1	-1	1

Bucher and Bourgund (1990) suggested an alternative process of selecting the sampling points in order to improve the accuracy of RSM. The mean value was chosen as the centre points at first and response surface function $\overline{G}(X)$ was obtained by interpolation using points along the axes x_i,

$$x_i = \bar{x}_i \pm f_i \sigma_i \tag{6.2}$$

where f_i is an arbitrary factor defined by user; σ_i is the standard deviation. The selection of f_i will influence the stability of convergence of the solution.

A design point x_D is then obtained using the $\overline{G}(X)$ on the interpolated limit state. Once x_D is found, $G(x_D)$ is evaluated and the new centre point x_M from linear

interpolation is chosen on a straight line from mean vector $\bar{x}$ to x_D so that G(X)=0.

$$x_M = \bar{x} + (\bar{x}_D - \bar{x}) \frac{G(\bar{x})}{G(\bar{x}) - G(x_D)} \tag{6.3}$$

This process is assumed to guarantee when the new centre points should be positioned reasonably closely to the original limit state. However, Rajashekhar and Ellinwood (1993) believe that the accuracy depends on the characteristics of the limit state being explored and one cycle of updating may not always be sufficient. Thus some ideas have been proposed to improve the response surface obtained from Bucher's algorithm and more iteration in searching for the design points are executed until a convergence criterion is satisfied.

Kim and Na (1997) proposed gradient projection method, in which the sampling points were selected to be reasonably close to the original failure surface by projecting the conventional sampling points on the response surface. A linear surface function was used and the effect of nonlinearity was considered by the optimised factor *f* to reduce the error produced by ignoring the squared terms. However, this might not be considered generic because it is not easy to obtain the optimum *f* for a realistic, complex problem. Das and Zheng (2000) proposed a modified version, in which a small angle is introduced to control the projection direction.

6.2.4 Determination of Response Surface

Multiple regression (Myers and Montgomery, 1995) can be used to determine the unknown coefficient in response surface function given in Eq. (6.1). The model may be written in matrix notation as

$$Y = XB + \varepsilon \tag{6.4}$$

where Y is an ($n\times1$) vector of the observations; $\boldsymbol{B}$ is an ($p\times1$) vector of the regression coefficients; X is an ($n\times p$) matrix of the variables; ε is an ($n\times1$) vector of random errors which are composed of the lack of fit error and a pure experimental error; A

normal distribution with mean zero and variance σ^2 is assumed for ε

The regression coefficients are determined so as to minimize the total error, e.g. the sum of squares of the errors can be minimized by using a least-squares-fit method. The sum of squares of the total error is

$$SS_E = \sum_{i=1}^{n} \varepsilon_i^{\,2} = (Y - XB)^T (Y - XB) \tag{6.5}$$

The normal equations for least squares estimators, b, may be obtained by minimising SS_E with respect to $\boldsymbol{B}$

$$(X^T X)b = X^T Y \tag{6.6}$$

Thus, the least squares estimators of $\boldsymbol{B}$ are

$$b = (X^T X)^{-1} X^T Y \tag{6.7}$$

where $X^T X$ is a ($p \times p$) symmetric matrix; $X^T Y$ is a ($p \times 1$) column vector

The fitted regression model is

$$\hat{Y} = Xb = X(X^T X)^{-1} X^T Y = HY \tag{6.8}$$

where H is the so-called "hat" matrix, which maps the vector of observed values into a vector of fitted values.

The vector of residuals from the fitted model is

$$e = Y - \hat{Y} \tag{6.9}$$

A response surface is only a simper function between the structural responses and the basic variables. In general, there is always some 'lack of fit' present. Hence, it is an important step to know how well the model predicts the response at the points of interest. The total sum of squares S_{yy} is composed of a sum of squares SS_R due to the model and a sum of squares SS_E due to residual.

$$S_{yy} = SS_R + SS_E \tag{6.10}$$

The Table 6.3 summarises the test procedure. Different checking procedures can be found in (Böhm and Brückner-Foit, 1992) (Khuri and Cornell, 1996) and (Myers and Montgomery, 2002).

Table 6.3 Analysis of variance in multiple regression

Source of variation	Sum of squares	Degree of freedom	Mean square
Regression	SS_R	p-1	$SS_R/(p\text{-}1)$
Residual or error	SS_E	n-p	$SS_E/(n\text{-}p)$
Total	S_{yy}	n-1	$S_{yy}/(n\text{-}1)$
$R^2 = \frac{SS_R}{S_{yy}} = 1 - \frac{SS_E}{S_{yy}}$ or $R_{adj}{}^2 = 1 - \frac{SS_E(n-p)}{S_{yy}/(n-1)}$			

6.3 The GLAREL Program

GLAREL, a response surface analysis program developed in-house, was used to construct the response surface (Yu, et al., 2002). Figure 6.2 shows how the response surface method is used for reliability analysis based on finite element method. The initial experimental points can be the mean values or the initial points that you choose. A pure linear response surface with the sampling points centred at $\mu_i \pm f_i\sigma_i$ and their centre μ_i is fitted by stepwise regression as the first approximation. The factor f is used to define the sampling range, usually f = 3 is used in the first approximation to cover as much information as possible in the failure region (Das and Zheng, 2000). As the estimated design point approaches the actual one, f can be reduced gradually until $f \approx 1$ according to $f^{(i)} = \sqrt{f^{(i-1)}}$.

FORM is performed to calculate the reliability index $\beta^{(1)}$ and the corresponding design point $\boldsymbol{X}^{*(1)}$ by using the initial response surface function. A new response surface by experiments at sampling points $X_i^* \pm f_i\sigma_i$ and X_i^* is gained. And then new centre point $\boldsymbol{X}^{*(k)}$ and the corresponding reliability index $\beta^{(k)}$ (k = 2, 3,…) are calculated. If $\left|X^{*(k)} - X^{*(k-1)}\right|$ or $\left|\beta^{(k)} - \beta^{(k-1)}\right|$ is less than the given tolerances, calculate the probability of failure $P_f = \Phi(-\beta^{(k)})$. Otherwise go back to find new evaluation points. Once the response surface is obtained, the reliability analysis can be made with this response surface as the limit-state surface in place of the original complicated limit-state surface of the model.

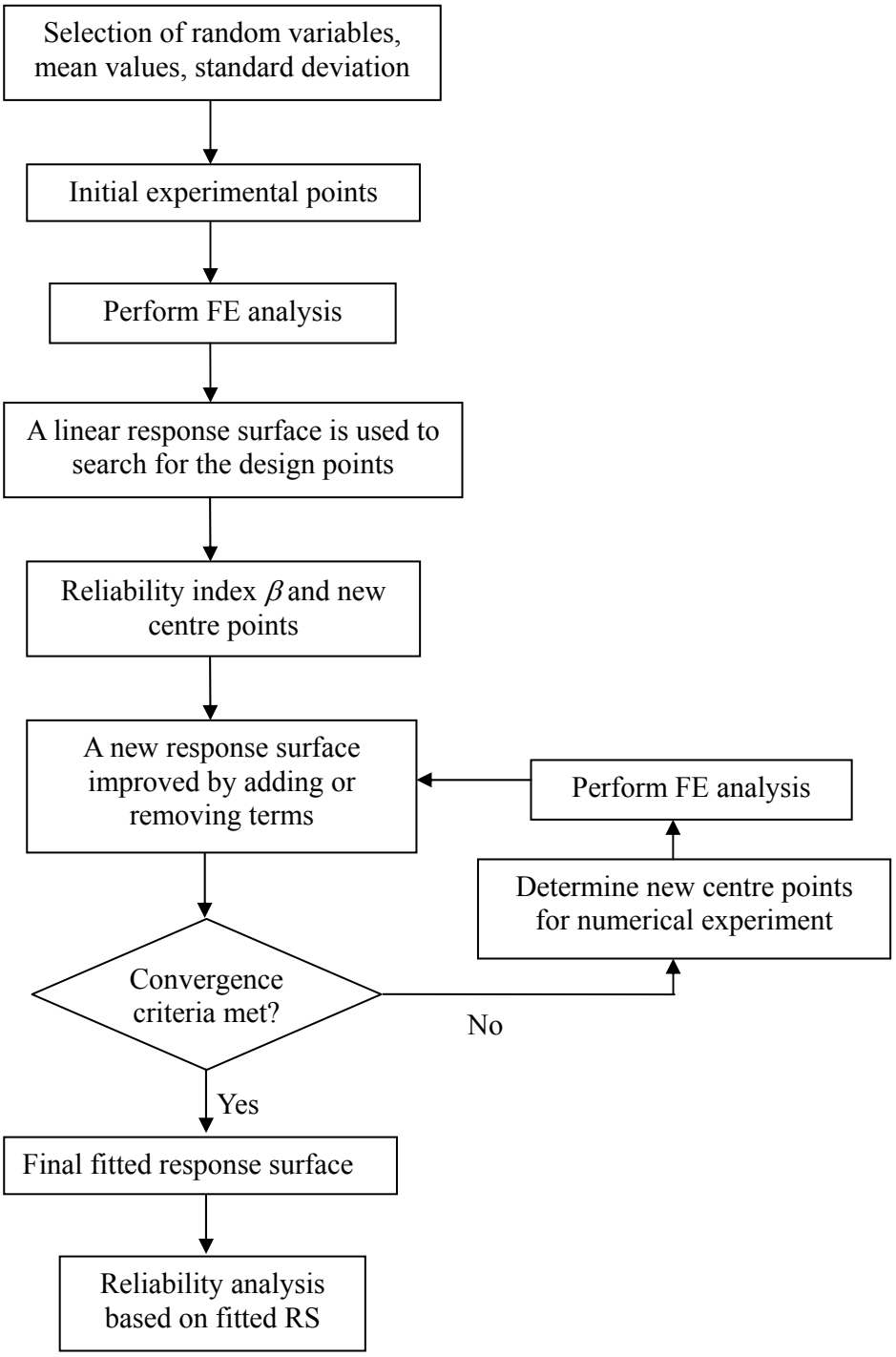

Figure 6.2 Flow chart of using the response surface method coupled with finite element analysis

6.4 The Application of RSM for Composite Structures

6.4.1 Finite Element Analysis

A stiffened composite panel with a configuration consisting of a flat skin and five equally spaced longitudinal hat-shape stiffeners is considered. The stiffened panel is 1500mm long and 2000mm wide having 12 mm thick flat skin. The stiffeners are 132mm deep having 8mm thick table, webs and flanges. Only one material is defined, since all layers are made of the same woven roving lamina with thickness of lamina t = 1.0mm. The typical mechanical properties of the material for this study are given in Table 6.5.

In order to perform the reliability analysis of stiffened panel using response surface method coupled with finite element method, it is essential to determine accurately their behaviour and strength. The idealised finite element model must be sufficient to capture all the mechanisms that could lead to collapse of the structure. For a deterministic analysis, such analysis needs to be performed only once. However, the present research is concerned with reliability assessment, in which repeated computations are required to consider the uncertainty in material properties, loading and geometric properties. A simple model that can represent the whole structure is desirable. Thus, the stiffened composite panel is modelled and analyzed using two different finite element models

(a) Finite Element Model I

The structure is modelled with shell element for the flat panel and five stiffeners. The transverse bulkhead is not modelled with elements, but it is simulated with simply supported at the edges of stiffened composite panel. Symmetry condition can be used to minimize the complexity of the analysis thereby reducing the time necessary to generate results. Therefore, only an half of stiffened panel is modelled due to symmetry.

(b) Finite Element Model II

The second finite element model consists of the central longitudinal stiffener along with attached flange with proper boundary condition as the stiffened panel has odd number of evenly spaced stiffeners. The width of the model is taken as the distance between the centre-lines of adjacent longitudinal stiffeners.

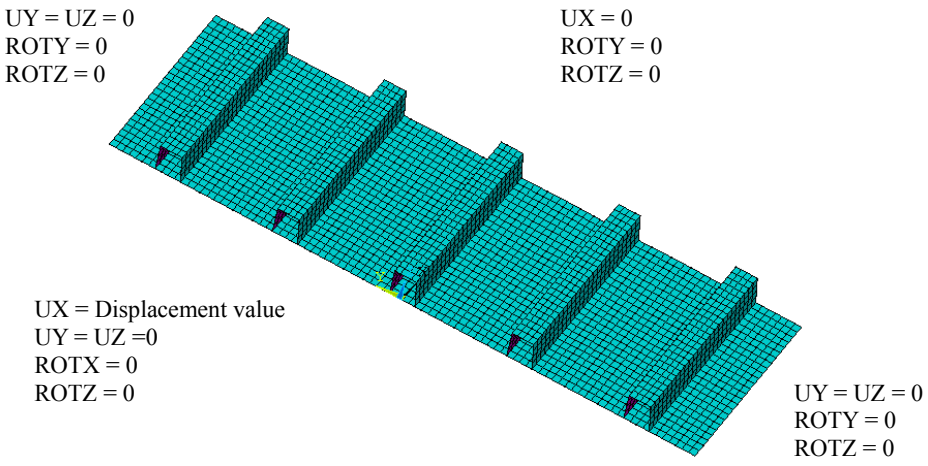

(a) Finite Element Model I

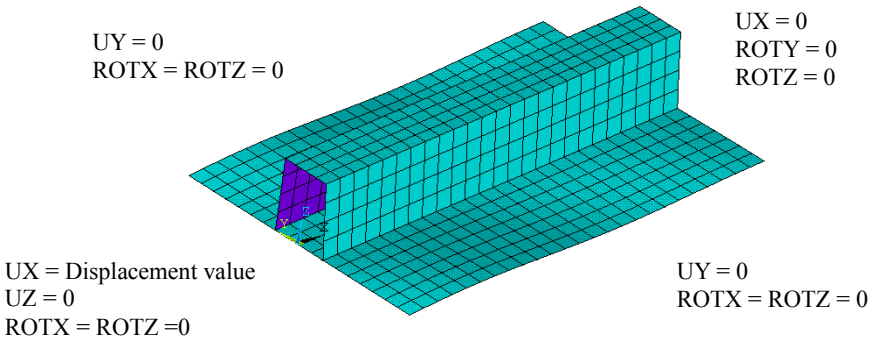

(b) Finite Element Model II

Figure 6.3 Idealised finite element models of stiffened panel with boundary conditions

The stiffened panel is discretized into 25 elements along the compressive load direction and 14 elements in-between the stiffeners. Each stiffener is discretized so that it has 4 elements along the depth of the stiffeners and 4 elements for the crown of the stiffeners. These two finite element models in conjunction with boundary conditions are illustrated in Figure 6.3(a) and (b). The end-shortening curve versus the applied load for the different finite element models are presented in Figure 6.4. The deformations of the stiffened panel at the ultimate failure load for two finite element models are shown in Figure 6.5(a) and (b).

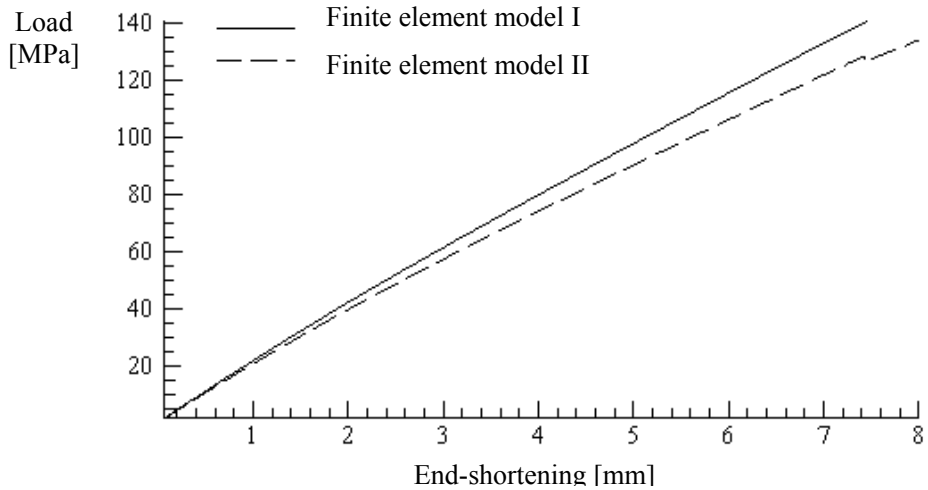

Figure 6.4 The end-shortening versus applied load for the different finite element models

Linear buckling analysis predicted that the initial local buckling loads for two finite element models agreed well as shown in Table 6.4. For the nonlinear analysis, the first local buckling mode with amplitude 5 mm is assumed to be the initial deformations of the stiffened panel. The collapse is caused by material failure in the shell laminate resulting from local buckling while stiffener attachment is maintained over most of the post collapse load range.

The deformed shapes at the ultimate load appear very similar for these two finite element models. The load curve of the finite element model II is slightly lower than that obtained from the finite element model I. The ultimate load estimated by the idealised model II differs only less than 3% from the finite element model I.

Furthermore, it is well known that the boundary condition at the edges of the stiffened panel are generally idealised as simply supported even though the true boundary condition lies somewhere between simply supported and clamped. This assumption generally gives a conservative prediction of the ultimate strength. Thus, finite element model II can be used as an idealised model, for which the results will be sufficiently accurate to simulate the stiffened panel considering the requirement of accuracy, efficiency and at the same time keeping the run times and necessary disk space reasonably low, noting that a large number of computations are required for reliability analysis.

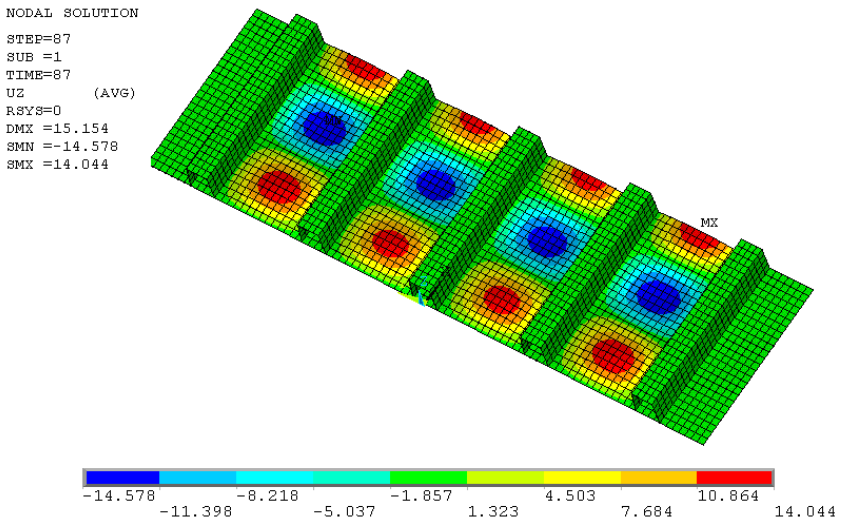

(a) Finite element model I

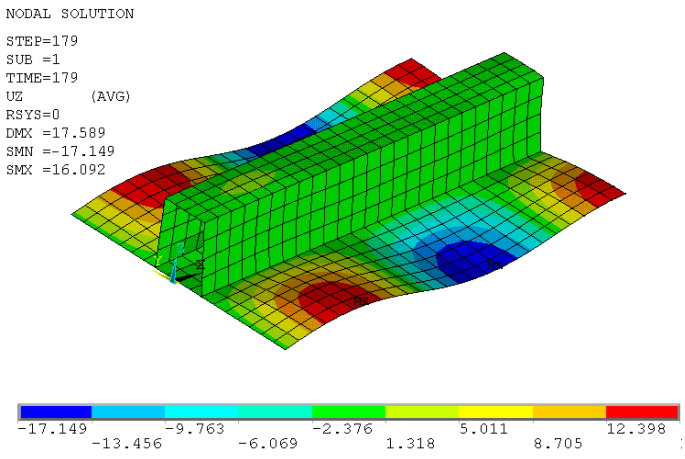

(b) Finite element model II

Figure 6.5 The out-of-plane deflection at the ultimate load

Table 6.4 The comparison between the different finite element models

Number of elements	Results description	Model I (MPa)	Model II (MPa)
800	Initial local buckling	66.4	62.7
	Ultimate load	140.7	143.8
1320	Ultimate load	-	127.7
1680	Ultimate load	-	124.4
2080	Ultimate load	-	122.7
2520	Ultimate load	-	121.5

The size of the finite element mesh should be determined based on the requirement of accuracy, efficiency and time constraint. The usual procedure for the convergence of finite element results is obtained using various mesh sizes to examine the mesh dependency. The comparison for different number of elements is also shown in Table 6.4. After a preliminary sensitivity study on the element size, it is found that satisfactory results are obtained as the number of mesh increases. In order to achieve both accuracy and efficiency, the finite element model with 40 elements along the compressive load direction and 28 elements in-between the stiffeners, 6 elements along the depth of the stiffeners and 6 elements for the crown of the stiffeners is chosen in the following reliability analysis.

6.4.2 Reliability Analysis

The reliability of a structure is defined as the probability that the structure will perform its intended function without failing. For the present analysis, the resistance model represents the ultimate strength of the structural component where the component is unable to carry any increase in load and is considered to have failed.

$$G = X_u \sigma_{ult} - \sigma \tag{6.11}$$

where X_u is the modelling uncertainty factor; σ_{ult} is the estimated ultimate load; σ is the load applied on the structure.

Table 6.5 Statistical properties of random variables for stiffened panels

Type	Symbol	Distribution	Mean value	COV
Material Properties	$E_1 = E_2$	Lognormal	17180MPa	0.10
	G_{12}	Fixed value	3520MPa	-
	$G_{13} = G_{23}$	Fixed value	5150MPa	-
	v_{12}	Fixed value	0.17	-
Strength Properties	$X_t = Y_t$	Lognormal	238.6MPa	0.10
	$X_c = Y_c$	Lognormal	324.5MPa	0.10
	S_{12}	Fixed value	80.9MPa	-
	$S_{23} = S_{13}$	Fixed value	60.7MPa	-
Thickness	t	Normal	1.0mm	0.05
Load	P	Weibull	500KN	0.20
Uncertainty of model	X_u	Normal	1.0	0.10

Six variables are considered as independent random variables, including the thickness of each layer, the Young's modulus, the strength properties, applied compressive load and model uncertainty as shown in the Table 6.5. RSM-reliability analysis is carried out using the implemented program GLAREL coupled with finite element program ANSYS. The design point is not known in advance. Initial points should be selected carefully so that the required number of iterations is as small as possible. In this application, the initial experimental design points are selected on the mean values of the random variables. A tolerance $\varepsilon = 10^{-3}$ is given and the computation is terminated at the eighth cycle of the iterations and costs 72 times of structural analysis. The process of iteration is shown in Table 6.6. The reliability index and the sensitivity factors of reliability index with respect to random variables are presented in Table 6.9.

Accordingly, the RSM-FEM coupling analysis is run without the model uncertainty while keeping other variables same with previous case. The computation is terminated at the eleventh cycle of the iterations and costs 99 times of structural analysis. The process of iteration is shown in Table 6.7. The reliability index increases greatly from 3.79 to 5.38. It shows that how different formulations for the reliability problem induce significantly change in the results when the variable having the most important impact on the failure probability is not considered. Therefore, great care must be taken in the choice of their coefficient of variation.

In order to improve the computational efficiency and reduce the space of random variables, the analysis is also run with the three variables in the following probability analysis, i.e. the applied load, thickness and compressive strength, which are more influential on the reliability or safety, while other two variables are replaced by deterministic values. The process of iteration is shown in Table 6.8. Not surprisingly small difference is obtained from probability analyses with five variables and three variables as these two variables have small effect on the probability failure.

This methodology, incorporating finite element method and probability algorithms, performs a probabilistic assessment of composite structure. The numerical application shows the efficiency of the RSM-FEM coupling, through the analysis of complex nonlinear structures with a reasonable number of mechanical calls. Following this procedure, it is possible to provide means for decomposition of the reliability index β of a structure into partial safety factors associated with the individual design variables which is ultimately used in the codes of practice. In the absence of other information, the partial factors presented could be used as a first-step in a reliability-based design procedure.

Table 6.6 Intermediate result of the iteration process for six random variables

Iteration step		1	2	3	4	5	6	7	8
Sampling centre X*		238.6	222.659	234.191	223.416	225.548	224.087	224.238	224.140
		324.5	290.555	302.267	313.428	302.477	299.338	299.387	299.091
		1.0	0.925410	0.934842	0.942635	0.938011	0.943330	0.941495	0.941086
		1.7180×10^{4}	1.67337×10^{4}	1.67362×10^{4}	1.68184×10^{4}	1.67962×10^{4}	1.68532×10^{4}	1.68595×10^{4}	1.68522×10^{4}
		5.0×10^{5}	6.57065×10^{5}	6.91990×10^{5}	6.73387×10^{5}	6.87968×10^{5}	6.88679×10^{5}	6.87216×10^{5}	6.86845×10^{5}
		1.0	0.758176	0.721869	0.699296	0.719211	0.722954	0.723070	0.723704
G(X*)		4.59608×10^{-7}	2.1420×10^{-8}	-1.89524×10^{-7}	5.34579×10^{-7}	3.80911×10^{-7}	6.05360×10^{-9}	8.63336×10^{-7}	2.74740×10^{-8}
Reliability index		3.54343	3.82959	3.81210	3.82563	3.79795	3.79544	3.79332	3.79265
Failure probability		1.9748×10^{-4}	6.4178×10^{-5}	6.8897×10^{-5}	6.5218×10^{-5}	7.2950×10^{-5}	7.3692×10^{-5}	7.4323×10^{-5}	7.4524×10^{-5}

Table 6.7 Intermediate result of the iteration process for five random variables

Iteration step		1	2	3	4	5	6	7	8	9	10	11
Sampling centre X*		238.6	209.107	243.573	190.609	218.403	220.409	221.366	222.107	223.899	224.603	225.228
		324.5	263.861	264.373	296.825	274.820	263.355	261.755	263.804	260.937	263.417	263.259
		1.0	0.842853	0.859104	1.07773	0.83100	0.840573	0.84448	0.84068	0.847642	0.842803	0.84523
		1.7180×10^{4}	1.63594×10^{4}	1.42436×10^{4}	1.4061×10^{4}	1.4848×10^{4}	1.51593×10^{4}	1.52966×10^{4}	1.52341×10^{4}	1.54866×10^{4}	1.54563×10^{4}	15499.7
		5.0×10^{5}	7.47712×10^{5}	7.71073×10^{5}	6.46075×10^{5}	7.68261×10^{5}	7.82947×10^{5}	7.84208×10^{5}	7.86069×10^{5}	7.91038×10^{5}	7.90023×10^{5}	7.93424×10^{5}
G(X*)		3.2736×10^{-7}	1.8627×10^{-9}	4.6566×10^{-9}	-3.7253×10^{-9}	2.60770×10^{-8}	6.51926×10^{-9}	1.10827×10^{-7}	3.16650×10^{-8}	1.86265×10^{-9}	6.69388×10^{-9}	7.91624×10^{-9}
Reliability index		4.97718	5.17001	3.77523	5.27092	5.39147	5.35797	5.39779	5.37445	5.38181	5.38791	5.38243
Failure probability		3.2259×10^{-7}	1.1704×10^{-7}	7.9930×10^{-5}	6.7871×10^{-8}	3.4942×10^{-8}	4.2081×10^{-8}	3.3734×10^{-8}	3.8408×10^{-8}	3.6870×10^{-8}	3.5642×10^{-8}	3.6744×10^{-8}

Table 6.8 Intermediate result of the iteration process for three random variables

Iteration step	1	2	3	4	5	6
Sampling centre X*	324.5	259.804	263.359	348.402	266.375	266.097
	1.0	0.828148	0.796812	1.00669	0.807719	0.809867
	5.0×10^{5}	7.60314×10^{5}	7.71438×10^{5}	7.67694×10^{5}	7.75762×10^{5}	7.77175×10^{5}
G(X*)	1.04774×10^{-9}	2.67755×10^{-9}	-7.45058×10^{-9}	4.59841×10^{-8}	5.95464×10^{-8}	5.72181×10^{-8}
Reliability index	5.17483	5.66452	3.40438	5.51296	5.50146	5.50213
Failure probability	1.14058×10^{-7}	7.3717×10^{-9}	3.3158×10^{-4}	1.7642×10^{-8}	1.8833×10^{-8}	1.8762×10^{-8}

Table 6.9 Reliability analysis results

Basic variables	Distribution type	Mean value	COV	Six variables $\beta = 3.79$ $P_f = 7.433\times10^{-5}$			Five variables $\beta = 5.38$ $P_f = 3.634\times10^{-8}$			Three variables $\beta = 5.50$ $P_f = 1.860\times10^{-8}$		
				Design point	Sensitivity factor	Partial safety factor	Design point	Sensitivity factor	Partial safety factor	Design point	Sensitivity factor	Partial safety factor
$X_t = Y_t$	Lognormal	238.6MPa	0.10	224.3	-0.1504	1.0637	225.4	-0.1046	1.0585	-	-	-
$X_c = Y_c$	Lognormal	324.5MPa	0.10	298.9	-0.2038	1.0857	263.5	-0.3770	1.2315	265.4	-0.3569	1.2226
t	Normal	1.0mm	0.05	0.9403	-0.3147	1.0635	0.8419	-0.5876	1.1878	0.8118	-0.6839	1.2318
$E_1 = E_2$	Lognormal	17180MPa	0.10	16840	-0.0391	1.0202	15440	-0.1877	1.1127	-	-	-
P	Weibull	500KN	0.20	686.5	0.5534	1.373	789.5	0.6829	1.579	778.9	0.6363	1.5578
X_u	Normal	1.0	0.10	0.7241	-0.7273	1.3810	-	-	-	-	-	-

6.5 Reliability-based Design Format

6.5.1 Introduction

Generally, reliability-based design of ship structures requires the considerations of the following three components (1) Loads (2) Structural strength (3) Method of reliability analysis. Two approaches were suggested for methodology of reliability-based design of ship structures:

- Direct Reliability-Based Design
- Load and Resistance Factor Design (LRFD)

As was already reviewed in Section 3.3 for the introduction of reliability levels, Level II is based on the mean and variance of random variables and Level III is based on the complete probabilistic characteristics of random variables. These two levels are included in direct reliability-based design. Reliability analysis based on Level III is difficult to apply in practices as the lack of complete information on the full probabilistic characteristics of the random variables and to evaluate to the resulting multiple integrals. Level II methods of reliability analysis have the advantage that they are relatively easy to use while still giving a good measure of a structure's probability of failure. Although Level II is easier to apply in practice, it is still of limited use to practitioners.

One way to deal with this is through a systematic evaluation of a range of designs using the higher level methods. Appropriate partial factors can be derived for each of the variables affecting the safety of the structures to ensure that the structure attains a certain reliability level, i.e. a target reliability. Level II approaches are the most suitable to this process as they provide an assessment of safety with an accuracy approaching that of Level III procedures while keeping numerical calculation within reasonable time.

This process of developing load and resistance factor design rules is called code

calibration. The load and resistance factors are used to amplify and reduce the response and the strength for a selected failure mode, respectively. One of the most useful aspects of this level of reliability analysis is that the LRFD-based method is the simplest way to use in practise as it can be used by engineers in design without a direct use of probabilistic description of the variables once the target reliability has been identified and while maintaining the simplicity of deterministic design practice.

6.5.2 LRFD Format

The load and resistance factor design format was proposed by Ravindra and Galambos (1978). The general form is given by

$$\phi R \geq \sum_{i=1}^{m} \gamma_i L_i \tag{6.12}$$

where ϕ is resistance factor; R is design strength; γ_i is Load factor for the i^{th} load; L_i is design value for the i^{th} load.

These factors are determined using structural reliability methods based on the probabilistic characteristics of basic random variables. Generally, the resistance factor ϕ always has a value less than unity to account for variability in strength due to variability of material properties, dimensions, fabrication or the uncertainty due to assumptions used in determining the resistance equations. γ is the corresponding load factor, which is generally greater than unity.

6.5.3 Reliability Analysis

Generally, derivation of the partial factors for use in the LRFD format using an advanced Level II approach is to calibrate these factors based on the reliability level in designed structures. The derivations for establishing the relationship between Level I and Level II are detailed in Appendix D. Table 6.9 presents the basic variables, the distribution type, mean value and COV assumed for each variable. The design points, the sensitivity factors and the partial safety factors for each of the

variables are also shown in the same table for the different probability analysis with the different variables. However, the reciprocal of these partial safety factors are used in relation to resisting variables in the design formats.

In this format, load effects are increased and strength is reduced by multiplying the corresponding characteristic values with factors, which are called resistance and load factors respectively. The higher the uncertainty associated with a load, the higher the corresponding load factor. These factors are determined probabilistically so that they correspond to a prescribed safety level.

The limit state equation Eq.(6.12) now becomes

$$G(\frac{x_{k_i}}{\gamma_{mi}},...\gamma_{fj}x_{kj},...) = 0 \quad i=1,,,m, \quad j=m+1,,,n \tag{6.13}$$

Eq.(6.13) can then be used to study the reliability index β achieved with different resistance factors ϕ, as a function of the statistics for the resistance variables and the applied load. This method is illustrated through the following example.

The partial safety factor of thickness t is assumed to be fixed value, say 1.1 and the partial safety factor of strength property X_c is assumed to be 1.15, 1.2 and 1.3. The reliability index β for a given resistance variable will depend on the ratios (P / P_{ult}). Figure 6.6 shows the results obtained with Eq.(6.13) for reliability index β corresponding to different resistance factors. The lower curve in Figure 6.6 corresponds to a partial safety factor of 1.3 for strength property X_c; The upper curve, on the other hand, corresponds to a partial safety factor of 1.15.

When the ratio of P_{ult} / P equals to 2.0, in other words a safety factor 2.0 is given, then quite different partial safety factor result in a range $2.8 < \beta < 3.2$. Generally, the partial load and resistance factors for use in the LRFD format are calibrated on a reliability level. A corresponding target reliability value is used to determine the load and resistance partial safety factors such that they minimize the deviation of the calculated reliability from the target level over the range of design applications.

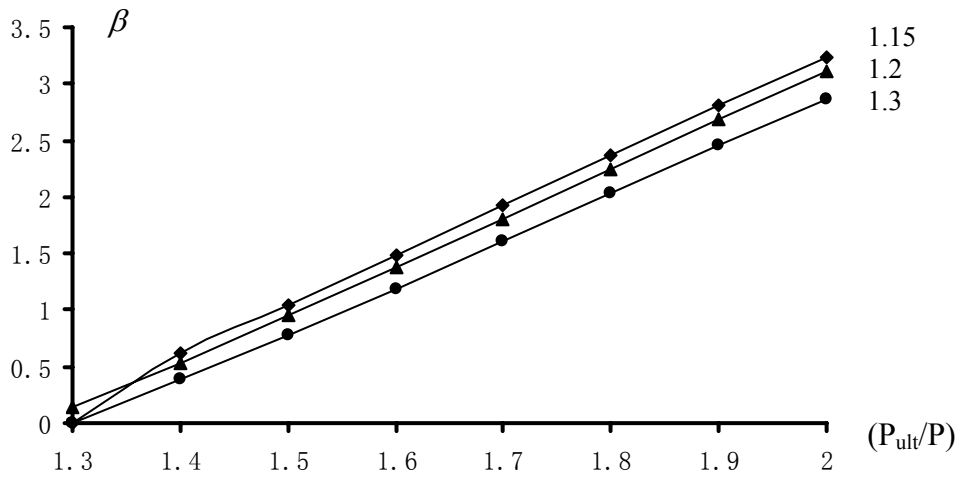

Figure 6.6. Reliability index β versus different resistance factors

6.6 Summary

An application methodology for structural reliability analysis of the composite structures based on the response surface method in conjunction with nonlinear finite element analysis is demonstrated in this chapter. After a closed-form relationship is defined between the input and output parameter, FORM is applied to establish the failure model. The numerical application shows the efficiency of the RSM-FEM coupling through the analysis of complex nonlinear structures with a reasonable number of mechanical calls.

Based on these methods a reliability-based design code format has been suggested for partial safety factors which can be used in design for certain target reliability level. With the fitted response surface obtained in this chapter, further developments for defining partial safety factors for composite design purpose are now possible.

Chapter 7:
Discussions and Conclusions

7.1 Discussions

On the basis of the work outlined in this thesis a number of issues deserve brief discussion, and they are as follows.

The primary objective of the research presented in this thesis is to develop a stochastic approach to the design of composite structures that is able to account for variations in material properties, geometric properties, load effects and processing techniques. Two main aspects need to be considered for the composite structures in the reliability analysis. One important aspect is that the mechanical model should be suitable for the development of a reliability-based design method for composite structures of ships. The second important aspect is that the probabilistic model has to be carefully chosen to consider computational efficiency which may restrict their applicability.

The study begins with the background of the design for the composite structures. Different methods available to calculate the strength of unstiffened and stiffened plates were reviewed and their advantages and disadvantages were discussed. In order to indentify all possible uncertain variables at all stages of the fabrication process, a brief overview of production defects for single-skin laminates and face laminates of sandwich structures and their causes and effects were given.

Four different levels of reliability analysis that depend mainly on the available input information and the application of the probabilistic approach were discussed. The practicability of structural reliability analysis methods for a specific limit state depends to a great extent on the complexity of the formulation of the limit state. The

approximate methods such as FORM and SORM are carried out based on the existence of closed-form expressions for the failure function. FORM is usually sufficient to get a rational estimate of the structural reliability in the situation where the limit state function is not strongly nonlinear. The advantage of FORM is that the computing time is small. However, if the limit state surface has significant curvature, SORM may yield better estimates of the failure probability, but it is computationally more intensive than the FORM. If the limit state function is not differentiable or the failure domain cannot be represented by linear or quadratic form, simulation-based method is feasible as one of the most attractive alternatives. After giving sufficient simulations, this method will always converge to the same result. The disadvantage of the simulation-based method is the number of simulations required may be very large even it has been improved a lot by variance reduction techniques and adaptive iteration.

For practical problems the performance function of the structures may be evaluated numerically by the commercial software, the FORM, SORM and simulated-based method may not suitable. Response surface method is used as a vehicle for incorporating finite element analysis into structural reliability computation through constructing a predictive equation. Once the response surface is fitted, the reliability analysis can be carried out by any of the methods previously described.

An analytical method, which is suitable for a simple topology, i.e. unstiffened FRP plate structure, was produced. The probabilistic design approach was proposed to laminate composite plates at design stages in order to tackle the design in a more realistic way. The design process is then a matter of selecting appropriate nominal member sizes and strengths so that the overall probability of failure does not exceed a chosen value. However, analytical methods are limited to specific shapes of plates with a limited set of boundary conditions. For more general structures with arbitrary geometries and boundary conditions, numerical methods are the most effective means. Hence, a progressive failure analysis method was developed for predicting the ultimate strength of laminated composite plates under compressive load using commercial software ANSYS. The multi-frame restart analysis was used to consider

the effect of degradation of material properties

The benchmark study was performed on a number of fibre reinforced plates with various thicknesses and imperfections. Three failure modes i.e. matrix cracking, fibre breakage and fibre/matrix interface failure were taken into account in the models. The limited stiffness reduction model was introduced and the elastic material properties associated with that mode of failure was set to a small fraction of the original properties of the undamaged material once failure was detected somewhere. Based on these studies, the following main concluding remarks can be made:

- The procedure of progressive failure analysis using the multi-frame restart analysis with Tsai-Wu failure criterion is feasible by comparing the results with those obtained from published experiments.

- For the benchmark study, good correlation with the test results was found for the most cases. The possible reasons for the most significant difference between the experimental measurements and numerical predictions may be due to the use of nonlinear boundary conditions and conservative damage modelling.

- A probabilistic analysis requires more information than the corresponding deterministic methods. The primary sources of error to apply the probabilistic approach at the design stage are the lacking of adequate data of the uncertainties associated with the variables in the limit state equation. Thus, the sensitivity analysis should be performed to study the effects of the various variables and statistical distribution.

The strength assessments of hat-stiffened panels made of composite material were developed based on the grillage model and beam-column model. Equivalent elastic properties were used for laminate composite plates. A complete program has been generated and validated by comparing the results obtained from finite element calculations and experimental results published in the literatures. From the study conducted the following specific conclusions can be drawn:

- The numerical results showed that this simplified analytical procedure is feasible and very fast for effectively analysing the stiffened composite panel in the preliminary and reliability-based design stages.

- A unique feature of fibre-reinforced polymers is the flexibility in their composition which enables a designer to design a structure to specifically meet constraints. The analytical method provides a useful means for initial design purposes and explores quantitatively the influence of the various constituent properties on reliability. This has enabled the variables having the greatest influence on reliability to be identified and may allow the engineer to concentrate on these more important variables.

- Reliability analysis shows that not only mean value but also COV of random variables plays a very important role in determining the reliability of the structures. The uncertainties of variables are generally caused by the lack of data, modeling simplifications, human errors or inadequate knowledge of physical phenomena, etc. The parametric study provided an insight into COV of various parameters to the effect on the reliability index.

- The model uncertainty and applied loads are very sensitive to the statistics of variables. Thus more precisely knowing the statistics of these two design variables will induce more meaningful results in the reliability analysis. Improving the accuracy of analysis method, such as by applying more advanced analysis method can minimise the modelling error and its variation so as to increase the safety index.

- The variation in component thicknesses from design and the fibre content within a component is also sensitive to the reliability calculation. In other words, the minor variation in these two variables has a major effect on the reliability. Therefore, if the uncertainties of such random variables can be reduced through approximate care or the stricter quality control, the reliability can be increased.

- The influence of the variation in the fibre modulus E_f is stronger than in the shear modulus G_m on reliability. That indicates that it is better to reduce the uncertainty of E_f rather than G_m in terms of their relative importance with respect to variations in their standard deviations. More testing would be required to control the scatter of this significant variable.

As discussed in Chapter 2, numerical methods are the most effective means for the structures with arbitrary geometries and boundary conditions. For practical problems, the performances of the structures may evaluate numerically by the commercial software such as ANSYS or ABAQUS. In these situations, the FORM, SORM and simulated-based method may not suitable. Therefore, an application methodology for structural reliability analysis of the composite structures based on the response surface method in conjunction with nonlinear finite element analysis was demonstrated. The response function for the ultimate failure is generated using quadratic polynomial. Stepwise response surface method is used to fit the true limit state function. The numerical application shows the efficiency of the RSM-FEM coupling, through the analysis of complex nonlinear structures with a reasonable number of mechanical calls.

Based on these methods a reliability-based design code format has been suggested for partial safety factors which can be used in design for certain target reliability level. The load and resistance factor design formats can be used by designers to account for uncertainties without a direct use of probabilistic description of the variables and while maintaining the simplicity of deterministic design practice. In the absence of other information, the partial factors presented could be used as a first-step in a reliability-based design procedure. With the fitted response surface obtained in this chapter, further developments for defining partial safety factors for composite design purpose are now possible.

7.2 Achievements and Contributions

Main contributions of this research work are summarized as follows

- An establishment of reliability framework, which could be applied to composite structure.

- An adaptation of the simplified methods for analysing unstiffened and stiffened plates. These simplified analytical procedures are feasible and very fast for effectively analysing the composite structures in the preliminary and reliability-based design stages.

- The reliability analysis and sensitivity analysis are performed based on the constituent level. This allows the engineers to concentrate on these more important factors in terms of design or manufacture.

- Structural reliability analysis of the composite structures based on the response surface method in conjunction with nonlinear finite element analysis is applied.

- Based on these methods a reliability-based design code format has been suggested, the partial safety factors can be obtained using this form for certain target reliability.

7.3 Recommendations for Future Research

- The failure criteria and the property degradation models could be further developed for marine composite materials to provide a more reasonable basis for the strength prediction.

- As the collapse of composite structures strongly affects by the delamination and the debonding of the stiffeners, such failure modes might be considered for the future research

- Although some of failure modes can be analysed by the present simplified method to a certain degree of accuracy, the interaction between different failure modes should be investigated further.

- There are problems with the data that are not well defined in reliability analysis. Once adequate and sufficient data are known with more precisely, the reliability results become more reliable, especially for the variable which is very sensitive to the performance of structure.

- Component reliability is addressed for individual independent failure modes. The response calculation incorporating the system reliability would be more accurate as multiple failure modes, as well as multiple interacting failure modes, are generally involved in structure failure.

- The optimisation of these partial safety factors for an assumed target reliability need to be evaluated which can be used in codified design.

References

Abu-Farsakh, G., & Abdel-Jawad, Y. (1994). A new failure criterion for nonlinear composite materials. *Journal of Composites Technology and Research*, Vol. 16(2), pp.138–145.

Al-Rifaie, W. N., & Evans, H. R. (1979). An approximate method for the analysis of box girder bridges that are curved in plan. *Proc. Int. Association of Bridges and Structural Engineering*, Int. Association for Bridge and Structural Engineering (IABSE), pp.1–21.

Ambur, D. R., Jaunky, N., Dávila, C. G., & Hilburger, M. W. (2001). Progressive failure studies of composite panels with and without cutouts. *NASA/CR-2001-211223*, ICASE Report, No.2001-27.

ANSYS User Manuals version 11.0, ANSYS Inc, USA

Åström, B. T. (1997). *Manufacturing of polymer composites*. Chapman & Hall, London, UK.

Azzi, V. D., & Tsai, S. W. (1965). Anisotropic strength of composites. *Experimental Mechanics*, pp.283-288.

Baranski, A. T., & Biggers, S. B. (1999). Postbuckling analysis of tailored composite plates with progressive failure. *Compos. Struct.* Vol. 46, pp.245–255.

Berggreen, C., Tsouvalis, N., Karantzas, V., Douka, C., & Delarche, A. (2009). Experimental round-robin measurement of material properties for UD laminates

applied in composite plate tests. *MARSTRUCT Report: MAR-D4-3-DTU-NTUA -01(2)*.

Bjerager, P., & Krenk, S. (1989). Parametric sensitivity in first-order reliability theory. *J. Eng. Mech., ASCE*, Vol.115 (7) pp.1577-1582.

Böhm, F., & Brückner-Foit, A. (1992). On criterion for accepting a response surface model. *Probabilistic Engineering Mechanics*, Vol. 7(3), pp.183-190.

Boote, D. (2007). Parametric evaluation of the effective breadth for GRP beams with FEM calculation. *Maritime Industry*, *IMAM 2007*, Varna, Bulgaria.

Box, G. E. P., & Wilson, K. B. (1951). On the experimental attainment of optimum conditions. *Journal of the Royal Statistical Society Series B*, Vol. 13(1), pp.1– 45.

Box, G. E. P., & Behnken, D. W. (1960). Some new three level designs for the study of quantitative variables. *Technometrics 2*, pp. 455-475.

Brown, D. K. (1990). Design consideration for MCMV. *Naval forces,* Vol.11(1), pp.31-38.

Bucher, C. G., & Bourgund, U. (1990). A fast and efficient response surface approach for structural reliability problems. *Structural Safety*, Vol. 7 (1), pp.57-66.

Cappello, F., & Tumino, D. (2006). Numerical analysis of composite plates with multiple delaminations subjected to uniaxial buckling load. *Composites Science and Technology*, Vol. 66(2), pp.264-272.

Cassenti, B. N. (1984). Probabilistic static failure of composite material. *AIAA Journal*, Vol.22 (1), pp.103-110.

Cederbaum, G., Elishakoff, I., & Librescu, L. (1990). Reliability of laminated plates

via the first-order second-moment method. *Composite Structures,* Vol.15, pp.161-167.

Chai, H., Babcock, C. D., & Knauss, W. G. (1981). One dimensional modeling of failure in laminated plates by delamination buckling. *International Journal of Solids and Structures*, Vol.17 (11), pp.1069–1083.

Chalmers, D. W., Osburn, R. J., & Bunney, A. (1984). *Hull construction of CMVs in the United Kingdom*. Proceedings of the International Symposium on Mine Warfare Vessels and Systems, London, Paper 13.

Chamis, C. C. (1969). Failure criteria for filamentary composites. *Composite Materials: Testing and Design, STP 460. American Society for Testing and Materials*, Philadelphia, pp.336-351.

Chang, F. K., & Chang, K. Y. (1987). A progressive damage model for laminated composites containing stress concentrations. *J. Compos. Mater*, Vol.21, pp.834–855.

Cheetham, M. A. (1986). Naval applications of reinforced plastics. *Plastics Polym*. Vol.36 (121), pp.15-20.

Chen, N. Z., & Soares, C. G. (2007). Reliability assessment of post-buckling compressive strength of laminated composite plates and stiffened panels under axial compression. *International Journal of Solids and Structures*, Vol.44(22-23), pp.7167-7182.

Chen, W., & Wu, Z. (2005). A new higher-order shear deformation theory and refined beam element of composite laminates. *Acta Mechanica Sinica*, Vol. 21(1), pp.65-69.

Chen, X., & Lind, N. C. (1982). *A new method for fast probability integration*. University of Waterloo, Research Paper, No.171, Waterloo, Canada.

Chen, Z. N., & Soares C.G. (2007). Reliability assessment for ultimate longitudinal strength of ship hulls in composite materials. *Probability Engineering Mechanics,* Vol. 22(4), pp.330-342.

Cheung, M. S., Bakht, B., & Jaeger, L. G. (1982). Analysis of box girder bridges by grillage and orthotropic plate methods. *Canadian Journal of Civil Engineering*, Vol.9 (4), pp.595-601.

Cheung, Y. K. (1976). *Finite strip method in structural analysis*. Pergamon Press, Oxford.

Christensen, R. M. (1988). Tensor transformations and failure criteria for the analysis of fiber composite materials. *Journal of Composite Materials*, Vol.22 (9), pp.874-897.

Clarkson, J. (1965). *The elastic analysis of flat grillage*. Cambridge University Press, Cambridge.

Cobb, B. (1968). Design, construction and economic considerations in fibreglass trawler construction. *Proc. Conf. on Fishing Vessel Construction Materials*, Montreal.

Cornell, C. A. (1969). A probability-based structural code. *Journal of the American Concrete Institute,* Vol. 66 (12), pp. 974-985.

Daniels, H. E. (1945). The statistical theory of the strength of bundles and threads. *Proc. Royal Soc. A183, London,* pp.405- 435.

Das, P. K., & Zheng, Y. (2000). Cumulative formation of response surface and its use in reliability analysis. *Probabilistic Engineering Mechanics*, Vol.15, pp. 309-315.

Datoo, M. H. (1991). *Mechanics of fibrous composites*. Elsevier, Science Publishers.

Dawe, D. J., & Peshkam,V. (1996). A note on finite strip buckling analysis of composite plate structures. *Composite Structures*, Vol.34, pp.163-168.

Der Kiureghian, A., Lin, H. Z., & Hwang, S. J. (1987). Second-order reliability approximations. *Journal of Engineering Mechanics*, Vol.113 (8), pp.1208-1225.

Der Kiureghian, A., & De Stefano M. (1991). Efficient algorithm for second-order reliability analysis. *Journal of Engineering Mechanics*, Vol.117 (12), pp. 2904-2923.

Ditlevsen, O. (1973). *Structural Reliability and the Invariance Problem*. Research Report, No. 22, Solid Mechanics Division, University of Waterloo, Waterloo.

Ditlevsen, O., & Madsen, H. O. (1996). *Structural reliability methods*. New York, John Wiley & Sons Inc.

DNV (2003). Offshore Standard DNV-OS-C501. Composite Components.

Engelstad, S. P., Reddy, J. N., & Knight, N. F. (1992). Postbuckling response and failure prediction of graphite-epoxy plates loaded in compression. *AIAA J.* Vol. 30(8), pp. 2106–2113.

Engelstad, S. P., & Reddy, J. N. (1993). Probabilistic nonlinear finite element analysis of composite structures. *AIAA Journal,* Vol.31(2), pp.362-369.

Engelund, S., & Rackwitz, R. (1993). A benchmark study on importance sampling techniques in structural reliability. *Structural Safety*, Vol.12 (4), pp.255-276.

Evans, H. R. (1984). Simplified methods for the analysis and design of bridges of cellular cross-section. *Proc. NATO Advanced Study Institute on Analysis and Design of Bridges*, Cesme, Izmir, Turkey, Vol.74, pp.95–115.

Evans, H. R., & Shanmugam, N. E. (1984). Simplified analysis for cellular structures. *Journal of Structural Engineering*, Vol.110 (3), pp.531–543.

Evans, H. R., Ahmad, M. K. H., & Kristek, V. (1993). Shear lag in composite box girders of complex cross-sections. *Journal of Constructional Steel Research*, Vol. 24(3) pp.183–204.

Fan, S., Kroeplin, B., & Geier, B. (1992). Buckling, postbuckling and failure behaviour of composite stiffened panels under axial compression. *In: Proceedings of 33rd AIAA Structures, Structural Dynamics and Materials Conference AIAA-19 92-2285*, pp. 264–273.

Faravelli, L. (1989). Response surface approach for reliability analysis. *Journal of Engineering Mechanics,* ASCE, Vol.115 (12), pp.2763-2781.

Faulkner, D., Soares, C. G. & Warwick, D.M. (1988). Modelling requirements for structural design and assessment. In: D. Faulkner, A. Incecik and M.J. Cowling, Editors, *Integrity of Offshore Structures* Vol. 3, pp.17–27.

Fiessler, B., Neumann, H. J., & Rackwitz, R. (1979). Quadratic limit states in structural reliability. *Journal of the Engineering Mechanics Division*, ASCE, Vol.105(4), pp.661-676.

Frangopol, D. M., & Recek, S. (2003). Reliability of fiber-reinforced composite laminated plates. *Probabilistic Engineering Mechanics*, Vol. 18(2), pp.119-137.

Ganesan, R., & Zhang, D. (2004). Progressive failure analysis of composite laminates subjected to in-plane compressive and shear loadings. *Science and Engineering of Composite,* Vol. 11(2/3).

Goldberg, J. E., & Leve, H. L. (1957). Theory of prismatic folded plate structures. *Int. Ass. Bridge Struct. Eng.* Vol.17, pp. 59–86.

Graner, W. R. (1982). *Marine applications*, in Handbook of Composites. Van Nostrand Reinbold, New York.

Graves-Smith, T. R., & Sridharan, S. (1978). A finite strip method for buckling of plate structures under arbitrary loading. *International Journal of Mechanical Science* Vol.20, pp.685-93.

Greene, E. (1990). *Use of fibre reinforced plastics in the marine industry*. Ship Structure Committee，Report SSC-360.

Gullberg, O., & Olsson, K. A. (1990). Design and construction of GRP sandwich ship hulls. *Marine structures*, Vol.3, pp. 93-109.

Gurvich, M. R., & Pipes, R. B. (1995). Probabilistic analysis of multi-step failure process of a laminated composite in bending. *Composite Science and Technology*, Vol. 55(4) pp.413-421.

Harlow, D. G., & Phoenix, S. L. (1981). Probability distribution for the strength of composite materials I: two-level bounds. *Intl. J. Fracture*, Vol.17, pp.321-336.

Harlow, D. G., & Phoenix, S. L. (1982). Probability distributions for the strength of fibrous materials under local load-sharing, I: two-level failure and edge effects. *Adv. Appl. Probab*, Vol.14, pp.68–94.

Hashin, Z. (1980). Failure criteria for unidirectional fiber composites. *Journal of Applied Mechanics*, Vol.47, pp.329-334.

Hasofer, A. M., & Lind, N. C. (1974). Exact and invariant second-moment code format. *Journal of Engineering Mechanics*, ASCE, Vol.100 (1), pp.111-121.

Heller, S. R. (1967). The use of composite materials in naval ships. *Mechanics of Composite Materials*: *Proceedings of the Fifth Symposium on Structural Mechanics*,

Oxford Pergamon Press, pp.69-111.

Henton, D. (1967). Glass reinforced plastics in the Royal Navy. *Trans, RINA*, Vol.109, pp.487-501.

Hill, R. (1950). *The mathematical theory of plasticity*. Oxford University Press, London, pp.318.

Hinton, M. J., Kaddour, A. S., & Soden, P. D. (2002). A comparison of the predictive capabilities of current failure theories for composite laminates, judged against experimental evidence. *Composite Science and Technology*, Vol.62, pp.1725-1797.

Hoffman, O. (1967). The brittle strength of orthotropic materials. *Journal of Composite Materials*, Vol.1, pp.200-206.

Hohenbichler, M., & Rackwits, R. (1981). Non-normal dependent vectors in structural safety. *Journal of the Engineering Mechanics Division*, Vol. 107(6), pp.1227-1238.

Hohenbichler, M., & Rackwitz, R. (1986). Sensitivity and importance measures in structural reliability. *Civil Eng. Systems*, Vol. 3(4), pp.203-209.

Hohenbichler, M., Gollwitzer, S., Kruse, W., & Rackwitz, R. (1987). New light on first- and second-order reliability methods. *Structural Safety*, Vol.4, pp.267-284.

Hohenbichler, M., & Rackwitz, R. (1988). Improvement of second-order reliability estimates by importance sampling. *Journal of Engineering Mechanics*, Vol.114 (12), pp.2195-2199.

Hosseini-Toudeshky, H., Ovesy, H. R., & Kharazi, M. (2005). The development of an approximate method for the design of bead-stiffened composite panels. *Thin-Walled Structures*, Vol. 43(11), pp.663-1676.

Ibnabdeljalil, M., & Curtin, W. A. (1997). Strength and reliability of fiber reinforced composites: localized load-sharing and associated size effects. *International Journal of Solids and Structures*, Vol.34 (21), pp.2649-2668.

Ibrahim, Y. (1991). Observations on applications of importance sampling in structural reliability analysis. *Structural Safety*, Vol.9(4), pp.269-281.

Jang, C. D., Seo, S. I., & Kim, S. K. (1996). A study on the optimum structural design of surface effect ships. *Marine Structures,* Vol.9, pp.519-544.

JeffWu, C. F., & Hamada, M. (2002). *Experiments planning, analysis and parameter design optimization*. John Wiley & Sons, Inc.

Jeong, H. K., & Shenoi, R. A. (1998). Reliability analysis of mid-plane symmetric laminated plates using direct simulation method. *Composite Structures*, Vol.43(1), pp.1–13.

Jeong, H. K., & Shenoi, R.A. (2000). Probabilistic strength analysis of rectangular FRP plates using Monte Carlo simulation. *Computers & Structures*, Vol.76 (1-3), pp.219–235.

Johansson, A. (2005). *Dry-zones in sandwich panels*. MSC thesis, Royal Institute of Technology, Stockholm, Sweden.

Kam, T. Y., Lin, S. C., & Hsiao, K. M. (1993). Reliability analysis of nonlinear laminated composite plate structures. *Composite Structures*, Vol. 25(1-4), pp.503-510.

Kam, T. Y., & Sher, H. F. (1995). Nonlinear and first-ply failure analysis of laminated cross-ply plates. *Journal of Composite Materials*, Vol.29, pp.463-482.

Kam, T. Y., & Chang, E. S. (1997). Reliability formulation for composite laminates

subjected to first-ply failure. *Composite Structures*, Vol.38 (1-4), pp.447-452.

Kant, T., & Manjunatha, B. S. (1994). On accurate estimation of transverse stresses in multilayer laminates. *Computers & Structures*, Vol. 50 (3), pp.351-365.

Khdeir, A. A. (1989). An exact approach to the elastic state of stress of shear deformable antisymmetric angle-ply laminated plates. *Composite Structures*, Vol.11, pp.245-258.

Khdeir, A. A., & Reddy, J. N. (1991). Analytical solutions of refined plate theories of cross-ply composite laminates. *Journal of Pressure Vessel Technology, Transactions of the ASME*, Vol.113, pp. 570-578.

Khuri, A. I., & Cornell, J. A. (1987). *Response surface, designs and analyses*. statistics textbooks and monographs series, Vol.81, Marcel Dekker, New York.

Kim, S. H., & Na, S. W. (1997). Response surface method using vector projected sampling points. *Structural Safety*, Vol. 19(1), pp.3-19.

Klug, J., Wu, X. X., & Sun, C. T. (1996). Efficient modeling of postbuckling delamination growth in composite laminates using plate elements. *AIAA Journal*, Vol.34 (1), pp.178–184.

Knight, N. F., Rankin, C. C., & Brogan, F. A. (2000). Controlling a nonlinear solution procedure during a progressive failure analysis. *AIAA/ASME/ASCE/AHS /ASC Structures, Structural Dynamics, and Materials Conference and Exhibit*, 41st, Atlanta, GA, United States.

Kong, C. W., Lee, I. C., Kim, C. G., & Hong, C. S. (1998). Postbuckling and failure of stiffened composite panels under axial compression. *Composite Structures*, Vol.42 (1), pp.13–21.

Kristek, V., Evans, H. R., & Ahmad, M. K. M. (1990). Shear lag analysis for composite box girder. *Journal of Constructional Steel Research*, Vol.16(1), pp.1-21.

Laros, W. P. J. (1984). Tripartite MCMV. *Proc. Int. Symp. on Mine Warfare Vessels and Systems*, RINA, London

Lee, J. D.(1982). Three-dimensional finite element analysis of damage accumulation in composite laminate. *Computers and Structures*, Vol.15 (3), pp.335-350.

Lee, K. H., Senthilnathan, N. R., Lim, S. P., & Chow, S. T. (1990). An improved Zig-Zag model for the bending of laminated composite plates. *Composite Structures*, Vol.15, pp.137-148.

Lemiere, Y. (1992). The evolution of composite materials in submarine structures. *Proceedings of the International Conference on Nautical Construction with Composite Materials*, Paris, Paper 43.

Lin, S. C., Kam, T. Y., & Chu, K. H. (1998). Evaluation of buckling and first-ply failure probabilities of composite laminates. *International Journal of Solids and Structures*, Vol. 35(13), pp.1395-1410.

Lin, S. C. (2000). Reliability predictions of laminated composite plates with random system parameters. *Probabilistic Engineering Mechanics*, Vol. 15(4), pp.327-338.

Liu, P. L., Lin, H. Z., & Der Kiureghian, A. D. (1989). *CALREL user manual*. Department of Civil Engineering, University of California at Berkeley.

Liu, P. L, & Der Kiureghian, A. D. (1990). Optimization algorithms for structural reliability. *Structural Safety,* Vol.9(3), pp.161-177.

Liu, P. F., & Zheng, J. Y. (2008). Progressive failure analysis of carbon fiber/epoxy composite laminates using continuum damage mechanics. *Material Science and*

Engineering, pp.711-717.

Lloyd's Register Rules and Regulations - Rules and Regulations for the Classification of Special Service Craft, July 2004

Loughlan, J., & Delaunoy, J. M. (1993). The buckling of composite stiffened plates with some emphasis on the effects of fibre orientation and on loading configuration. *Composite Structures*, Vol.25 (1-4), pp. 485- 494.

Loughlan, J. (1996). The buckling of composite stiffened box sections subjected to compression and bending. *Composite Structures*, Vol.35, pp.101-116.

Madsen, H. O., Krenk, S., & Lind, N. C. (1986). *Methods of structural safety*. Prentice-Hall.

Maisano, A. J. (2003). Manufacturing processes of composite materials for a human powered submarine. *Oceans Conference*, Vol.5, pp.2678-2681.

Maneepan, K., Shenoi, R. A., Blake, J. I. R., & Jeong, H. K. (2007). Genetic algorithm (GAs) based optimisation of FRP composite plated grillages in ship structures. *Transactions of the Royal Institution of Naval Architects*, *Part A: International Journal of Maritime Engineering*, Vol.149, pp.1-19.

Mansour, A. E. (1977). Cross panel strength under combined loading. *Ship Structure Committee*, SSC-270, Washington, DC.

Mansour, A. E., & Wirsching, P. H. (1995). Sensitivity factors and their application to marine structures. *Marine Structures*, pp.229-255.

Marsh, J. G., & Taylor, P. (1990). PC program for orthotropic plate box girder bridges. *Australia Second National Structural Engineering Conference*, Institution of Engineers, Australia. pp. 224–235.

Marsh, G. (2001). Composite ship shafts shape up. *Reinforced Plastics*, Vol. 45(11), pp.32-36.

Mau, S. T. (1973). A refined laminate plate theory. *Journal of Applied Mechanics*, Vol.40, pp.606-607.

Melchers, R. E. (1990). Search-based importance sampling. *Structural Safety*, Vol.9 (2), pp.117-128.

Melchers, R. E. (1999). *Structural reliability analysis and prediction*. 2nd edition, Chichester.

Meyer, C., & Scordelis, A .C. (1971). Analysis of curved folded plate structures. *Journal of the Structural Division*, Vol.97 (10), pp.2459–2480.

Miki, M., Murotsu, Y., Shao, S., & Tanaka, T. (1990). Reliability of unidirectional fibrous composites. *AIAA Journal*, Vol.28 (11), pp.1980-1986.

Mindlin, R. D. (1951). Influence of rotary inertia and shear on flexural motions of isotropic, elastic plates. *J Appl Mech,* Vol.18, pp.31–38.

Mouritz, A. P., Gellert, E., Burchill, P., & Challis, K. (2001). Review of advanced composite structures for naval ships and submarines. *Composite Structures*, Vol.53, pp.21-41.

Mukhopadhyay, M. (1989a). Vibration and stability analysis of stiffened plates by semi-analytic finite difference method, Part I: consideration of bending displacements only. *Journal of Sound and Vibration*, Vol.130 (1), pp.27-39.

Mukhopadhyay, M. (1989b). Vibration and stability analysis of stiffened plates by semi-analytic finite difference method, Part II: consideration of bending and axial displacements only. *Journal of Sound and Vibration*, Vol.130 (1), pp.41-53.

Murray, Y., & Schwer, L. (1990). Implementation and verification of fibre composite damage models, failure criteria and analysis in dynamic response. *ASME*, AMD-Vol.107, pp.21-30.

Murthy, M. V. V. (1981). An improved transverse shear deformation theory for laminated anisotropic plates. *NASA technical Paper 1903*, pp.1–37.

Myers, R. H., & Montgomery, D. C. (1995). *Response surface methodology: process and product optimization using designed experiments.* New York, Wiley.

Myers, R. H., & Montgomery, D. C. (2002). *Response surface methodology: process and product optimization using designed experiments*. Second Edition, Wiley, New York.

Nahas, M. N. (1986). Survey of failure and post-failure theories of laminated fibre-reinforced composites. *Journal of Composite Technology and Research*, Vol.8 (4), pp.138-153.

Nishii, S. (1983). On the FRP-made motor yacht Asian lady. *J. Fishing Boat Asso.* Vol.91, Japan.

Ochoa, O. O., & Engblom, J. J. (1987). Analysis of failure in composites. *Compos. Sci. Technol.*, Vol.28, pp. 87–102.

Onkar, A. K., Upadhyay, C. S., & Yadav, D. (2007). Probabilistic failure of laminated composite plates using the stochastic finite element method. *Composite Structures*, Vol. 77(1), pp.79-91.

Orificia, A. C., Thomson, R. S., Herszzberg, I., Weller, T., Degenhardt, R., & Bayandor, J. (2008). An analysis methodology for failure in postbuckling skin-stiffener interfaces. *Composite Structures*, Vol. 86 (1-3), pp.186-193.

Ovesy, H. R., & Assaee, H. (2001). Buckling analysis of some composite stiffened plate structures due to in-plane compression and shear loading using finite strip method. *Proceedings of ISME-2001*, Vol.4, Iranian Society of Mechanical Engineers, pp.75-82.

Ovesy, H. R., & Assaee, H. (2003). Buckling characteristics of some composite stiffened boxes under longitudinal compression or bending using finite strip approach. *44th AIAA/ASME/ASCE/AHS /ASC Structures*, *Structural Dynamics and Materials Conference*, Norfolk, Virginia.

Padhi, G. S., Shenoi, R. A., Moy, S. S. J., & Hawkins, G. L. (1998). Progressive failure and ultimate collapse of laminated composite plates in bending. *Composite Structures*, Vol.40 (3-4), pp, 277-291.

Petit, P. H., & Waddoups, M. E. (1969). A method of predicting the nonlinear behaviour of laminated composites. *Journal of Composite Materials*, Vol.3(1), pp.2-19.

Pugsley, A. el at., (1955). Report on structural safety. *Structural Engineer,* Vol. 33(5) pp.141-149.

Rackwitz, R., & Fiessler, B. (1977). An algorithm for calculation of structural reliability under combined loading. *Berichte zur Sicherheitheorie der Bauwerke*, Munchen.

Rackwitz, R., & Fiessler, B. (1978). Structural reliability under combined random load sequence. *Computers and Structures*, Vol.9, pp.484–494.

Rackwitz, R. (1982). *Response surfaces in structural reliability*. Berichte zur Zuverlässigkeitstheorie der Bauwerke, Heft 67, München.

Rajashekhar, M. R., & Ellingwood, B. R. (1993). A new look at the response surface approach for reliability analysis. *Structural Safety*, Vol. 12(3), pp.205-220.

Razzaq, R. J., & EI-Zafrany, A. (2005). Non-linear stress analysis of composite layered plates and shells using a mesh reduction method. *Engineering analysis with boundary elements*, Vol.29 (12), pp.1115-1123.

Ravindra, M. K.& **Galambos**, T. V., (1978). Load and resistance factor design for steel, *Journal of the Structural Division,* Vol. 104(9) pp. 1337-1353.

Reddy, J. N. (1984). A simple higher order theory for laminated composite plates. *J Appl. Mech.*, Trans ASME, Vol.51, pp. 745–752.

Reddy, J. N., Khdeir, A. A., & Librescu, L. (1987). Levy type solutions for symmetrically laminated rectangular plates using first-order deformation theory. *Journal of Applied Mechanics*, Vol.54, pp.740-742.

Reddy, J. N. & Pandey, A. K. (1987). A first-ply failure analysis of composite laminates. *Computers & Structures*, Vol.25, pp.371-393.

Reddy, J. N. (1990). A general non-linear third-order theory of plates with moderate thickness. *International Journal of Non-Linear Mechanics*, Vol. 25(6), pp. 677-686.

Reddy, J. N. (2004). *Mechanics of laminated composite plates and shells: theory and analysis*. 2nd ed. CRC Press.

Reddy, Y. S. N. & Reddy, J. N. (1992). Linear and non-linear failure analysis of composite laminates with transverse shear. *Composites Science and Technology*, Vol.44(3), pp.227-255.

Reddy, Y. S., & Reddy, J. N. (1993). Three-dimensional finite element progressive failure analysis of composite laminates under axial extension. *Journal of Composites*

Technology and Research, Vol. 15(2), pp.73- 87.

Reissner, E. (1945). The effect of transverse shear deformation on bending of elastic plates. *J. Appl. Mech.,* Vol.12, pp.A69–A77.

Reissner, E., & Stavsky, Y. (1961). Bending and stretching of certain types of heterogeneous aelotropic elastic plates. *ASME J. Appl. Mech.,* Vol. 28, pp.402–408.

Reitung, K. (1984). Asymptotic approximations for multinormal integrals. *J. Eng. Mech. ASCE*, Vol. 110(3), pp.357-366.

Ren, J. G. (1986). A new theory of laminated plates. *Composite Science and Technology*, Vol.26, pp.225-239.

Rosen, B. W. (1964). Tensile failure of fibrous composites. *AIAA Journal* 2 pp.1985–1991.

Rowlands, R. E. (1985). Strength theories and their experimental correlation, Chapter II, *Handbook of Composites*, vol. III, *Failure Mechanics of Composites*, Edited by G. C. Sih and A. M. Skudra, Elsevier Science Publishers.

Sandhu, R. S. (1974). Nonlinear behaviour of unidirectional and angle ply laminates. *AIAA Journal of Aircraft*, Vol.13, pp.104-111.

Scott, R. J., & Sommella, J. H. (1971). *Feasibility study of glass reinforced plastic cargo ship*. US Ship Structures Committee, Report SSC-224.

Schueller, G. I., & Stix, R. (1987). A critical appraisal of methods to determine failure probabilities. *Structural Safety,* Vol.4 (4), pp.293-309.

Shahid, I., & Chang, F. K. (1995). An accumulative damage model for tensile and shear failures of laminated composite plates. *J. Compos. Mater.*, Vol.29 (7), pp.926-

981.

Sharpe, R. (1999). *Jane's fighting ship 1999-2000*. Coulsdon, UK: Jane's Information group limited.

Shenoi, R. A., & Wellicome, J. F. (1993). *Composite materials in maritime structures*. Cambridge University Press, UK.

Shinozuka, M. (1983). Basic analysis of structural safety. *Journal of Structural Engineering*, ASCE, Vol. 109(3), pp 721-740.

Short, G. J., Guild, F. J., & Pavier, M. J. (2002). Delaminations in flat and curved composite laminates subjected to compressive load. *Composite Structures*, Vol. 58(2), pp.249-258.

Singh, S. B., & Kumar, A. (1998). Postbuckling response and failure of symmetric laminates under in-plane shear. *Compos. Sci. Technol.*, Vol.58, pp.1949–1960.

Sjogron, J., Celsing, C. G.., Olsson, K. A., Levander, C. G.., & Hellbratt, S. E. (1984). Swedish development of MCMV hull design and construction. *Proc. Int. Symp. on Mine Warfare Vessels and Systems, RINA,* London.

Sleight, D.W., Knight, N. F. Jr., & Wang, J. T. (1997). Evaluation of a progressive failure analysis methodology for laminated composite structures. *In: Proceedings of the 38th AIAA/ASME/ASCE/AHS/ASC Structures, Structural Dynamics, and Materials Conference*, Reston, VA, pp. 2257–72.

Sleight, D. W. (1999). Progressive failure analysis methodology for laminated composite structures. *Technical Report: NASA-99-tp209107*.

Smith, C. S. (1966). Elastic analysis of stiffened plating under lateral loading. *Transactions of the Royal Institution of Naval Architects*, Vol.108, pp.113-131.

Smith, C. S. (1968). Bending, buckling and vibration of orthotropic plate beam structures. *Journal of Ship Research*, Vol.12 (4), pp.249-268.

Smith, C. S., & Dow, R. S. (1985). Compressive strength of Longitudinally Stiffened GRP Panel. *In: I.H. Marshall, Editor, Composite structures 3*, Elsevier Science Publishers, pp.468–490.

Smith, C. S., & Dow, R. S. (1987). Interactive buckling effects in stiffened FRP panels. *In: I.H. Marshall, Editor, Composite structures 4*, Vol.1, Elsevier Science Publishers, pp.122–137.

Smith, C. S. (1990). *Design of Marine Structures in Composite Materials*. Elsevier Applied Science, London.

Soares, C. G.. (1997). Reliability of components in composite materials. *Reliability Engineering and System Safety*, Vol.55 (2), pp.171-177.

Soden, P. D., Hinton, M. J., & Kaddour, A. S. (2002). Experimental failure stresses and deformations for a range of composite laminates subjected to uniaxial and biaxial loads: failure exercise benchmark data. *Composite Science and Technology*, Vol.62, pp.1489–1514.

Starnes, J. H. Jr., & Rouse, M. (1981). Postbuckling and failure characteristics of selected flat rectangular graphite-epoxy plates loaded in compression. *Proc. 22nd AIAA/ASME/ASCE/ AHS Structures, Structural Dynamics and Materials Conf*, pp.422-423.

Stroud, W. J., Greene, W. H., & Anderson, M. S. (1984). Buckling loads of stiffened panels subjected to combined longitudinal compression and shear: results obtained with PASCO, EAL and STAGS Computer Programs. *NASA TP-2215*.

Sutherland, L. S., & Soares, C. G. (1997). Review of probabilistic models of the

strength of composite materials. *Reliability Engineering and System Safety*, Vol. 56(3), pp. 183-196.

Szilard, R. (1974). *Theory and analysis of plates: classical and numerical methods*. Prentice-Hall, New Jersey.

Tafreshi, A., & Oswald, T. (2003). Global buckling behavior and local damage propagation in composite plates with embedded delaminations. *International Journal of Pressure Vessels and Piping*, Vol.80 (1), pp.9–20.

Tarunjit, S. B. & Wolfe, W. E. (2002). A strain-energy-based non-linear failure criterion: comparison of numerical predictions and experimental observations for symmetric composite laminates. *Composites Science and Technology*, Vol.62 (12-13), pp.1697-1710.

Thoft-Christensen, P., & Baker, M. J. (1982). *Structural Reliability Theory and its Application*. Springer-Verlag, Berlin, Heidelberg.

Timoshenko, S. P., & Woinowsky-Krieger, S. (1959). *Theory of plates and shells*. McGraw-Hill, New York.

Torng, T. Y., Lin, H. Z., & Khalessi, M. R. (1996). Reliability calculation based on a robust importance sampling method. *In: Proc. 37th AIAA/ASME/ASCE/ AHS/ASC Structures, Structural Dynamics, and Materials Conference*, Salt Lake City, pp.1316–1325.

Bogetti, T.A., Hoppel, C.P.R. & Harik, V. M. (2004). Predicting the nonlinear response and progressive failure of composite laminates. *Composites Science and Technology*, Vol.64, 329–342.

Trimming, M. (1984). Monocoque GRP minehunters. *Proc. Int. Symp. on Mine Warfare Vessels and Systems*, RINA, London.

Tsai, S. W. (1968). Strength theories of filamentary structures in fundamental aspects of fiber reinforced plastic composites. *Conference Proceedings,* Dayton, Ohio, Wiley Interscience, New York, pp.3-11.

Tsai, S. W., & Wu, E. M. (1971). A general theory of strength for anisotropic materials. *Journal of Composite Materials*, Vol.5, pp.371-393.

Tsai, S. W. (1984). A survey of macroscopic failure criteria for composite materials. *Journal of Reinforced Plastics and Composites*. Vol.3, pp.40-63.

Vedeler, G. (1945). *Grillage beams in ships and similar structures*. OLSO.

Viswanathan, A. V., Tamekuni, M., & Baker, C. C. (1973). Elastic Stability of Laminated Flat and Curved Long Rectangular Plates Subjected to Combined In-plane Loads. Report, NASA CR-2330, 88pp.

Wang, X. W., Pont-Lezica, I., Harris, J. M., Guild, F. J., & Pavier, M. J. (2005). Compressive failure of composite laminates containing multiple delaminations. *Composites Science and Technology,* Vol.65 (2) pp.191-200.

Weibull, W. (1939). A statistical theory of the strength of materials. *Ing. Vetenskaps. Akad. Handl.* Vol.151. pp.45.

Whitney, J. M., & Sun, C. (1973). A higher order theory for extensional motion of laminated composites. *Journal of Sound and Vibration*, Vol. 30(1), pp. 85-97.

Whitney, J. M. (1973). Shear correction factors for orthotropic laminates under static load. *Journal of Applied Mechanics*, Vol.40(1), pp.302-304.

Wildman, D. (1971). Reinforced plastics for small craft. *Proc. Symp. on Small Craft,* RINA, Southampton.

Wimmers, H. W. (1966). *Consideration of the Design and Construction of Larger Glass Fiber Reinforced Polyester Ships*. Schip en Werf.

Wittrick, W. H. (1968). A unified approach to the initial buckling of stiffened panels in compression. *Aeronautical Quarterly*,Vol.19, pp.265-283.

Wittrick, W. H., & Williams, F. W. (1974). Buckling and vibration of anisotropic or isotropic plate assemblies under combined loadings. *International Journal of Mechanical Sciences*, Vol.16(4), pp.209-239.

Wittrick, W. H. (1987). Analytical three-dimensional elasticity solutions to some plate problems and some observations on Mindlin's plate theory. *International Journal of Solids and Structures,* Vol.23, pp.441-464.

Wolfe, W. E., & Butalia, T. S. (1998). A strain-energy based failure criterion for non-linear analysis of composite laminates subjected to biaxial loading. *Composites Science and Technology,* Vol.58, pp.1107–1124.

Wong, F. A. (1985). Slope reliability and response surface method. *Journal of Geotechnical Engineering*, Vol. 111(1), pp.32-53.

Wu, Y. T. (1994). Computational methods for efficient structural reliability and reliability sensitivity analysis. *AIAA Journal*, Vol. 32 (8), pp.1717-1723.

Xavier, P. B., Chew, C. H., & LEE, K. H. (1995). Buckling and vibration of multilayer orthotropic composite shells using a simple higher-order layerwise theory. *International Journal Solids and Structures,* Vol.32, pp. 3479–3497.

Yang, P. C., Norris, C. H., & Stavsky, Y. (1966). Elastic wave propagation in heterogeneous plates. *Int J Solids Struct*, Vol.2, pp.665–684.

Yang, Y. S., Lee, J. O., & Kim, B. J. (1996). Structural reliability analysis using

commercial FEM package. *Proceeding of the 6th International Offshore and Polar Engineering Conference*, Vol.4, pp.387-394, USA.

Yoda, T., & Atluri, S. N. (1992). Postbuckling analysis of stiffened laminated composite panels using a higher-order shear deformation theory. *Computational Mechanics*, Vol. 9(6), pp.390-404.

Yu, L., Das, P. K., & Zheng, Y. (2002). Stepwise response surface method and its application in reliability analysis of ship hull structure. *J. Offshore Mech. Arct. Eng*, Vol.124 (4), pp.226-231.

Yuan, W. X., & Dawe, D. J. (2004). Free vibration and stability analysis of stiffened sandwich plates. *Composite Structures*, Vol. 63(1), pp.123-137.

Zaharia, R., & El-Zafrany, A. (2009). Progressive failure analysis of composite laminated stiffened plates using the finite strip method. *Composite Structures,* Vol. 87 (1) pp.63-70.

Zhang, Y., & Der Kiureghian, A. (1994). Two improved algorithms for reliability analysis. reliability and optimization of structural systems. *Proc. 6th IFIP WG 7.5 working conference on reliability and optimization of structural systems*, pp.297–304.

Züleyha, A., & Mustafa, S. (2009). Buckling behavior and compressive failure of composite laminates containing multiple large delaminations. *Composite Structures*, Vol. 89(3), pp.382-390.

Zweben, C., & Rosen, B. W. (1970). A statistical theory of material strength with application to composite materials. *J. Mech. Phys. Solids*, Vol.18, pp. 189–206.

Appendix A:
Navier Solution Using FSDT

The different analytical solutions based on the FSDT have been developed to obtain the exact solutions of laminated plates such as the Navier method, the Lévy method and the Ritz methods depending on the boundary conditions. Navier solutions have been developed by Reddy for rectangular laminate with two sets of simply supported boundary conditions (SS-1 and SS-2). The Navier solutions for rectangular laminated plates using SS-1 boundary conditions may exist only for laminates whose stiffnesses A_{16}, A_{26}, B_{16}, B_{26}, D_{16}, D_{26} and A_{45} are zero. Thus, the Navier solutions for the SS-1 boundary conditions can be developed for laminates with a single generally orthotropic layer, symmetrically laminated plates with multiple specially orthotropic layers, and antisymmetric cross-ply laminated plates. Similar, the Navier solutions using SS-2 boundary condition may exist when stiffnesses A_{16}, A_{26}, B_{11}, B_{12}, B_{22}, B_{66}, D_{16}, D_{26} and A_{45} are zero, i.e., for laminates with a single generally orthotropic layer, symmetrically laminated plates with multiple specially orthotropic layers, and antisymmetric angle-ply laminated plates (Reddy, 2003).

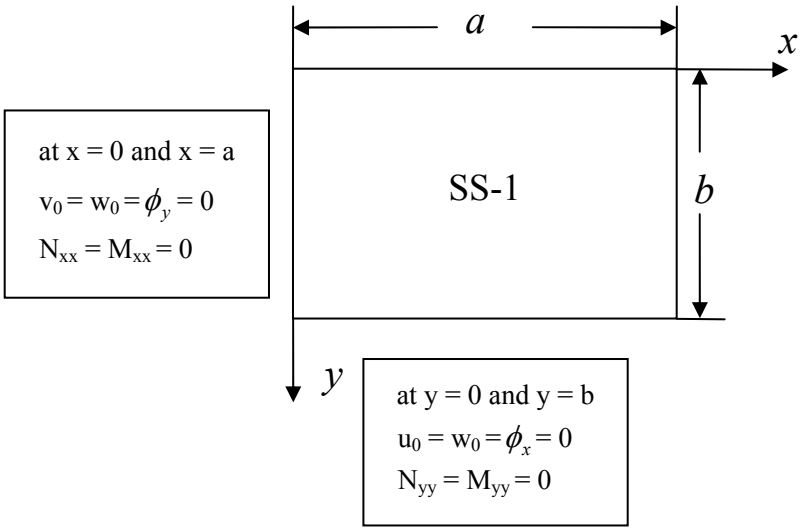

Figure A.1 Navier solution for SS-1 boundary condition

In the Navier method, the displacements are expanded in a double trigonometric series when the displacement boundary condition of SS-1 is satisfied. The displacement boundary conditions of SS-1 are satisfied by assuming the following form of the displacements

$$\begin{aligned} u_0(x,y) &= \sum_{n=1}^{\infty}\sum_{m=1}^{\infty} U_{mn}\cos\alpha x\sin\beta y \\ v_0(x,y) &= \sum_{n=1}^{\infty}\sum_{m=1}^{\infty} V_{mn}\sin\alpha x\cos\beta y \\ w_0(x,y) &= \sum_{n=1}^{\infty}\sum_{m=1}^{\infty} w_{mn}\sin\alpha x\sin\beta y \\ \phi_x(x,y) &= \sum_{n=1}^{\infty}\sum_{m=1}^{\infty} X_{mn}\cos\alpha x\sin\beta y \\ \phi_y(x,y) &= \sum_{n=1}^{\infty}\sum_{m=1}^{\infty} Y_{mn}\sin\alpha x\cos\beta y \end{aligned} \tag{A.1}$$

The mechanical force q should also be expanded in the same form.

$$q(x,y) = \sum_{n=1}^{\infty}\sum_{m=1}^{\infty} Q_{mn}\sin\alpha x\sin\beta y \tag{A.2}$$

where $\alpha = \dfrac{m\pi}{a}$, $\beta = \dfrac{n\pi}{b}$ and $\left(U_{mn}, V_{mn}, W_{mn}, X_{mn}, Y_{mn}\right)$ are coefficients to be determined. Once these coefficients are determined, the solution $\left(u_0, v_0, w_0, \phi_x, \phi_y\right)$ can then be computed from Eq.(A.1).The in-plane stresses of a simply supported laminated plate can be obtained by the stress-strain relations Eqs.(4.4) and (4.5)

Bending Strength of laminated Plate with SS-1

For antisymmetric cross-ply laminated plates, the stresses in each layer can be obtained using equations

$$\begin{Bmatrix}\sigma_{xx}\\ \sigma_{yy}\\ \sigma_{xy}\end{Bmatrix}^{(k)} = \sum_{m=1}^{\infty}\sum_{n=1}^{\infty}\begin{bmatrix}\overline{Q}_{11} & \overline{Q}_{12} & 0\\ \overline{Q}_{12} & \overline{Q}_{22} & 0\\ 0 & 0 & \overline{Q}_{66}\end{bmatrix}^{(k)}\begin{Bmatrix}(R_{mn}^{xx}+zS_{mn}^{xx})\sin\alpha x\sin\beta y\\ (R_{mn}^{yy}+zS_{mn}^{yy})\sin\alpha x\sin\beta y\\ (R_{mn}^{xy}+zS_{mn}^{xy})\cos\alpha x\cos\beta y\end{Bmatrix} \tag{A.3}$$

$$\begin{Bmatrix}\sigma_{yz}\\ \sigma_{xz}\end{Bmatrix}^{(k)} = \sum_{m=1}^{\infty}\sum_{n=1}^{\infty}\begin{bmatrix}\overline{Q}_{44} & 0\\ 0 & \overline{Q}_{55}\end{bmatrix}^{(k)}\begin{Bmatrix}(Y_{mn}+\beta W_{mn})\sin\alpha x\cos\beta y\\ (X_{mn}+\alpha W_{mn})\cos\alpha x\sin\beta y\end{Bmatrix} \tag{A.4}$$

where

$$\begin{Bmatrix}R_{mn}^{xx}\\ R_{mn}^{yy}\\ R_{mn}^{xy}\end{Bmatrix} = \begin{Bmatrix}-\alpha U_{mn}\\ -\beta V_{mn}\\ \beta U_{mn}+\alpha V_{mn}\end{Bmatrix} \quad \begin{Bmatrix}S_{mn}^{xx}\\ S_{mn}^{yy}\\ S_{mn}^{xy}\end{Bmatrix} = \begin{Bmatrix}-\alpha X_{mn}\\ -\beta Y_{mn}\\ \beta X_{mn}+\alpha Y_{mn}\end{Bmatrix}$$

Buckling Strength of laminated Plate with SS-1

For buckling analysis, we assume that the only applied loads are the in-plane forces and all other mechanical loads are zero

$$\hat{N}_{xx} = -N_0 \qquad \hat{N}_{yy} = -kN_0 \tag{A.5}$$

The buckling load can be obtained by

$$N_0 = \frac{1}{\alpha^2+k\beta^2}\left(\hat{s}_{33} - \frac{\hat{s}_{34}\overline{s}_{55}-\hat{s}_{35}\overline{s}_{45}}{\overline{s}_{44}\overline{s}_{55}-\overline{s}_{45}\overline{s}_{45}}\hat{s}_{34} - \frac{\overline{s}_{44}\hat{s}_{35}-\overline{s}_{45}\hat{s}_{34}}{\overline{s}_{44}\overline{s}_{55}-\overline{s}_{45}\overline{s}_{45}}\hat{s}_{35}\right) \tag{A.6}$$

where

$$\hat{s}_{11} = (A_{11}\alpha^2 + A_{66}\beta^2)\ \hat{s}_{12} = (A_{12}+A_{66})\alpha\beta \qquad \hat{s}_{14} = (B_{11}\alpha^2 + B_{66}\beta^2)$$

$$\hat{s}_{15} = (B_{12}+B_{66})\alpha\beta \quad \hat{s}_{22} = (A_{66}\alpha^2 + A_{22}\beta^2) \quad \hat{s}_{25} = (B_{66}\alpha^2 + B_{22}\beta^2)$$

$$\hat{s}_{24} = \hat{s}_{15} \quad \hat{s}_{33} = K(A_{55}\alpha^2 + A_{44}\beta^2) \quad \hat{s}_{34} = KA_{55}\alpha \quad \hat{s}_{35} = KA_{44}\beta$$

$$\overline{s}_{44} = \hat{s}_{44} - \hat{s}_{14}\frac{\hat{s}_{14}\hat{s}_{22}-\hat{s}_{12}\hat{s}_{24}}{\hat{s}_{11}\hat{s}_{22}-\hat{s}_{12}\hat{s}_{12}} - \hat{s}_{24}\frac{\hat{s}_{11}\hat{s}_{24}-\hat{s}_{12}\hat{s}_{14}}{\hat{s}_{11}\hat{s}_{22}-\hat{s}_{12}\hat{s}_{12}}$$

$$\overline{s}_{45} = \hat{s}_{45} - \hat{s}_{15}\frac{\hat{s}_{14}\hat{s}_{22}-\hat{s}_{12}\hat{s}_{24}}{\hat{s}_{11}\hat{s}_{22}-\hat{s}_{12}\hat{s}_{12}} - \hat{s}_{25}\frac{\hat{s}_{11}\hat{s}_{24}-\hat{s}_{12}\hat{s}_{14}}{\hat{s}_{11}\hat{s}_{22}-\hat{s}_{12}\hat{s}_{12}}$$

$$\overline{s}_{55} = \hat{s}_{55} - \hat{s}_{15}\frac{\hat{s}_{15}\hat{s}_{22} - \hat{s}_{12}\hat{s}_{25}}{\hat{s}_{11}\hat{s}_{22} - \hat{s}_{12}\hat{s}_{12}} - \hat{s}_{25}\frac{\hat{s}_{11}\hat{s}_{25} - \hat{s}_{12}\hat{s}_{15}}{\hat{s}_{11}\hat{s}_{22} - \hat{s}_{12}\hat{s}_{12}}$$

Appendix B:
Effective Breadths

Table B.1 Effective Breadths, B_e, as calculated by Classification Societies (Boote, 2007)

	Steel and light alloy	GRP
R.I.Na (1995, 2003)	$\lambda = 0.25\left(\frac{L}{B}\right) - 0.016\left(\frac{L}{B}\right)$ if $L/B \le 8$ RNA '99	$B_e = B$
	$\lambda = 1$ if $L/B > 8$ RINA '99 $B_e = B$ stiffeners RINA 2000 $B_e = B_o$ 0.2 L primary beams RINA 2000	
A.B.S (2000, 2001)	$B_e = 80\,t$ steel $B_e = 60\,t$ light alloy	*Single skin* $Be = b_1 + 18\,t \le 36\,t$ *Sandwich* $Be = b_1 + 9\,t_c$
B.V. (1993, 2004)	$B_e = B$ stiffeners $B_e = B_o$ 0.2 L_o B primary beams	$B_e = B$ or 0.2 L "I" beams $B_e = B$ or $0.2\,L + b_1$ hat beams
DNV (2000)	$B_e = B$ stiffeners $B_e = CB$ primary beams Unif.load $C = 0.004(L/B)^3 - 0.074(L/B)^2 + 0.466(L/B) - 0.0044$ Point load $C = 0.0157(L/B)^2 + 0.2233(L/B) - 0.0058$	$\lambda = \left(1 + 3.3\frac{E}{G}\left(\frac{B}{L}\right)^2\right)^{-1}$
GL (2006)	$B_e = B$ stiffeners $B_e = C$ B primary beams Unif.load $C = 0.003(L/B)^3 - 0.065(L/B)^2 + 0.436(L/B) - 0.004$ Point load $C = 0.0124(L/B)^2 + 0.213(L/B) - 0.0027$	As for steel
Lloyd's	$\lambda = 0.3\left(\frac{L}{B}\right)^{2/3}$ if $L/B \le 6$ $\lambda = 1$ if $L/B > 6$	*Single skin* $1/2\ Be = 0.5\,b_1 + 10\,t$ *Sandwich* $1/2\ Be = 0.5\,b_1 + (t_o + t_i)$
ISO (2006)		$B_e = 9\,t_c + B$ (2000) $B_e = 20\,t_c + B$ (2005)

Appendix C:
Ply Properties of Laminates

Elastic properties for a unidirectional layer should be established ideally by tests, however, for initial design purpose, a very wide variety of fibre combinations are possible and representative test data are unlikely to be available. They may be obtained by several simple approximations to the elastic constants with reasonable accuracy. Semi-empirical equations of moduli derived by Halpin and Tsai are sufficiently accurate for most composites except those with a very high fibre content (Smith, 1990). Young's modulus E_1 in the fibre direction, Young's modulus E_2 in the transverse direction normal to the fibre, Poisson's ratio ν_{12} and shear modulus G_{12} as follows

$$E_1 = E_f V_f + E_m V_m \tag{C.1}$$

$$\nu_{12} = \nu_f V_f + \nu_m V_m \tag{C.2}$$

$$M = M_m \times \frac{1 + \xi\eta V_f}{1 - \eta V_f} \tag{C.3}$$

$$\eta = \frac{M_f / M_m - 1}{M_f / M_m + \xi} \tag{C.4}$$

where E_f and E_m are fibre and matrix moduli, respectively; V_f is the fibre volume fraction; $V_m = 1 - V_f$ is the corresponding matrix volume fraction; $M = E_2$ or G_{12}, $M_f = E_f$ or G_f, $M_m = E_m$ or G_m, respectively; Reinforcing factor $\xi_G = 1$ for the prediction of shear G_{12} and $\xi_E = 2$ for the Young's modulus E_2 approximately.

The strengths of a unidirectional composite layer can be obtained using simple equations as follows

Longitudinal tensile strength

$$X_t = E_f V_f \varepsilon_f^* \qquad \text{When } \varepsilon_f^* > \varepsilon_m^* \qquad \text{(C.5)}$$

$$X_t = (E_f V_f + E_m V_m)\varepsilon_f^* \qquad \text{When } \varepsilon_f^* < \varepsilon_m^* \qquad \text{(C.6)}$$

Transverse tensile strength and in-plane shear strength

$$Y_t = \left(1 - (\sqrt{V_f} - V_f)\left(1 - \frac{E_m}{E_2}\right)\right)\sigma_m^* \qquad \text{(C.7)}$$

$$S_t = \left(1 - (\sqrt{V_f} - V_f)\left(1 - \frac{E_m}{E_2}\right)\right)\tau_m^* \qquad \text{(C.8)}$$

where ε_f^* and ε_m^* is strains to failure of the fibre and resin, respectively; σ_m^* is the matrix tensile strength; τ_m^* is the matrix shear strength. The longitudinal and transverse compressive strength can be approximately estimated by the same equation.

Appendix D:
Partial Safety Factor

Random variables X can be standardized to Y through (Melchers, 1999).

$$y_i = \frac{(x_i - \mu_{x_i})}{\sigma_{x_i}} \tag{D.1}$$

The coordinates of the checking point y_i^* in Y space were found to be given by

$$y_i^* = -\alpha_i \beta \tag{D.2}$$

From these two expressions it follows that the coordinates of the checking point in X space are

$$x_i^* = \mu_{x_i} - \alpha_i \beta \sigma_{x_i} \quad \text{(i=1,..,n)} \tag{D.3}$$

When the X space is non-normal, the general expression $x_i^* = F_{x_i}^{-1}[\Phi(y_i^*)]$ must be used instead.

The limit state function evaluated at the checking point x^* is

$$G(x_i^*) = G[\mu_{x_i}(1 - \alpha_i \beta_C V_{x_i})_{i=1,...n}] = 0 \tag{D.4}$$

Generally, the concept of safety is established by comparison of an upper characteristic value of applied stress with a lower characteristic value of resistance in engineering applications. For resistance, the characteristic value is estimated on the low side of the mean

$$R_k = \mu_R (1 - K_R V_R) \tag{D.5}$$

where μ_R and V_R are mean resistance and the coefficient of variation of R, respectively.

Similarly, for stress, the characteristic value is defined on the high side of the mean

$$S_k = \mu_S(1 + K_S V_S) \tag{D.6}$$

where μ_s and V_s are mean resistance and the coefficient of variation of S, respectively. K_R and K_S are percentile characteristic values of R and S, respectively.

Let the subset X_i, i=1,,,m be resistance basic variables, Converting from means to characteristic values by the use of Eqs.(D.3) and (D.5)

$$x_i^* = \frac{1 - \alpha_i \beta_C V_{x_i}}{1 - K_{x_i} V_{x_i}} x_{k_i} \tag{D.7}$$

Equation (D.7) may be written also as

$$x_i^* = \mu_{x_i}(1 - \alpha_i \beta_C V_{x_i}) = \frac{x_{k_i}}{\gamma_{mi}} \tag{D.8}$$

where $\frac{1}{\gamma_{mi}} = \frac{1 - \alpha_i \beta_C V_{x_i}}{1 - K_{x_i} V_{x_i}} = \frac{x_i^*}{x_{k_i}}$ is defined as the partial factor on the resistance random variables.

Similarly, let X_i, i = m+1,…n represent loading basic variables. Then using Eq.(D.6)

$$x_i^* = \frac{1 - \alpha_i \beta_C V_{x_i}}{1 + K_{x_i} V_{x_i}} x_{k_i} = \gamma_{f\,i} x_{ki} \tag{D.9}$$

where $\gamma_{fi} = \frac{x_i^*}{x_{k_i}}$ is defined as the partial factor on the load random variables.

Appendix E:
Papers

The papers written based on the thesis and published in journal or presented for international conferences are as follows:

[1] Blake, I.R., Shenoi, R.A., Das, P.K. & **Yang, N.** (2009). The application of reliability methods in the design of stiffened FRP composite panels for marine vessels. *Ships and Offshore Structures*.Vol.4(3) , pp. 287 – 297.

[2] **Yang, N.**, Das, P.K. & Yao, XL (2009). Ultimate strength and reliability assessment of composite plates under axial compression, *Ships and Offshore Structures*. (Accepted to be published)

[3] **Yang, N.**, Das, P.K. Blake, I.R., Sobey, A.J. & Shenoi, R.A., (2010) The application of reliability methods in the design of stiffened composite plate under in-plane loading (submitted to *Ship and Offshore Structures*)

[4] **Yang, N.**, Das, P.K. & Yao, XL (2007). An application of response surface method for reliability analysis of composite structure, *12th International Congress of International Maritime Association of the Mediterranean* (IMAM) 2-6 September 2007, Varna, Bulgaria.

[5] **Yang, N.**, Das, P.K. & Yao, XL (2008). Reliability analysis of stiffened composite panel. *4th International ASRANET Colloquium*, 25-27 June 2008 Athens, Greece.

[6] **Yang, N.**, Das, P.K. & Yao, XL (2009). Ultimate strength and reliability assessment of laminated composite plates under axial compression. *2nd*

MARSTRUCT Conference, 16 – 18 March 2009, Lisbon, Portugal

[7] **Yang, N.**, Das, P.K. & Yao, XL (2009). The application of reliability methods in the design of stiffened composite panels under in-plane loading. *1st International Conference on Light Weight Marine Structures*, 7-8 September, 2009, Glasgow,UK

[8] Misirlis, K., Dow, R.S., Downes, J., Berggreen,C., Delarche, A., Larsen C. L., Hayman, B., Touvalis, N., Das, P.K. & **Yang, N.** (2009) Investigations on the Ultimate Compressive Strength of Composite Plates with Geometrical Imperfections. *17th International Conference on Composite Materials* (ICCM17), 27-31. July 2009, Edinburgh, UK.

[9] **Yang, N.**, Subin, K.K.& Das, P.K., (2010). Application of response surface method for the reliability analysis of stiffened laminated plates. *ASRANet2010 Conference*, 14th - 16th June 2010, Edinburgh, Scotland